

**Institute of Polar Studies**

**Report No. 78**

# **Snow stratigraphic investigations at Dome C, East Antarctica**

**by  
Julie M. Palais**

**Institute of Polar Studies  
and  
Department of Geology and  
Mineralogy**

**1984**

**GOLDTHWAIT POLAR LIBRARY  
BYRD POLAR RESEARCH CENTER  
THE OHIO STATE UNIVERSITY  
1090 CARMACK ROAD  
COLUMBUS, OHIO 43210 USA**



**The Ohio State University  
Institute of Polar Studies  
Columbus, Ohio 43210**

INSTITUTE OF POLAR STUDIES

Report No. 78

Snow stratigraphic investigations at Dome C  
Antarctica: A study of depositional  
and diagenetic processes

by

Julie M. Palais

Institute of Polar Studies

and

Department of Geology and Mineralogy

1984

Copyright 1980

Used by permission of the author

Institute of Polar Studies  
The Ohio State University  
Columbus, Ohio 43210



INSTITUTE OF POLAR STUDIES

Report No. 15

Snow accumulation investigations at Point Barrow

Investigation of a study of deposition

and climatic processes

Copies of this and other publications  
of the Institute of Polar Studies are available from:

Institute of Polar Studies  
The Ohio State University  
125 South Oval Mall  
Columbus, Ohio 43210

Department of Geology and Mineralogy

1964

Copyright 1964

Used by permission of the author

Institute of Polar Studies

The Ohio State University

Columbus, Ohio 43210

## ABSTRACT

Current interest in studies of past climatic changes as revealed in long ice cores has stressed a need for understanding the development of the record preserved in these cores. This study investigates whether the record preserved at depth is more a function of depositional processes or of processes acting during or soon after burial. The temporal and areal variability of accumulation are investigated with a view to understanding how representative a single core is for a certain region, both in time and space. The validity of certain stratigraphic interpretations for dating is also assessed.

Evidence from snow pit studies made at Dome C, East Antarctica, (74°34'S, 123°10'E) suggests that a major part of the depositional features are preserved with depth. Visible annual strata are composed of thin hard crusts overlying thicker layers of soft to medium hard snow. Depth hoar-like low density layers, when they occur, are most often found below the thin hard crusts. Cycles in the concentration of gross Beta radioactivity and microparticles occur and can be accurately dated when studied in conjunction with a detailed record of the visible stratigraphy.

Accumulation stake measurements are used to study the formation of annual layers at Dome C. These measurements support the belief that depositional processes can account for a major part of the stratigraphic record.

Strong near surface temperature gradients and the associated effects of thermal conduction, vapor diffusion and air convection contribute to the development of depth hoar and with time may lead to significant changes in the variations in hardness, density, grain size and possibly impurity concentration and total mass preserved in individual layers.

## ABSTRACT

Current interest in studies of past climatic changes as revealed in long ice cores has stressed a need for understanding the development of the record preserved in these cores. This study investigates whether the record preserved in depth is more a function of depositional processes or of processes acting during or soon after burial. The known and recent variability of accumulation are investigated with a view to understanding how representative a single core is for a certain region, both in time and space. The reliability of certain stratigraphic interpretations for dating is also assessed.

Information from snow pit studies such as from C. East Antarctica, 15° 30' S, 115° 10' E suggests that a major part of the depositional record is preserved with depth. While the annual strata are composed of thin, dense, overlapping layers of ice, in some parts they are more often found below the thin hard crust. Cycles in the deposition of these thin layers and the deposition of ice can be accurately dated when studied in conjunction with a detailed record of the whole stratigraphy.

Information from snow pit studies are used to study the formation of annual layers at Dome C. These measurements support the belief that depositional processes are important for a major part of the stratigraphic record.

Strong near surface temperature gradients and the associated effects of thermal contraction, vapor diffusion and air convection contribute to the development of depth hard and thin ice layers in significant changes in the variation in density, density, grain size and possibly layering concentration and total mass preserved in individual layers.

## ACKNOWLEDGMENTS

This work has been realized through the contributions of many people. I would like to thank Dr. Ian Whillans for giving me the opportunity to go to Dome C and for his ceaseless patience through many hours of helpful discussions.

I would also like to thank Dean Colin Bull for helping in my understanding of many aspects of polar snow stratigraphy and for his encouragement and moral support throughout this research.

Dr. John Bolzan, Dr. Robert Reynolds and Mr. Ron Coffman provided much needed assistance with the field work. Their comments and suggestions have been invaluable.

The microparticle sample analyses and data synthesis were made by Dr. Lonnie Thompson and Ellen Mosley-Thompson of the Institute of Polar Studies, The Ohio State University. They also provided many hours of advice and encouragement.

The gross  $\beta$  radioactivity samples were analyzed by Michel Pourchet and Francis Pinglot of the C.N.R.S. Laboratoire de Glaciologie in Grenoble, France. Jean-Robert Petit provided comparative information and helpful discussions concerning the Dome C stratigraphy. Many thanks to my French colleagues.

I would also like to thank Drs. Gunter Faure and Dominique Raynaud for reading the manuscript and making many helpful suggestions to improve this work.

Finally, the men and women of the U.S. Navy's Operation Deep Freeze, and Holmes and Narver, Inc., provided excellent logistic support in the field.

This work has been supported by National Science Foundation grant DPP 76-23428 to Dr. I. Whillans and The Ohio State University Research Foundation.

# ACKNOWLEDGMENTS

This work has been carried through the contributions of many people. I would like to thank Dr. Ian Williams for giving me the opportunity to go to Paris and for his constant patience through many hours of helpful discussions.

I would also like to thank Dr. G. Bell for helping in my understanding of many aspects of polar wave stratigraphy and for his encouragement and moral support throughout this research.

Dr. John Kojan, Dr. Robert Reynolds and Mr. Ken Collins provided much needed assistance with the field work. Their comments and suggestions have been invaluable.

The stratigraphic sample analyses and data synthesis were made by Dr. John Thompson and Ellen Hooton-Thompson at the Institute of Polar Studies, The Ohio State University. They also provided many hours of advice and encouragement.

The Gross & radiometric sample were analyzed by Michel Fournier and Francis Planchet at the C.N.R.S. Laboratoire de Géochimie à Grenoble, France. Jean-Robert Bell provided comparative information and helpful discussions concerning the Gross & stratigraphy. Many thanks to my former colleagues.

I would also like to thank Dr. G. Bell, Dr. Ken Collins and Dr. John Kojan for reading the manuscript and making very helpful suggestions to improve this work.

Finally, the men and women of the U.S. Navy's Operation Deep Freeze, and Holmes and Narver, Inc., provided excellent logistic support in the field.

This work has been supported by National Science Foundation Grant DUE 75-1312 to Dr. I. Williams and The Ohio State University Research Foundation.

# TABLE OF CONTENTS

	Page
ABSTRACT.....	iii
ACKNOWLEDGEMENTS.....	v
LIST OF ILLUSTRATIONS.....	ix
LIST OF TABLES.....	xi
INTRODUCTION.....	1
FIELD PROGRAM.....	3
Previous Work at Dome C.....	4
Accumulation Stakes.....	4
Snow Pit Studies.....	6
ANALYTICAL METHODS.....	7
Visible Stratigraphy.....	7
Gross $\beta$ Radioactivity.....	9
Microparticles.....	11
DATA ANALYSIS AND RESULTS.....	17
Accumulation Stakes.....	17
Snow Pit Studies.....	28
Visible Stratigraphy.....	28
Definition of Annual Units.....	37
Gross $\beta$ Radioactivity.....	38
Microparticles.....	41
Areal and Temporal Variability: Comparison of Profiles B and C.....	46
DEPOSITIONAL AND DIAGENETIC PROCESSES.....	49
Depositional Processes.....	49
Diagenetic Processes.....	51
CONCLUSIONS.....	57
REFERENCES.....	61
APPENDICES.....	67



# TABLE OF CONTENTS

Page	
411	ABSTRACT.....
412	ACKNOWLEDGMENT.....
413	LIST OF ILLUSTRATIONS.....
414	LIST OF TABLES.....
415	INTRODUCTION.....
416	FIELD STUDIES.....
417	.....
418	.....
419	.....
420	.....
421	.....
422	.....
423	.....
424	.....
425	.....
426	.....
427	.....
428	.....
429	.....
430	.....
431	.....
432	.....
433	.....
434	.....
435	.....
436	.....
437	.....
438	.....
439	.....
440	.....
441	.....
442	.....
443	.....
444	.....
445	.....
446	.....
447	.....
448	.....
449	.....
450	.....
451	.....
452	.....
453	.....
454	.....
455	.....
456	.....
457	.....
458	.....
459	.....
460	.....
461	.....
462	.....
463	.....
464	.....
465	.....
466	.....
467	.....
468	.....
469	.....
470	.....
471	.....
472	.....
473	.....
474	.....
475	.....
476	.....
477	.....
478	.....
479	.....
480	.....
481	.....
482	.....
483	.....
484	.....
485	.....
486	.....
487	.....
488	.....
489	.....
490	.....
491	.....
492	.....
493	.....
494	.....
495	.....
496	.....
497	.....
498	.....
499	.....
500	.....
501	.....
502	.....
503	.....
504	.....
505	.....
506	.....
507	.....
508	.....
509	.....
510	.....
511	.....
512	.....
513	.....
514	.....
515	.....
516	.....
517	.....
518	.....
519	.....
520	.....
521	.....
522	.....
523	.....
524	.....
525	.....
526	.....
527	.....
528	.....
529	.....
530	.....
531	.....
532	.....
533	.....
534	.....
535	.....
536	.....
537	.....
538	.....
539	.....
540	.....
541	.....
542	.....
543	.....
544	.....
545	.....
546	.....
547	.....
548	.....
549	.....
550	.....
551	.....
552	.....
553	.....
554	.....
555	.....
556	.....
557	.....
558	.....
559	.....
560	.....
561	.....
562	.....
563	.....
564	.....
565	.....
566	.....
567	.....
568	.....
569	.....
570	.....
571	.....
572	.....
573	.....
574	.....
575	.....
576	.....
577	.....
578	.....
579	.....
580	.....
581	.....
582	.....
583	.....
584	.....
585	.....
586	.....
587	.....
588	.....
589	.....
590	.....
591	.....
592	.....
593	.....
594	.....
595	.....
596	.....
597	.....
598	.....
599	.....
600	.....

# LIST OF ILLUSTRATIONS

Figure		Page
1	Location map showing the Dome C site in central East Antarctica.....	2
2	Dome C camp showing orientation of strain net, location of snow pits, and intensive study area.....	5
3	Surface observations of aitken nuclei concentration at the South Pole, 1975.....	11
4	Microparticle profile showing criteria for annual peak interpretation.....	13
5	Frequency distribution of accumulation in the bamboo forest and accumulation cross.....	19
6	Changes in surface topography of the bamboo forest..	23
7	Sketch map of the accumulation cross.....	26
8	Profiles of the relative surface elevation in the bamboo forest.....	27
9-13	Composite of 3-meter pit studies.....	30-35
14	Microparticle profile from shallow pit at Dome C, 1975.....	43
15	Microparticle profile from shallow core section, Dome C, 1975.....	45
16	Schematic representation of the stratigraphy in Profiles B and C.....	47
17	Schematic representation of the possible position of a glazed surface with respect to other depositional units.....	50



# LIST OF TABLES

Table		Page
1	Accumulation rate data from the bamboo forest and accumulation cross at Dome C.. .....	18
2	Mean surface elevations and standard deviations of single measurements of stakes in the bamboo forest, made during the 1978-79 and 1979-80 seasons.....	17
3	Mean annual (1979) accumulation and description of surface conditions in the four branches of the accumulation cross.....	25
4	Accumulation rates obtained from gross $\beta$ radioactivity analyses of samples from 3-meter snow pits.....	39
5	Microparticle data showing values of the cleanest 30 percent of all samples in each pit.....	42

## INTRODUCTION

In recent years there has been heightened interest in the causes of the fluctuations of climate which have been inferred from the analysis of long cores from the major ice sheets and the deep ocean basins, as well as from tree rings (Global Atmospheric Research Programme, 1975). Particularly important have been the results of work on ice cores from Greenland and Antarctica which can provide high-resolution records of past fluctuations in some of the characteristics of climate for the past approximately 100,000 years, on scales of decades or years. Interest in understanding the large ice masses of Antarctica and Greenland and their response to local and global climate has shown the need for more detailed studies of the factors which affect the dynamics and mass budget of these ice sheets (National Academy of Sciences, 1974; Global Atmospheric Research Programme, 1975).

In order to interpret the stratigraphic record preserved in long ice cores it is important to understand the effects of ice flow at depth, the transport of snow to the glacier, and the processes occurring near the surface of the ice sheet. A study of part of these surface phenomena is the subject of the present work.

The thick interior portions of the East Antarctic ice sheet contain the longest records of snow accumulation in Antarctica. In preparation for deep drilling in one region, Dome C (Figure 1, 74° 30'S, 123° 10'E), investigations were conducted to obtain information concerning the surface regime and ice flow characteristics (Lorius and Donnou, 1978; Whillans, 1979). Studies of the present surface regime at Dome C have been conducted by both French and American glaciologists. The present study includes the results of two austral summers of surface investigations.

The use of new methods to date deep ice cores such as analyses of oxygen isotopes (Dansgaard and others, 1973) and microparticle profiles (Thompson, 1977; Mosley-Thompson, 1980) has led to comparisons with the theoretical predictions of age from flow models (Raynaud and others, 1979; Hammer and others, 1978). A knowledge of the current accumulation rate at the surface is important for the development of time scales in deep ice cores and for use in these theoretical calculations. In addition to the use of oxygen isotopes and microparticles, a method which has been developed to obtain this information involves the detection of levels in the snow exhibiting high concentrations of artificial radioactivity from the fission products of nuclear weapon testing. These levels in Antarctica correspond to approximately January 1955 and January 1965 and allow for the determination of mean annual accumulation since 1955.

A major portion of the interior of East Antarctica, including Dome C, has an annual accumulation of less than 50 kg/m<sup>2</sup>/a (Bull,

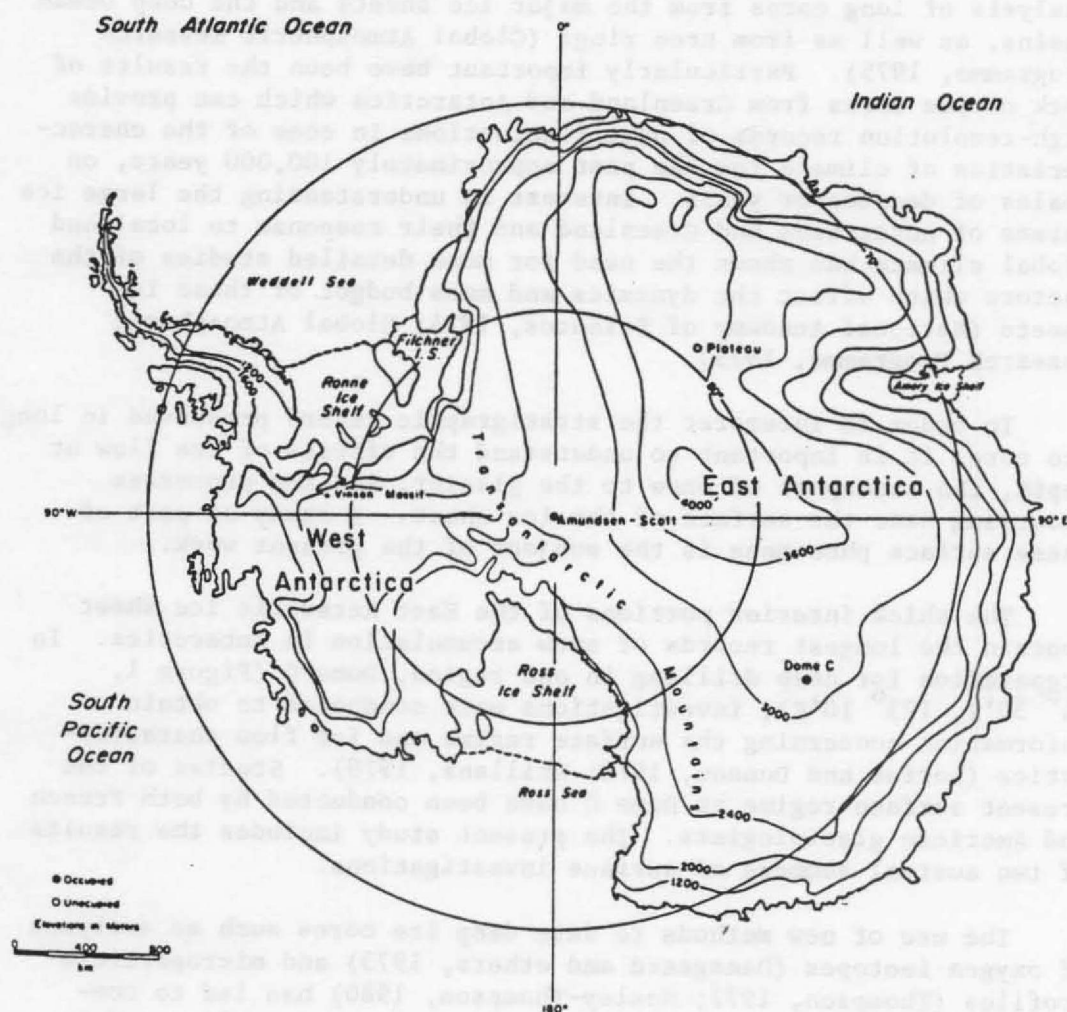


Figure 1. Location map showing the Dome C site in central East Antarctica; modified from Dalrymple, (1966).



1971). It is therefore important to determine whether the stratigraphy at the surface of the ice sheet (as revealed in surface snow pits) can be interpreted as it can in other parts of Antarctica (Cameron, 1964; Benson, 1970; Bull, 1971) where the accumulation rates are higher.

The following objectives were established for the work at Dome C.

- (1) To interpret accurately the stratigraphy in an area of low annual accumulation in terms of depositional and diagenetic processes.
- (2) To study the areal variability of the accumulation rate near the Dome C camp and the implications of this areal variability to stratigraphic interpretations.
- (3) To investigate whether some of the conventional snow stratigraphic methods of dating (that is, the interpretation of visible stratigraphy) and other more recently developed methods (involving measurements of microparticle concentration and gross  $\beta$ -radioactivity profiles) can be applied with confidence in areas of low annual accumulation such as Dome C. Comparatively few studies of this kind have been made in such regions (Picciotto and others, 1971; Taylor, 1971; Pourchet, 1979; Petit and others, 1980).

#### FIELD PROGRAM

Dome C is one of several ice ridges located in the central portion of the East Antarctic plateau. The mean elevation and mean annual air temperature are 3240 m and  $-53.5^{\circ}\text{C}$  respectively (Lorius and Donnou, 1978). Radio-echo and seismic sounding (Scott Polar Research Institute, 1974; Robin, 1975; Bentley and others, 1979) show that the ice there is approximately 3400 m thick.

The Antarctic Plateau, according to Dalrymple (1966) is that area of East Antarctica above 2000 m with an average surface slope of less than 1%. The homogeneous microclimate which is developed over the plateau is determined by the high elevation, low surface slope and low temperature. Relatively calm and stable conditions are established at the surface due to the presence of a strong temperature inversion which persists almost year round and isolates the ice sheet surface from the main part of the troposphere. A low pressure area develops over the ice sheet as a result of the temperature conditions but the high surface elevations generally prevent cyclones from penetrating to the interior of the continent. Thus, precipitation is high (up to  $800 \text{ kg/m}^2/\text{a}$ ) in the coastal regions and is much less on the plateau.

Meteorological observations at Dome C in December 1978 and January 1979 showed generally fair weather with low winds ( $< 5 \text{ m/s}$ )

and clear-sky ice crystal precipitation. About one week of stormy weather occurred at the end of December when relatively high winds (10 m/s), cloud cover, and snow fall were common.

Previous Work at Dome C. Work at the Dome C site has been carried out previously as part of the International Antarctic Glaciological Program (IAGP) by researchers from Australia, France, the United Kingdom, the United States and the Union of Soviet Socialist Republic. Surface glaciological studies (Lorius and Merlivat, 1977; Delmas and Boutron, 1978; Lambert and others, 1977; Petit and others, 1982) and deep ice core investigations (Lorius and others, 1979; Raynaud and others, 1979) have been undertaken to increase understanding of the present and past conditions of the East Antarctic ice sheet (National Academy of Sciences, 1974).

The present study was made to obtain information on the present surface conditions at Dome C. In the following section the 1978-79 field program of surface pit and stake measurements is described. In addition, shallow temperature studies were made and long-term experiments to measure the surface strain rate and firn densification were begun.

Accumulation Stakes. As a means of studying the accumulation rate and surface roughness, a network of bamboo stakes was established roughly 1 km grid SW of the Dome C camp (see Figure 2). This network, subsequently referred to as "the bamboo forest" consisted of poles, 3 m apart in a 10x10 grid. The poles were surveyed with a levelling instrument and numbered in rows (A-J) and columns (0-9). The top of the pole AO was chosen as a reference point and arbitrarily given an elevation of 10.00 m. The snow surface elevation was then obtained by measuring the exposed pole length on the grid N side using a tape measure and subtracting this from the elevation of the pole top. Measurements were made to the nearest 0.01 m. The bamboo forest was set up on December 5, 1978. Subsequent measurements of the exposed pole length were made on December 7, 23 and 29, 1978 and on January 16, 1979 and during the 1979-80 field season on November 30, 1979 and January 1, 1980. The data are given in Appendix I.

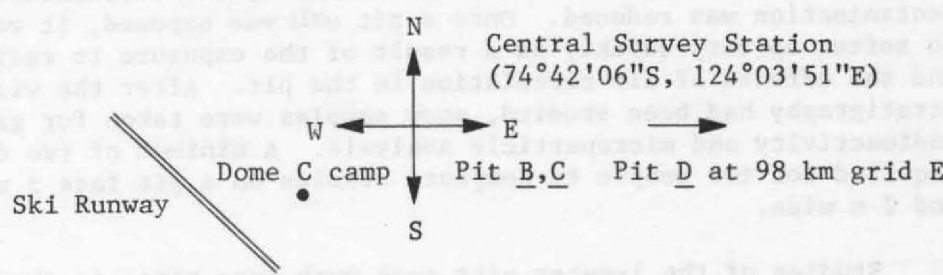
A second set of accumulation stakes was set up to measure accumulation over a larger region. This accumulation network had four branches oriented along the grid directions, each with 25 poles, separated by about 1 km. The first pole in each branch was 6 km from the central survey station (see Figure 2 and Figure 7), because the area within 5 km of the station was disturbed by human activity. Distances between poles were measured using an odometer wheel towed behind a snowmobile. Qualitative observations concerning the surface features and sastrugi development along the branches were also recorded. These poles were remeasured during the 1979-80 field season and additional poles were put at the ends of the East and West branches. The accumulation rates calculated from these studies are given in Appendix I.

During the 1975-76 austral summer, five strain-  
 gauged profiles were observed and compared in four 3-meter snow pits  
 of varying dimensions. In the four 3-meter pits, an experiment  
 was carried out in which the snow-water ratio, which varied from 10 to 20  
 percent, was studied to observe the changes in the strain  
 rate.

The 3-meter pits (labeled A-E, see Figure 2 for location) were  
 excavated in two stages. All work in the top 1.5 m was completed  
 before the remainder 1.5 m was excavated. This provided a continuous  
 working depth and, by not exposing the snow pit until it was  
 about to be studied, alteration by radiation, air circulation and  
 condensation was reduced. The 1.5 m pits were exposed in two 1-m  
 sections at the top of the exposure to facilitate  
 the work. After the work was done, the snow was  
 covered with a tarp and the pits were sealed for future use.

Studies of the 3-meter pits were made each time, in about 10-15  
 hours and about 10-15 minutes for the profile. In each 3-meter pit,  
 one of the exposed walls was marked. Dimensions and temperature were  
 measured and snow samples were taken from the pit. The snow was  
 covered with a tarp and the pits were sealed for future use.

The 3-meter pits were excavated in two stages. All work in the top 1.5 m was completed  
 before the remainder 1.5 m was excavated. This provided a continuous  
 working depth and, by not exposing the snow pit until it was  
 about to be studied, alteration by radiation, air circulation and  
 condensation was reduced. The 1.5 m pits were exposed in two 1-m  
 sections at the top of the exposure to facilitate  
 the work. After the work was done, the snow was  
 covered with a tarp and the pits were sealed for future use.



Pit A □ Intensive Study Area  
 (bamboo forest, densification experiment)

Pit E at Old French camp  
 ~6.5 km

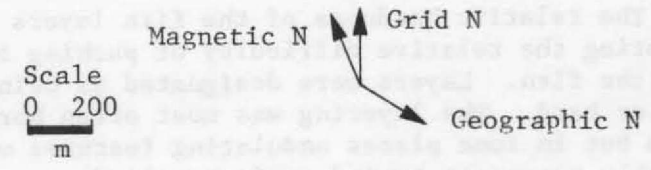


Figure 2. Dome C camp showing orientation of strain net and location of snow pits and intensive study area.

Snow Pit Studies. During the 1978-79 austral summer, five stratigraphic profiles were observed and sampled in four 3-meter snow pits of varying dimensions, in the Dome C area. In addition, an experiment was carried out in which six one-meter pits, within about 50 m of one another, were studied to observe the temporal changes, in the visible stratigraphy.

The 3-meter pits (lettered A-E, see Figure 2 for locations) were excavated in two stages: all work in the top 1.5 m was completed before the remaining 1.5 m was excavated. This provided a convenient working depth and, by not exposing the snow pit wall until it was about to be studied, alteration by radiation, air circulation and contamination was reduced. Once a pit wall was exposed, it was found to soften up very quickly as a result of the exposure to radiation and the effects of air circulation in the pit. After the visible stratigraphy had been studied, snow samples were taken for gross  $\beta$  radioactivity and microparticle analysis. A minimum of two days was required for two people to complete studies on a pit face 3 m deep and 2 m wide.

Studies of the 1-meter pits took much less time; in about four hours one person could complete the profile. In each 1-meter pit, one of the exposed walls was mapped, densities and temperatures were measured and snow samples were taken for analysis of oxygen isotopes by Dr. Minze Stuiver of the University of Washington, Seattle. The results of the oxygen isotope analyses are not available yet and will be discussed in a future publication.

Soon after a pit had been excavated, the selected wall was mapped. This involved qualitative observations of the hardness of layers, their thickness, extent, and two dimensional orientation. Where the surface was reasonably flat, the surface was used as a reference level for depth measurements. In other cases, a level reference line was made 0.05 to 0.10 m below the surface and the wall was mapped both up to the surface and down below the zero line. In all cases, zero is the defined reference level noted on each pit map.

The relative hardness of the firn layers in each pit was measured by noting the relative difficulty of pushing the blunt end of a pencil into the firn. Layers were designated as being very soft, soft, medium-hard or hard. The layering was most often horizontal on a scale of 2-3 m but in some places undulating features were observed, which probably represent buried surface relief.

While this mapping was being done, a second person measured temperatures with a dial thermometer. A section of the wall was cut into for a fresh surface and temperatures were measured every 0.10 m. The thermometer was allowed to equilibrate for approximately five minutes at each measurement point.

Density measurements were made by two different techniques, a block method and the standard 0.5 liter density-tube method. In the



first method, a block of firn approximately 0.30 m on a side was excavated and subsequently cut down to obtain parallel and orthogonal sides. The final block was usually 0.15 to 0.20 m on a side. All 12 edges were measured (to 1 mm) and the four edges in each orientation were averaged. From these measurements volume was calculated. The block was weighed on a triple beam balance to  $10^{-4}$  kg and the density was then calculated. Densities so obtained are accurate to about 2 percent.

The second method of density measurement was by using 0.5 liter density tubes. Vertical and horizontal samples were taken. The sample tube (after being weighed) was hammered into the wall with a rubber mallet and then sawed out of the wall. A plastic cap of known mass was added on the bottom of the tube. The sample and tube was weighed and the density calculated. This method was accurate to about 7 percent.

After these measurements had been completed, samples were collected for subsequent laboratory analysis of microparticle concentration, stable oxygen isotope ratios, and gross  $\beta$  radioactivity. The microparticle samples were usually taken first as these were the most susceptible to contamination. A plastic syringe about 40 mm in diameter was used to obtain samples from the pit wall. As in all the sampling, a section of the wall was cut out to expose a fresh surface. The sample was transferred directly into plastic bottles and sealed.

Adjacent samples were obtained for analyses of oxygen isotopes and gross  $\beta$  radioactivity. A small steel spatula was used to remove 20 mm (vertically) by approximately 50 mm (horizontally) samples (0.03-0.10 kg). These samples were placed directly in pre-labelled plastic bags and sealed.

The microparticle and oxygen isotope samples were shipped to the United States for analysis at The Institute of Polar Studies, The Ohio State University, and at the Department of Geological Sciences, University of Washington, respectively. The gross  $\beta$  samples were filtered at the Dome C camp and sent to the C.N.R.S. Laboratoire de Glaciologie in Grenoble, France, on ion exchange filter papers.

#### ANALYTICAL METHODS

Visible Stratigraphy. Visible stratigraphy was investigated in order to study the processes of layer formation and preservation. The criteria used to recognize annual units are based on previous work in areas of low annual accumulation (Gow, 1965; Koerner, 1971), snow stake measurements, and pit studies at Dome C. These criteria are described at page 17.

Work on snow stratigraphy in the dry facies of Greenland and Antarctica provided a basis for the interpretation of annual units of accumulation in snow pits (Liljequist, 1956; Schytt, 1958;

Giovinetto, 1960; Benson, 1962). The criteria established by these researchers involved primarily visual and other physical parameters such as density, hardness, crystal morphology, size, orientation, and thickness of various layers exposed in a pit wall. These characteristics are functions of original crystal size during precipitation, annual precipitation, temperature, and temperature gradients across the air-snow interface, and solar radiation, age, and effects of wind within the snow cover.

It has generally been agreed that snow deposited during the winter produces a hard compact layer of fine-grained dense firn. In contrast, summer deposited accumulation is generally coarser grained, softer, and lower in density (Benson, 1962; Bull, 1971). Annual accumulation units have been identified in various ways by different workers. Some have used grain size and hardness changes (Cameron, 1964) while others have used variations in density (Taylor, 1965; Benson, 1970) or a combination of all three (Giovinetto, 1960). Areas of fairly high annual accumulation and moderate air temperature with noticeable seasonal contrasts in these parameters, seem to provide the best conditions for such stratigraphic interpretations (Bull, 1971).

The mechanisms of post-depositional alteration of these properties (grain size, density, hardness) have been discussed by Seligman (1936), de Quervain (1963), Gow (1965), Benson (1970) and Taylor (1971). These authors attribute certain aspects of the visible stratigraphy to changes which take place after deposition. The theory behind these diagenetic processes and the mechanisms which produce these changes is discussed at page 49.

Gow (1965) used the annual formation of depth hoar (a diagenetic phenomenon) to determine the yearly accumulation in snow pits at the South Pole. Comparison with stake measurements led to the development of criteria for the recognition of years with little or no accumulation. In years where accumulation was absent, unusually thick depth hoar layers (0.04 to 0.05 m) were found just below the surface. In addition, thick crusts were often associated with and found just above these "hiatus-type" depth hoar layers (Gow, 1965). Unless yearly stake measurements are available, the main problem with such a criteria is that one does not know the length of time involved in the hiatus. The use of several stratigraphic methods simultaneously, however, may resolve such problems.

A different approach to the study of the effects of diagenesis on a snow cover in a region of low annual accumulation is due to Koerner (1971). In his study, 64 shallow (0.50 m) pits were excavated in early December at Plateau Station (Figure 1- 79° 15'S, 40° 30'E) before the effects of summer warmth and radiation could alter the physical properties of the previous winter's accumulation. Measurements of grain size, shape, density and hardness were made. The previous winter's accumulation was recognized by its fine (0.2mm), angular grains, in contrast to the coarser (0.4mm) rounder grains of the preceeding year's accumulation.



In late January, 50 more shallow pits were excavated in the same location to observe the effects of the summer season on the visible stratigraphy. During this two month interval, a thin (3-40 mm) fine grained hard layer had developed near the surface, with associated hoar layers and bonded grain crusts both above and below. The preceeding winter's snow had become a homogenized coarse grained (0.4 mm) soft layer without crusts or depth hoar layers. Annual units were recognized on the basis of the cyclical repetition of these hard, fine grained layers with associated depth hoar and the soft, coarse homogeneous layers. These soft layers contained the bulk of the annual accumulation and were deposited under varying conditions and subsequently homogenized during the summer.

With this background of the possible ways to interpret visible snow stratigraphy, an attempt was made to interpret the record preserved in the snow pits at Dome C. This analysis includes considerations of both depositional and post-depositional processes and is presented at page 17.

Gross  $\beta$  Radioactivity. The exploding of nuclear weapons high in the troposphere in the 1950's and 1960's produced a stratospheric burden of artificial radionuclides (fission products). The fallout of this material throughout the earth has led to many investigations of its transport, deposition and interaction with the atmosphere, biosphere, hydrosphere, lithosphere, and cryosphere (Martell, 1959; Junge, 1963; Wilgain and others, 1965).

The first measurements of atmospheric radioactivity in Antarctica were begun at Little America station in 1956. Two years later similar measurements were initiated at the South Pole. The information gained in these studies has allowed atmospheric scientists to trace the circulation patterns in the atmosphere over Antarctica (Martell, 1959; Junge, 1963; Lockhart and others, 1966). In addition, it was recognized that measurements of the variation with depth of the concentration of radioactivity of these fission products in the snow of polar and temperate glaciers could be used as a dating method (Picciotto and Wilgain, 1963; Picciotto and others, 1971).

The first measurements of radioactivity of snow in Antarctica (Picciotto and Wilgain, 1963; Wilgain and others, 1965; Lambert and others, 1967; Crozaz, 1969), used chemical coprecipitation techniques to measure the radioactivity of individual radionuclides. A new method has been developed (Delmas and Pourchet, 1977) in which ion exchange resin filters are used to collect particles and salts of artificial radioelements from firn samples. The samples which were collected at Dome C were prepared using this technique. Counting of the samples was made at the C.N.R.S. Laboratoire de Glaciologie in Grenoble, France on a low-level  $\beta$  counter designed and built specifically for this purpose (Pinglot, 1978; Pinglot and Pourchet, 1979).

The primary objective of these analyses was to locate the depths in each pit which correspond to the 1955 and 1965 peaks of gross  $\beta$  radioactivity. These peaks have been noted throughout Antarctica and correspond to the Ivy-Castle series of nuclear tests in the early 1950's and to the high-yield Soviet tests in the Arctic in the early 1960's, respectively. It was hoped that seasonal variations of radioactivity, which have been measured in the Antarctic atmosphere (Lockhart and others, 1966) and in southern hemisphere precipitation (Taylor, 1968) (summer maximum, winter minimum), could be detected in the Dome C pits. Snow stratigraphic dating, using  $\beta$  radioactivity peaks to determine annual layers, has already been used by Jouzel and others, (1979) at the South Pole where accumulation is  $80 \text{ kg/m}^2/\text{a}$ , twice as high as Dome C.

In a recent study, Pourchet and Pinglot, 1979, have used gross  $\beta$  radioactivity measurements to determine a variety of parameters related to the residence time, transport, and deposition of artificial radionuclides. A mean stratospheric residence time of  $1.5 \pm 0.2$  years was determined for the radioisotopes, based on the observed decrease in activity between 1965-69, at which time the stratospheric reservoir was homogeneous. Comparative measurements of the concentration of radioactivity in the air (g/S.C.M.) and the concentration in the snow (g/g) have allowed these authors to determine a value of one for the ratio between these two quantities (concentration in air/concentration in snow). Finally, the contribution of "dry fallout" to the total concentration of  $\beta$  activity in the snow was estimated as being from 10-15% in coastal sites, and as much as 20-30% in central regions of Antarctica (Pourchet and others, 1983).

The criteria which have been established to interpret the  $\beta$  profiles in this work are based on many analyses from pits in the Dome C area. These criteria, which are discussed below, were first established by Pourchet (1979). Because the  $\beta$  profiles presented in this work are very similar to those of Pourchet can be interpreted quite well using his criteria, it was decided that similar standards would be used. The January 1955 peak in each pit is taken to be the deepest sample where the level of activity first exceeds 1000 dph/kg of snow. Similarly, the January 1965 level is taken to be the lowest sample where the activity exceeds 2000 dph/kg of snow. It must be noted that these levels of activity apply only to samples taken at Dome C (or other Antarctic sites with a similar annual accumulation) and measured in January 1979, as the activity of the artificial nuclides is continuously decreasing according to the law of radioactivity.

The uncertainties in these measurements and the determination of mean annual accumulation from this information are related to several factors. These include:

- (1) Sampling error in the absolute depth of each sample from the reference horizon (= 1 sample or 0.02 m).

(2) Uncertainty in the exact date of the first arrival of radioactivity in Antarctic snows and errors in the precise placement of these fallout levels (1955 or 1965), according to the criteria described above ( $\approx 1$  sample or 0.02 m).

(3) Uncertainty in the exact age (depth) of a sample from the mean surface level due to buried surface microrelief.

These factors are believed to contribute only small errors to the exact determination of the depth to a particular radioactive level and thus to the mean accumulation rate calculated from such information.

**Microparticles.** The underlying assumptions in the interpretation of microparticle data are that concentration in the atmosphere varies cyclically with a period of one year and that this cyclicity is preserved within the snow stratigraphy. This assumption is supported by studies of microparticles from ice cores (Hamilton and Langway, 1967; Thompson, 1977; Mosley-Thompson, 1980) and from recent surface work at Dome C by J.R. Petit (Thompson and others, 1981). Further evidence for a seasonal variation in microparticle concentration comes from the one year of aerosol measurements at the South Pole (Hogan and Barnard, 1978) (Figure 3).

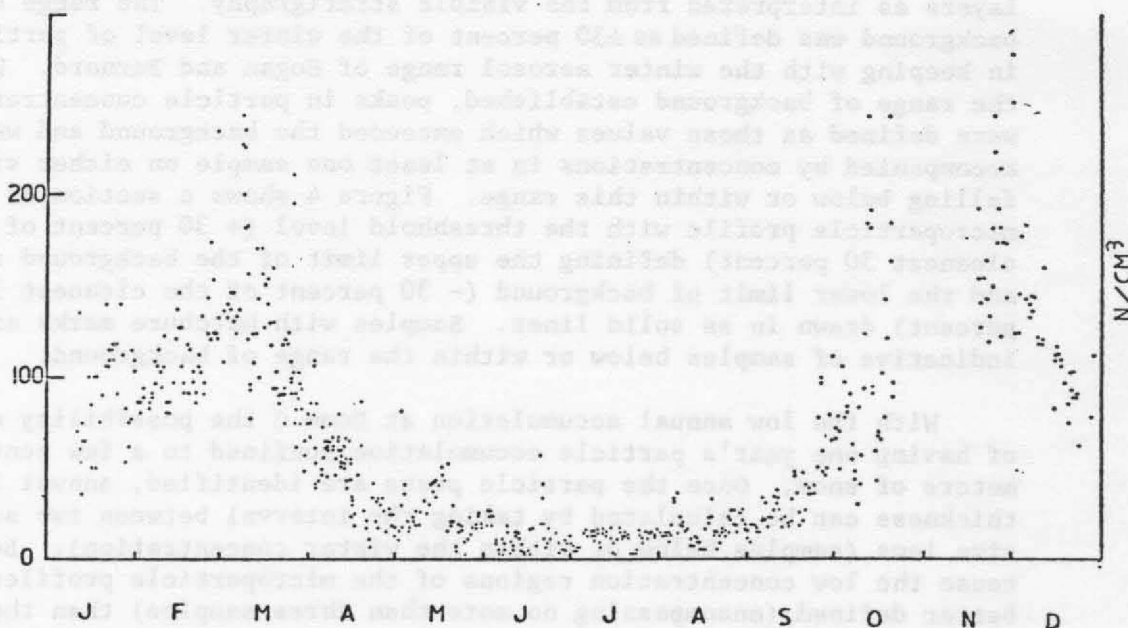


Figure 3. Surface observations of aiten nuclei concentration at the South Pole, 1975 (from Hogan and Barnard, 1978)



The information from these aerosol measurements has been used to define a set of criteria for the interpretation of the microparticle profiles.

It is assumed here and elsewhere (e.g. Mosley-Thompson, 1980), that a direct correlation exists between the atmospheric concentration of total aerosols and that of insoluble microparticles. It must also be assumed that there is a linear relationship between the atmospheric concentration of these particles and the concentration as measured in the snow. Furthermore, the effects of vapor transfer and mass loss during and after burial on the concentration of microparticles in the snow must also be considered. These assumptions and considerations have yet to be documented fully, requiring the direct measurement of atmospheric nuclei in the same size range as those measured by the microparticle analysis.

The aerosol measurements of Hogan and Barnard (1978) reveal "very low" levels in the winter (mean values of  $15 \pm 5$  nuclei/m<sup>3</sup>) and "much higher" levels during the summer (100-200 nuclei/m<sup>3</sup>) (Figure 3). In order to make a direct comparison with Hogan and Barnard's work, the concentration of microparticles in the cleanest 30 percent of the samples in each snow pit was computed. By taking the cleanest 30 percent as the winter level of particles, minor errors induced in the sampling and laboratory preparations are eliminated. In addition, the number of particles represented by the cleanest 30 percent appears to compare well with the concentration of particles found in winter snow layers as interpreted from the visible stratigraphy. The range of the background was defined as  $\pm 30$  percent of the winter level of particles, in keeping with the winter aerosol range of Hogan and Barnard. With the range of background established, peaks in particle concentration were defined as those values which exceeded the background and were accompanied by concentrations in at least one sample on either side falling below or within this range. Figure 4 shows a section of a microparticle profile with the threshold level (+ 30 percent of cleanest 30 percent) defining the upper limit of the background range and the lower limit of background (- 30 percent of the cleanest 30 percent) drawn in as solid lines. Samples with hatchure marks are indicative of samples below or within the range of background.

With the low annual accumulation at Dome C the possibility exists of having one year's particle accumulation confined to a few centimeters of snow. Once the particle peaks are identified, annual layer thickness can be calculated by taking the interval between two successive lows (samples below or within the winter concentration). Because the low concentration regions of the microparticle profiles are better defined (encompassing no more than three samples) than the regions defined as peaks (encompassing as many as 10 samples) annual layers are therefore counted between successive lows of particle concentration rather than between successive peaks. This gives more

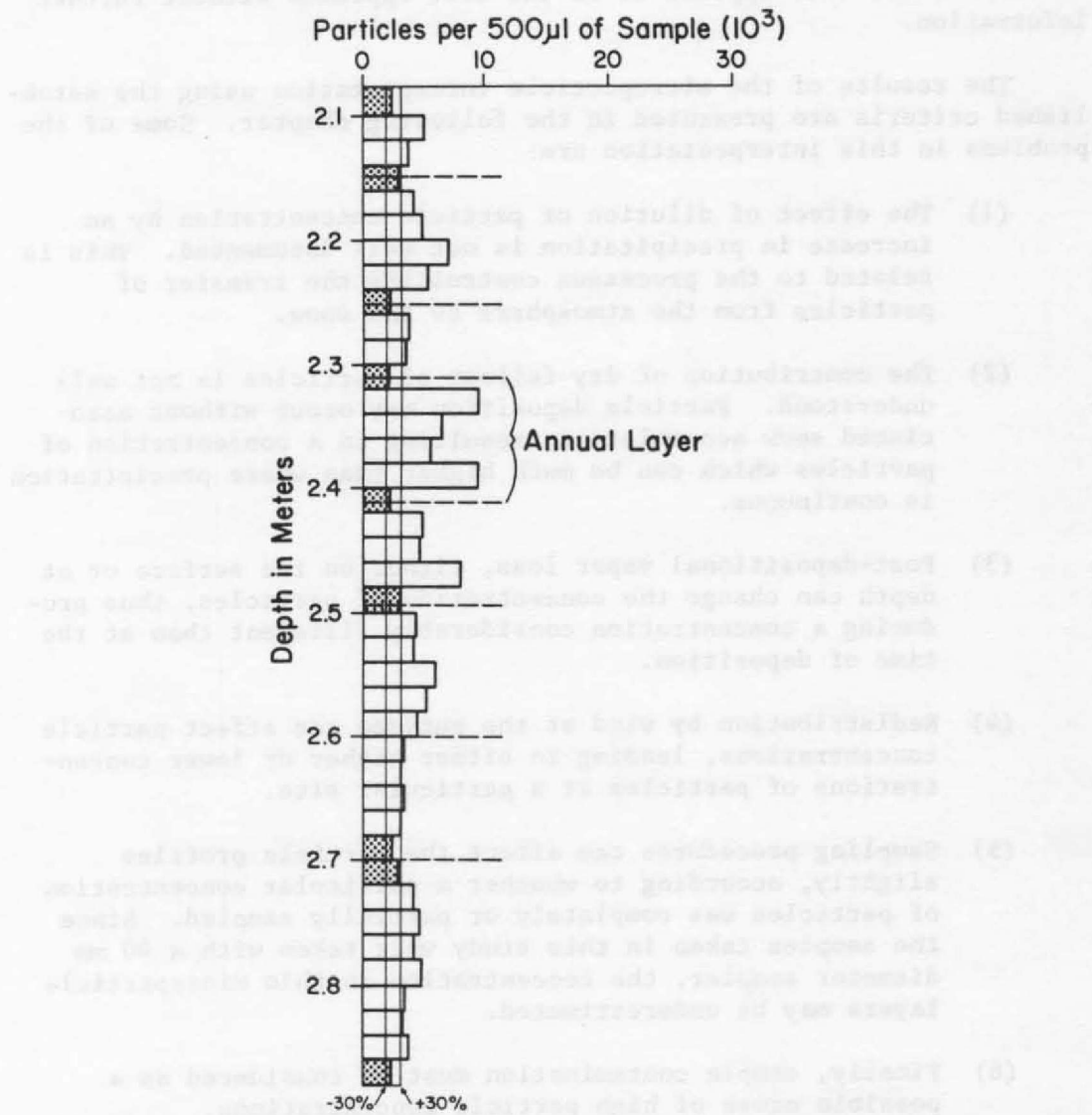


Figure 4. Microparticle profile showing criteria for annual peak interpretation.

precise temporal resolution than if one were to count between the more diffuse peak areas. As a low may extend for more than one sample, the low interval is divided in half and split between one year and the next. The exact partitioning of accumulation cannot be precisely determined but this appears to be the best approach without further information.

The results of the microparticle interpretation using the established criteria are presented in the following chapter. Some of the problems in this interpretation are:

- (1) The effect of dilution of particle concentration by an increase in precipitation is not well documented. This is related to the processes controlling the transfer of particles from the atmosphere to the snow.
- (2) The contribution of dry fallout of particles is not well understood. Particle deposition may occur without associated snow accumulation, resulting in a concentration of particles which can be much higher than where precipitation is continuous.
- (3) Post-depositional vapor loss, either on the surface or at depth can change the concentration of particles, thus producing a concentration considerably different than at the time of deposition.
- (4) Redistribution by wind at the surface can affect particle concentrations, leading to either higher or lower concentrations of particles at a particular site.
- (5) Sampling procedures can affect the particle profiles slightly, according to whether a particular concentration of particles was completely or partially sampled. Since the samples taken in this study were taken with a 40 mm diameter sampler, the concentration in thin microparticle layers may be underestimated.
- (6) Finally, sample contamination must be considered as a possible cause of high particle concentrations.

Little information is available concerning the relative importance of these effects: however several general comments can be made. Difficulties in the sampling and analysis of firn for microparticles make contamination potentially a greater problem than for similar analyses of ice. Sampling procedures (complete versus partial sampling of a particle layer) are important at sites such as Dome C because particles there are concentrated in thinner layers than at sites with a higher accumulation rate. Dry fallout was discussed in the previous section in relation to gross Beta radioactivity. Pourchet



and others (1983) estimated that dry fallout may contribute as much as 20-30 percent of the total  $\beta$  activity at a site like Dome C. A direct comparison between radioactivity microparticles, however, cannot be made at this time since the processes controlling the deposition of these impurities are not completely understood. Finally, changes in particle concentration occurring after burial are difficult to estimate. Detailed surface sampling for microparticle analysis, in conjunction with atmospheric aerosol measurements and vapor transfer studies, are necessary to understand the contributions from these effects.

and others (1982). It is suggested that the failure of correlation as such as in 19-20, is not a failure of the theory but a failure of the data. A direct comparison between the two sets of data is not possible because of the different methods used in the two experiments. The results of the two experiments are not directly comparable. Finally, changes in the correlation between the two sets of data are observed in certain cases. Detailed studies are needed for microstructural analysis in correlation with appropriate control experiments and other factors which are necessary to understand the correlation from these studies.

## DATA ANALYSIS AND RESULTS

Accumulation Stakes. The mean accumulation for 1979, computed for the 100 stakes in the bamboo forest and the 95 stakes in the accumulation cross, is presented in Table 1, with other comparable values from Petit and others (in press). Appendix I lists the complete data. A thorough discussion of the problems of firn settling and pole migration in the precise determination of annual accumulation from bamboo pole measurements has been presented by Whillans (1975). Errors in the balance calculated for the first time interval after a pole has been emplaced are estimated to be only 1 percent or about 0.001 m of snow at Dome C, and thus have been neglected.

The frequency distribution of the accumulation from these measurements is shown in Figures 5 a-e. These histograms indicate the spatial variability of accumulation in the Dome C area both on a small scale (900 m<sup>2</sup> -bamboo forest) and on a larger scale (3600 km<sup>2</sup> -accumulation cross). The time interval over which the measurements were made is indicated in the upper left hand corner of each histogram. All of the figures show a more or less normal distribution about the mean value. However, for the summer accumulation, there appears to be less spatial variability than for the annual accumulation. Based on these data for two years of measurements, summer snow appears to have been deposited and redistributed as a more uniform blanket than snow of other seasons. Perhaps summers are less stormy than other seasons or perhaps the measurement intervals were too short for the full roughness to develop.

An estimate of the surface roughness at Dome C can be obtained by calculating the standard deviation of the relative surface elevations ( $\sigma_s$ ) in the bamboo forest. These data are presented in Table 2.

Table 2. Mean Surfaces Elevations and Standard Deviations of Single Measurements of Stakes in the Bamboo Forest, made during the 1978-79 and 1979-80 Seasons.

<u>DATE</u>	<u>MEAN RELATIVE ELEVATION (m)</u>	<u><math>\sigma_s</math> (m)</u>
December 5, 1978	8.84	0.05
December 23, 1978	8.83	0.06
December 29, 1978	8.84	0.06
January 16, 1979	8.84	0.08
November 30, 1979	9.01	0.07
January 1, 1980	9.02	0.06

The relation between the standard deviation of surface elevation ( $\sigma_s$ ) and the standard deviation of layer thickness ( $\sigma_z$ ) is given in equation 1c on page 21. Taking the minimum value of  $\sigma_s$  in the bamboo forest (0.05 m), the corresponding  $\sigma_z$  (if one assumes that the surface roughness is preserved with depth) would be 0.07 m. This

Table 1. Accumulation rate data.

<u>ACCUMULATION INTERVAL</u>	<u>LAYER THICKNESS</u> (meters of snow)	<u>ACCUMULATION*</u> (kg/m <sup>2</sup> )	<u>ACCUMULATION RATE</u> (kg/m <sup>2</sup> /a)
<u>Bamboo Forest</u>			
Dec. 5, 1978-Nov. 30, 1979 (annual)	0.180 (0.076)**	62 (28)**	62 ( 2.8) <sup>+</sup>
Jan. 16, 1979-Jan. 1, 1980 (annual)	0.170 (0.087)**	59 (31)**	59 ( 3.1) <sup>+</sup>
Dec. 5, 1978-Jan. 16, 1979 (summer)	-0.005 (0.063)**	-1.7 (21)**	-11.9 (14.7) <sup>+</sup>
Nov. 30, 1979-Jan. 1, 1980 (summer)	+0.001 (0.035)**	+0.35 (24)**	+4.2 ( 5.0) <sup>+</sup>
<u>Accumulation Cross</u>			
Dec. 30, 1978-Dec. 30, 1979	0.098 (0.065)**	35 (24)**	35 ( 2.5) <sup>+</sup>
<u>French Stake Measurements</u> (after Petit and others, 1982)			
1 year interval	0.104 (0.075)**	36 (26)**	36 ( 4) <sup>+</sup>
4 year interval	0.440 (0.096)**	152 (32)**	38 ( 1.5) <sup>+</sup>

\*Conversion from snow layer thickness using mean surface density of 345 kg/m<sup>3</sup>

\*\*Standard deviation for single measurement

<sup>+</sup>Standard deviation of the mean

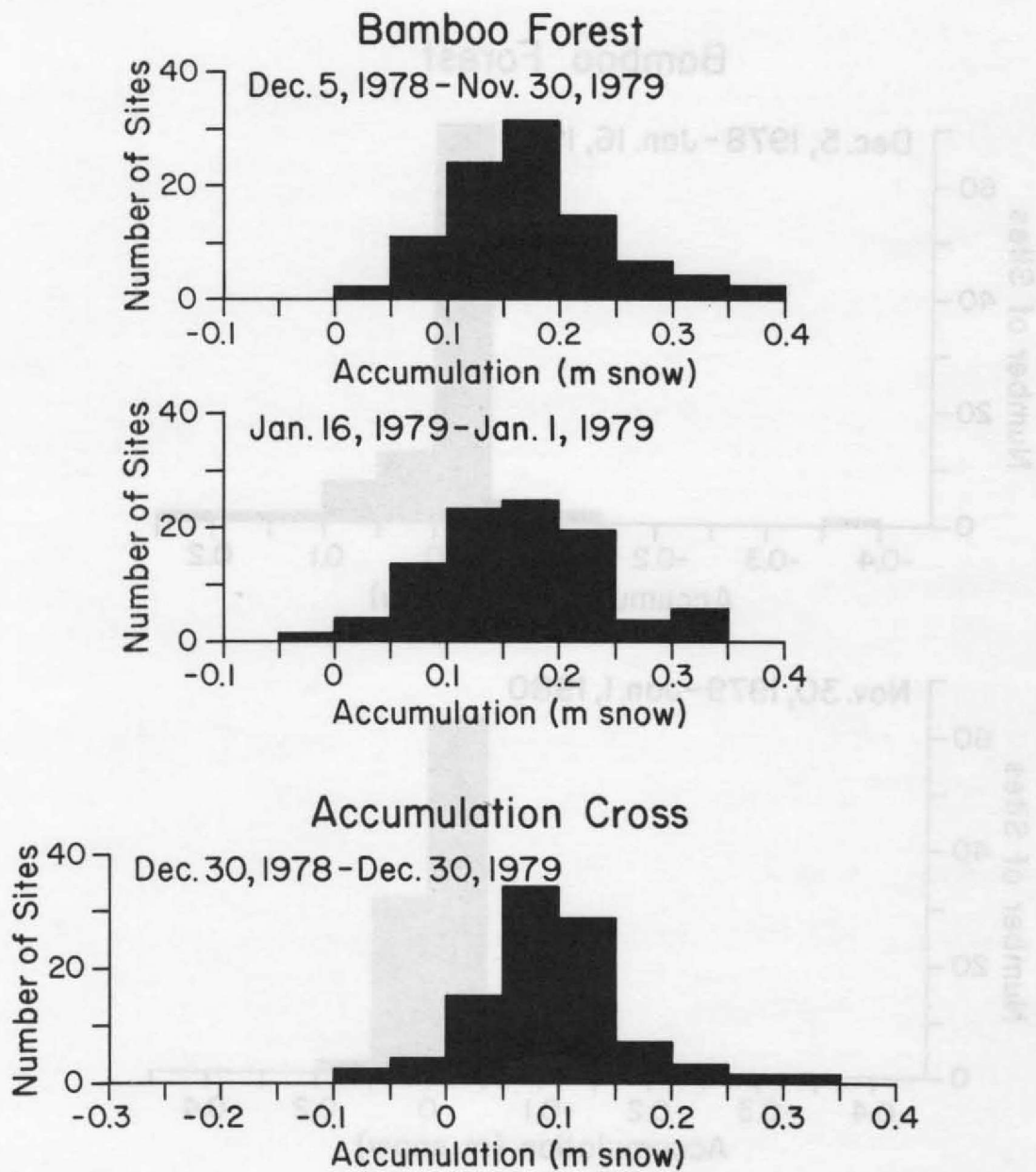


Figure 5. Frequency distribution of accumulation in the bamboo forest (a, b, d, e) and accumulation cross (c) in m of snow vs. number of sites.

## Bamboo Forest

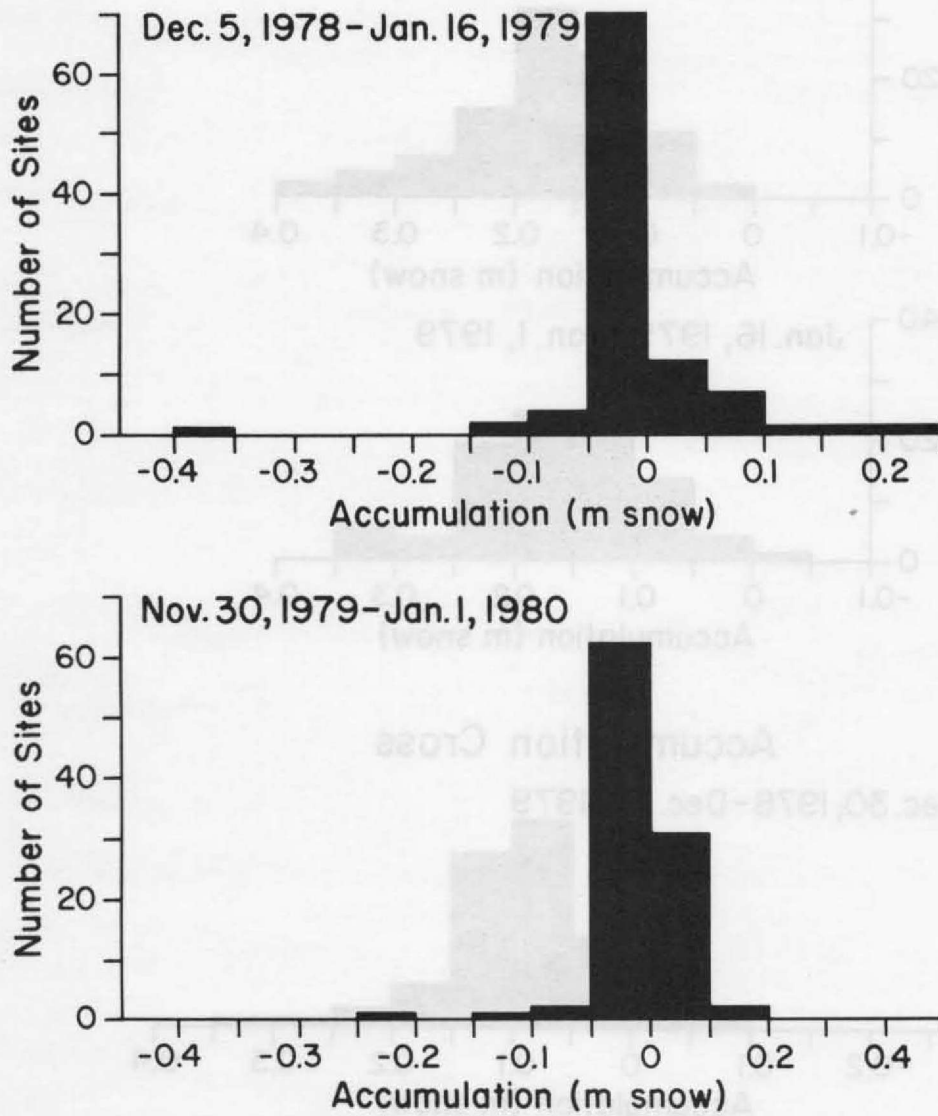


Figure 5. (cont'd)



number is similar to the standard deviation of annual accumulation found in the accumulation cross (0.065 m) and supports the assumption that surface features are preserved during burial. The high value of  $\sigma_s$  (0.08 m) which was measured at the end of the 1978-79 season (see Table 2) is believed to be anomalous due to the surface roughness which was developed at the end of that season (see discussion following and Figures 6 and 8).

A measure of this roughness can also be obtained by considering the variance of layer thickness from gross  $\beta$  radioactivity measurements. A value of  $\sigma_L$  (20 measurements) of 0.095 m was determined for the layer between 1955 and 1965 using data from Petit and others (1982). If one assumes, as a first approximation, that  $\sigma_{s55} = \sigma_{s65}$  and that post-depositional effects did not alter these surfaces, then one can compute  $\sigma_s$  for the 1955 and 1965 surfaces. This calculation is shown below:

$$(1a) \quad \sigma_{L55-65}^2 = \sigma_{s55}^2 + \sigma_{s65}^2$$

$$(1b) \quad \text{if } \sigma_{s55} = \sigma_{s65} ; \text{ then } \sigma_{L55-65}^2 = 2 \sigma_{s55}^2$$

$$(1c) \quad \sigma_{L55-65} = \sqrt{2} \sigma_{s55}$$

$$(1d) \quad \text{if } \sigma_{L55-65} = 0.095\text{m} ; \frac{0.095\text{m}}{\sqrt{2}} = \sigma_{s55}$$

$$(1e) \quad 0.067\text{m} = \sigma_{s55}$$

This number compares well with current estimates of surface roughness from the accumulation cross (see Table 1) and suggests that surface features are preserved upon burial and subsequently with depth.

The mean annual accumulation estimated from the bamboo forest is high compared with the accumulation cross (62 versus 35 kg/m<sup>2</sup>/a) and measurements of other workers (Petit and others, in press). The apparently higher than average accumulation has a number of possible explanations:

- (1) The high accumulation may not be significant at all if one considers the standard deviation on the measurement (28 kg/m<sup>2</sup>/a).
- (2) The bamboo forest may have been established on a site where the topography favored increased accumulation. No major surface

topography was observed at Dome C while in the field; however, very broad, low amplitude undulations if they exist, might not be detected visually. A detailed survey of surface elevations near the Dome C camp should solve this question.

- (3) Figure 6 (see especially profiles from December 29, 1978 and January 16, 1979) shows profiles of the surface along row A in the bamboo forest. A large change occurred between December 23 and December 29, 1978. Small (scale of a few meters) depressions which were developed in this period of stronger-than-average wind ( $> 6$  m/s) may have caused the higher-than-average accumulation, the low areas being preferentially filled in during the following winter.
- (4) The poles, being so closely spaced, may have acted as a barrier to drifting snow, causing enhanced deposition. The importance of this effect is difficult to assess since few stake networks with such closely spaced poles have ever been studied. Until further comparative work is made, this problem remains unsolved.
- (5) There may be regional (scale larger than  $900 \text{ m}^2$ ) patterns in accumulation unrelated to topography. This suggestion may be supported by observations made from the air of large linear features (with a spacing of about 1 km.) on the polar plateau near Dome C and observations made on the ground of greater surface roughness in the grid South and West directions (see Table 3).

In the bamboo forest, no stakes were found to have a zero or negative balance. With this information alone one could conclude that there is no chance of losing a year's accumulation at Dome C. Measurements of the 95 stakes in the accumulation cross provide a lower estimate of annual accumulation ( $35 \text{ kg/m}^2/\text{a}$ ) which may be more representative of the true annual accumulation at Dome C and which shows good agreement with the results of Petit and others, (1982). In the accumulation cross, 6 percent of the bamboo poles show a zero or negative net balance for the year 1978-79. Based on the interpretation of visible stratigraphy (see page 7 and Appendix V), it is estimated that about 6 percent of the annual layers between 1949 and 1979 are missing and according to the microparticle interpretation (see page 11) for a similar interval of time, 5 percent of the annual cycles appear to be missing. These values agree reasonably with estimates by Petit and others, (1982). who suggest that an annual layer is lost 10 percent of the time.

The probability of losing annual layers at Dome C due to erosion of non-deposition is estimated from the proportion of stakes showing either no accumulation or net ablation. This estimate of the probability of losing a year's accumulation was suggested was suggested by Koerner (1971) to be equal to the corresponding probability of a

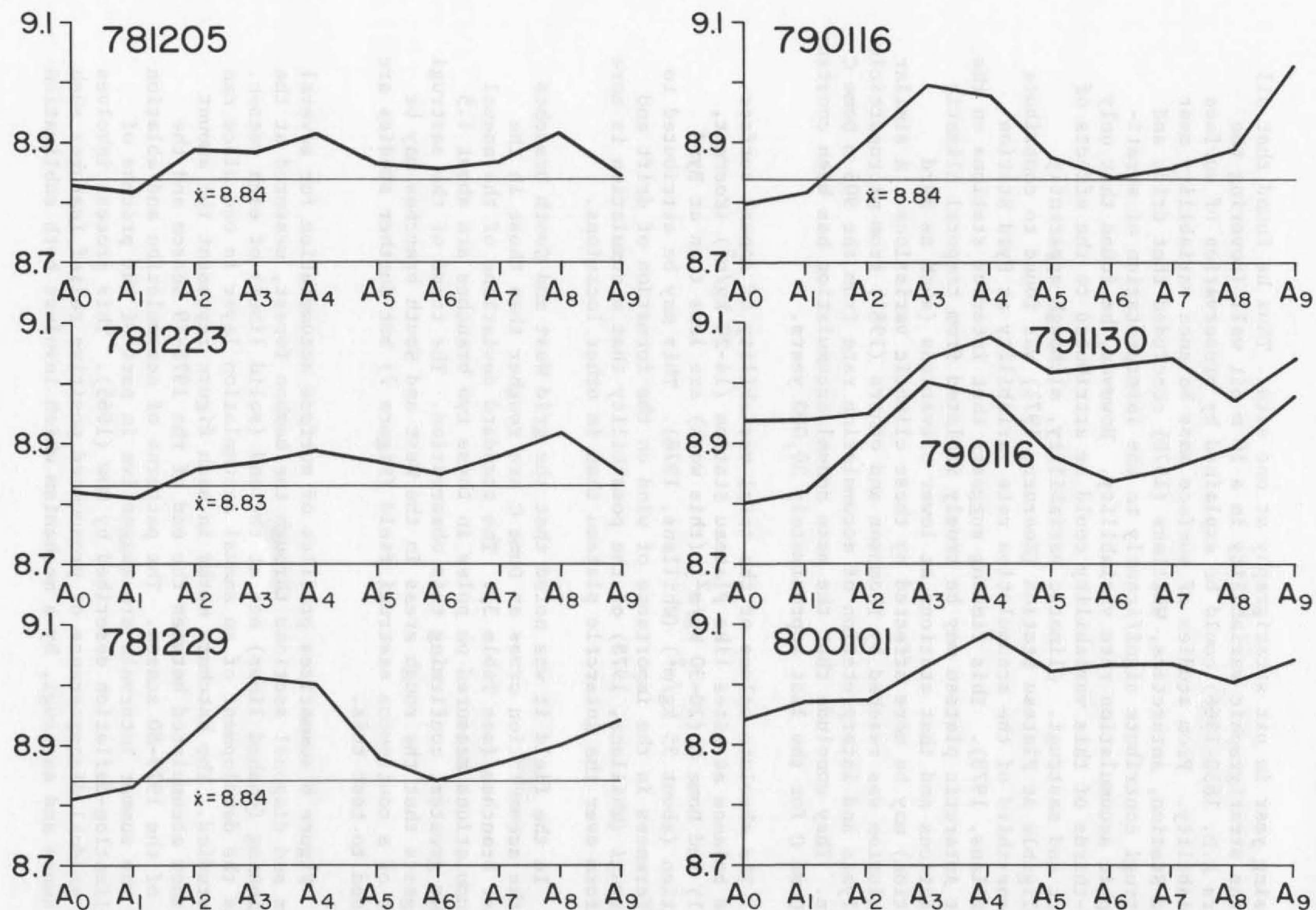


Figure 6. Changes in surface topography in row A<sub>0-9</sub> of the bamboo forest from Dec. 5, 1978 (781205) to Jan. 1, 1980 (800101).

missing year in pit stratigraphy at one site. Thus he found that all of the stratigraphic variability in a 10 m pit wall (covering the years A.D. 1830-1966) could be explained by preservation of surface variability. From studies of surface mass balance variability near Byrd Station, Antarctica, Whillans (1978) concluded that drift and sastrugi contribute significantly to the interpretation of stratigraphic accumulation rate variability. However, he found that only two-thirds of this variability could be attributed to the effects of drift and sastrugi. Climatic variability, although apparently negligible at Plateau Station (Koerner, 1971) was found to contribute to one-third of the accumulation rate variability at Byrd Station (Whillans, 1978). This finding suggests that interior stations on the East Antarctic plateau may be truly isolated from temporal climatic variations and that stations at lower elevations (such as Byrd Station) may be more affected by these climatic variations. A similar conclusion was reached by Thompson and others (1981) from microparticle analysis and interpretation of accumulation rate from the 905 m Dome C core. They conclude that the mean annual accumulation has been constant at Dome C for the last approximately 30,000 years.

The absolute values of the total variability of annual surface mass balance at sites like Plateau Station ( $14\text{--}20\text{ kg/m}^2$ ) (Koerner, 1971) and Dome C ( $20\text{--}30\text{ kg/m}^2$ ) (this work) are less than at Byrd Station (about  $35\text{ kg/m}^2$ ) (Whillans, 1978). This may be attributed to differences in the importance of wind on the formation of drift and sastrugi (Whillans, 1978) or the possibility that accumulation is more uniform over the Antarctic plateau than in other locations.

In the field it was noted that the grid West and South branches of the accumulation cross at Dome C are rougher than those in the other branches (see Table 3). The standard deviations of the annual accumulations measured on poles in these two branches are about 1.5 times greater, confirming this observation. The trend of the sastrugi suggests that the rough areas in the West and South branches may be part of a continuous sastrugi field (Figure 7) but further studies are needed to test this.

Figure 8 summarizes profiles of surface accumulation for several rows and diagonal sections through the bamboo forest, measured at the beginning (dashed lines) and at the end (solid lines) of each season. Thus the development of an annual accumulation layer in one place can be studied. The hatchure marks in each figure represent the amount of snow accumulated between the end of the 1978-79 season and the end of the 1979-80 season. The patterns of accumulation and ablation for the summer intervals are suggestive in part of the process of sublimation-deflation described by Gow (1965). This process involves the gradual disappearance of pronounced positive relief features such as dunes and sastrugi, by a mechanism which involves both sublimation



Table 3.

BRANCH	NOTES	ACCUMULATION RATE* <sup>(°e)</sup> (kg/m <sup>2</sup> )
North	Surface was relatively smooth. Sastrugi not very well developed.	36 (18)
South	Sastrugi poorly developed 56 to pole S- 20. Becomes very rough thereafter, average sastrugi height 0.15-0.18 m.	34 (29)
East	Surface is very smooth and soft, very low relief.	29 (17)
West	Sastrugi small but become very rough at W-20 and continue rough to the end.	32 (23)

\*Conversion from snow layer thickness using mean surface density of 345 kg/m<sup>3</sup>.

and deflation. The high angle of incidence of the sun on these features causes intense radiational heating and subsequent removal of material from within these features. The vapor which is lost recondenses as "scale-like" crystals on the sastrugi flanks and these crystals are then removed during periods of moderate winds and re-distributed over the surface.

This effect although in evidence at Dome C (lowering of high spots and filling in of lows) does not completely remove the large scale (10 m wavelength) surface roughness. This may be a result of lower windspeed at Dome C. Since the minimum pole separation is 3 m, the smallest wavelength feature which can be resolved is about 10 m. On this scale, there are three types of annual accumulation patterns which have been recognized. These are:

- (1) Preservation - Surface relief is preserved from one season to the next (Figure 8 a,d).
- (2) Inversion - Surface relief is inverted so that low areas in one season become highs in the next and vice-versa (Figure 8 e,f).
- (3) Undefined - In this case there is no clear correlation between surface relief in one season and the next (Figure 8 b,c).

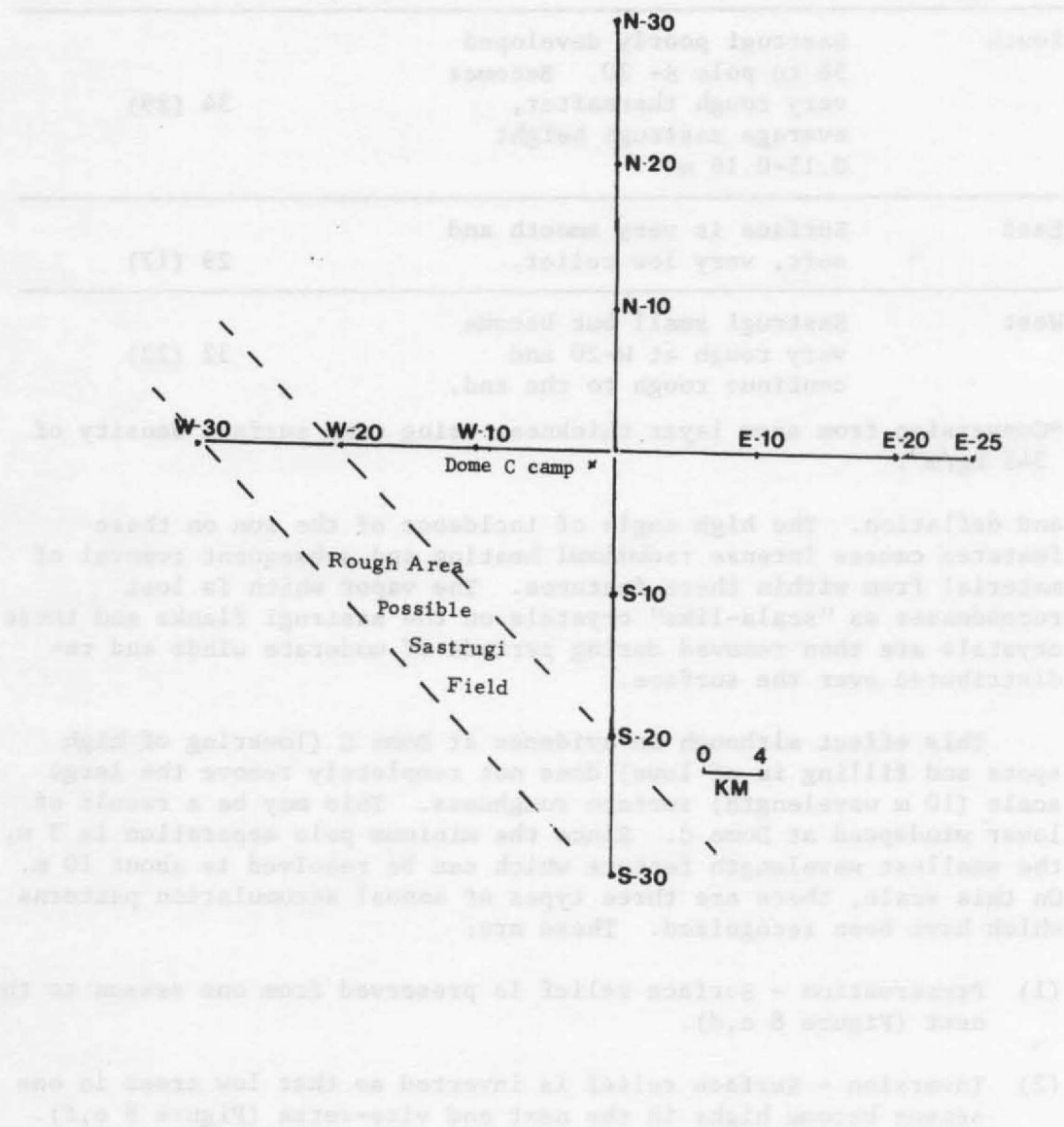


Figure 7. Sketch map of the accumulation cross, showing location of rough area and possible sastrugi field with respect to the Dome C camp.



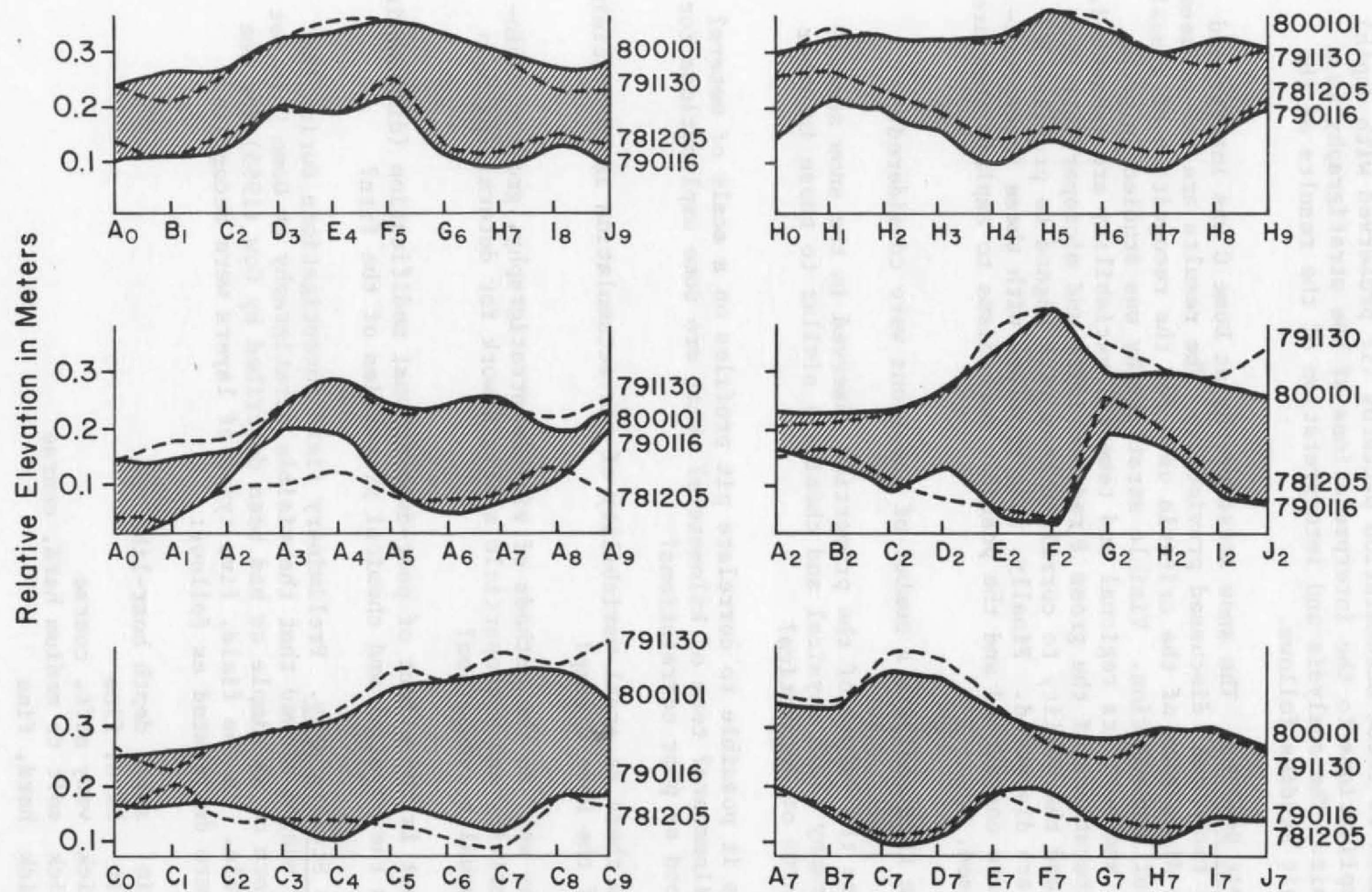


Figure 8. Profiles of the relative surface elevation in the bamboo forest, showing changes in surface topography from the beginning of the austral summer 1978/79 to the end of the austral summer 1979/80.

Each of these accumulation patterns (if preserved with depth) has implications to the interpretations of the stratigraphy in a snow pit. The analysis and interpretation of the results of the snow pit studies follows.

Snow Pit Studies. The snow stratigraphy at Dome C was interpreted by the techniques discussed previously. The results are now presented with a discussion of the criteria used for the recognition of annual units of accumulation. Visible stratigraphy was studied in great detail and both its regional and temporal variability are presented. Interpretations of the gross  $\beta$  radioactivity and microparticle profiles and the ability to correlate them with regard to profiles B and C are discussed. Finally, some problems with these interpretations are considered and the possible mechanisms to explain them are discussed.

In this analysis a number of questions were considered:

- (1) Are the values of the properties observed in the snow stratigraphy (both physical and chemical) similar to those in other parts of Antarctica?
- (2) Is it possible to correlate pit profiles on a scale of meters? kilometers? tens of kilometers? What are some explanations for good or poor correlations?
- (3) Is there an areal variability of the accumulation in the vicinity of the Dome C camp?
- (4) How well do the methods of visible stratigraphy, gross  $\beta$  Radioactivity and microparticle analysis work for determining mean annual accumulation?
- (5) What is the effect of post-depositional modification (diagenesis) on the physical and chemical properties of the firn?

Visible Stratigraphy. Preliminary field investigations during the 1978-79 season showed that the visible stratigraphy at Dome C is not as uniform or as simple as had been described by Gow (1965) for the South Pole. In the field, five types of layers were recognized. These were designated as follows:

- (a) thin soft, depth hoar-like
- (b) thin hard, fine
- (c) thick very soft, coarse
- (d) thick soft to medium hard, coarse
- (e) thick hard, fine

Although the non uniformity and discontinuous nature of the snow strata in the Dome C pits at first offered little chance of dating

the individual layers, in general the stratigraphic dating (as described below) appears to be fairly accurate. The results of these studies and specific examples of these layers are described below and are presented in Figures 9-13 and in Appendix 2.

Thinning, thickening, and occasionally the complete disappearance of some layers is not uncommon in the Dome C pits (see for example in Figure 9-Profile A at 2.10 and 2.30 m and Figure 13-Profile E at 0.90 m). These patterns probably mark the sloping surfaces of buried depositional features which have been truncated at the edge by new accumulation and appear as truncated layers due to the orientation of the pit wall with respect to the features. The layers which mark these features are usually the thin hard crusts, which are probably late-summer surfaces.

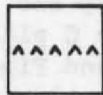
The layers which are designated as thick, soft, to medium-hard coarse grained firn are due to snow deposition from autumn through spring and constitute the bulk of the accumulation. These layers were recognized in the field as being inhomogeneous, which may be because these layers were deposited and subsequently modified under a wide variety of conditions.

Notable in the visible stratigraphy at Dome C are the low density depth-hoar-like layers. A possible origin for these layers is described in section 5, based on considerations of diagenetic processes.

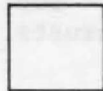
These low density layers were seen in all the pits (Figures 9-13), usually below the thin, hard crusts, but also along (see Figure 13-Profile E at 0.50 m) or with a crust below (see Figure 11-Profile C at 0.60 m). Another point of interest is that the low density layers were rarely found above 0.30 m, and were a persistent feature down to the bottom of the pits at 3.00 m. They cannot be used however to define annual layers, as was done by Gow (1965) at the South Pole, since they do not appear to be annual features and even when they do occur, they are not always laterally continuous.

In a few cases, especially thick, hard layers are found associated with particularly well developed low-density layers (see for example Figure 9-Profile A at 0.20-0.50 m and 0.90-1.10 m and in Figure 13-Profile E at 1.10-1.25 m). These thick, hard layers are similar to the thin crusts described above but are thicker and may be the product of long-term exposure to near-surface conditions (wind action, radiation, temperature gradients, and associated vapor transfer) as a result of a hiatus in deposition or erosion (Gow, 1965).

## LEGEND



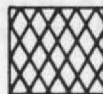
Low  
Density  
Layer



Very  
Soft



Soft



Medium  
Hard



Hard

Figures 9-13. Composite of 3-meter pit studies showing visible stratigraphy, gross  $\beta$  radioactivity and microparticle profiles.



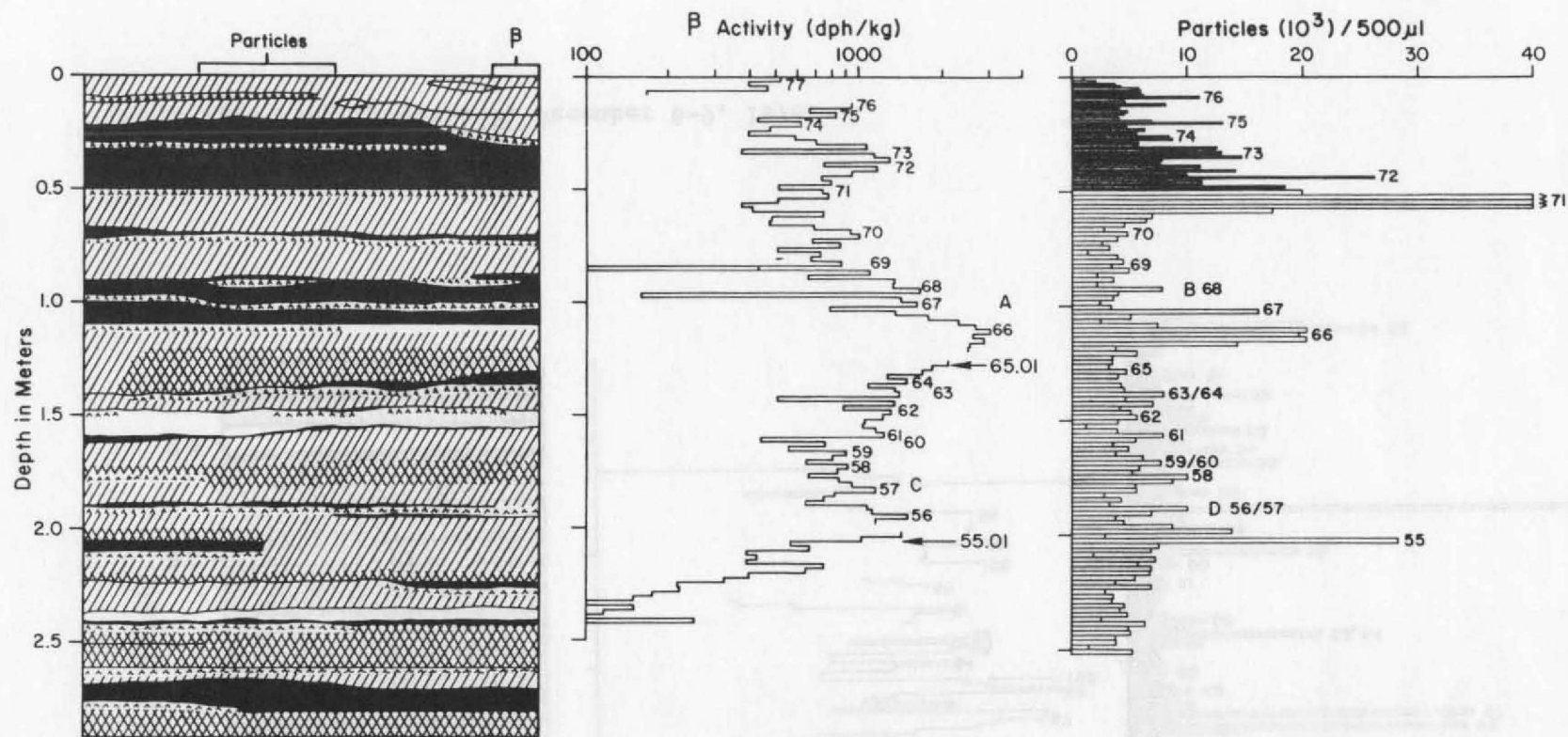


Figure 9. Profile A, December 2-5, 1978.



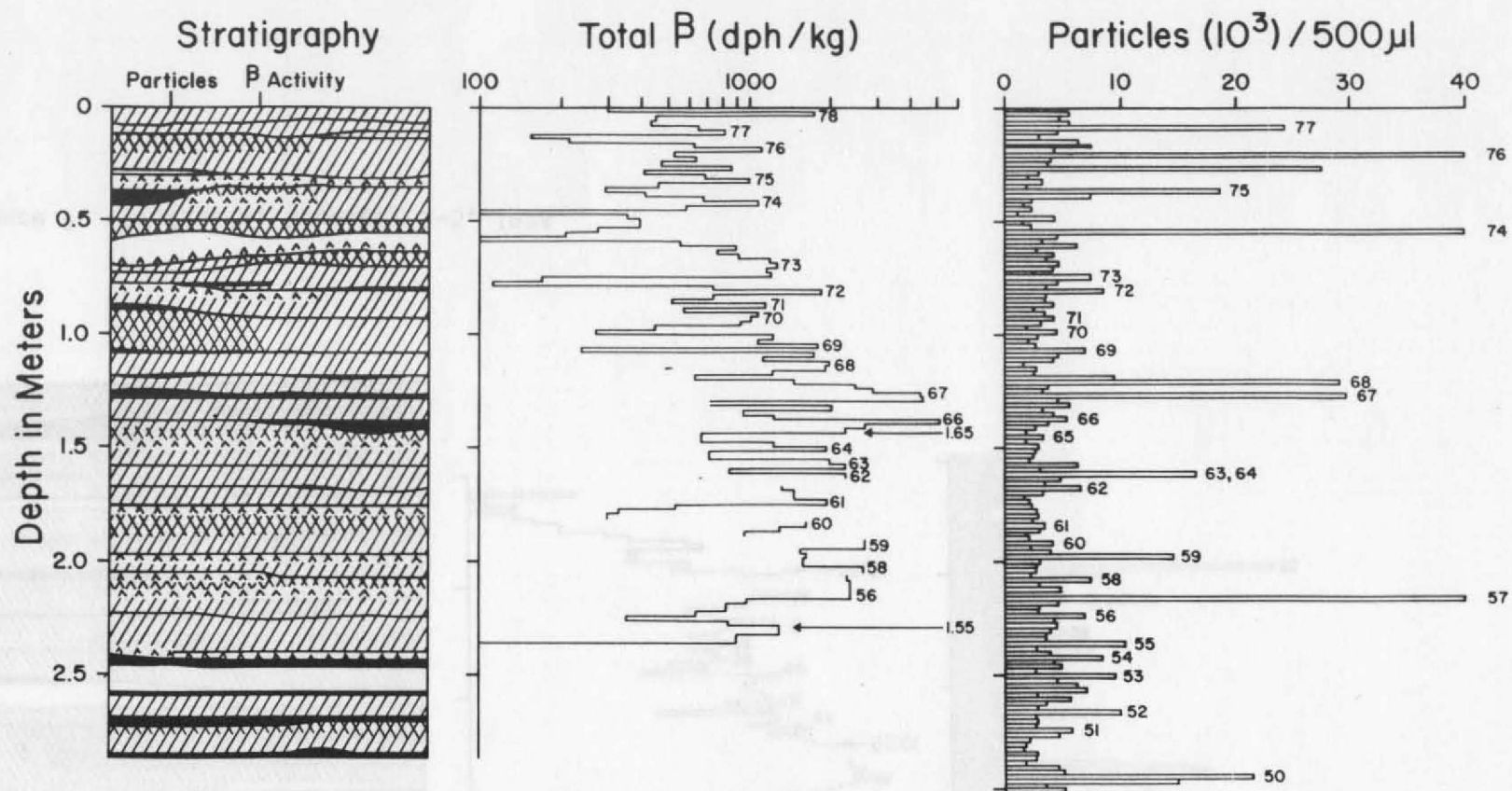


Figure 10. Profile B, December 6-9, 1978.

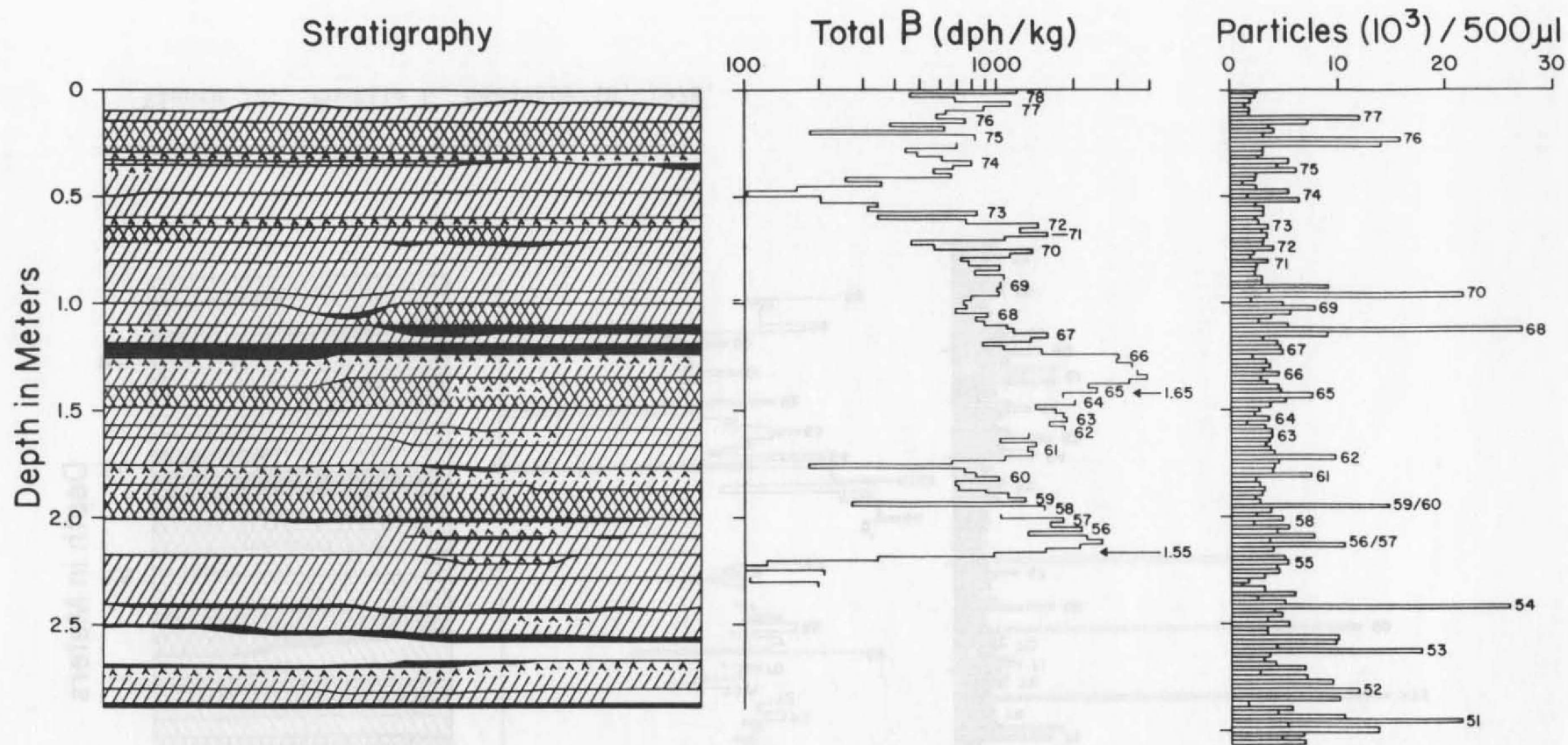


Figure 11. Profile C, December 6-9, 1978.

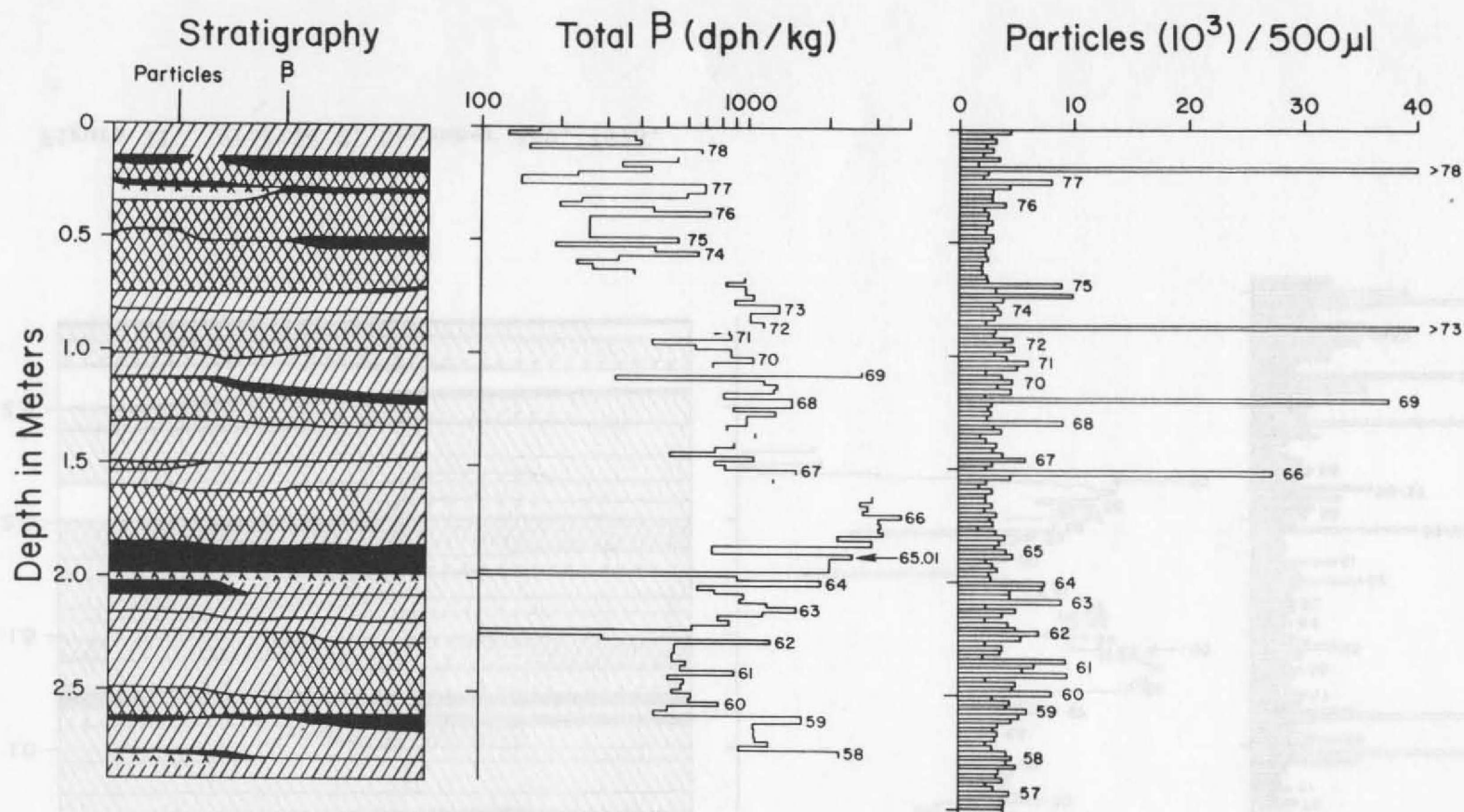


Figure 12. Profile D, December 18, 1978.

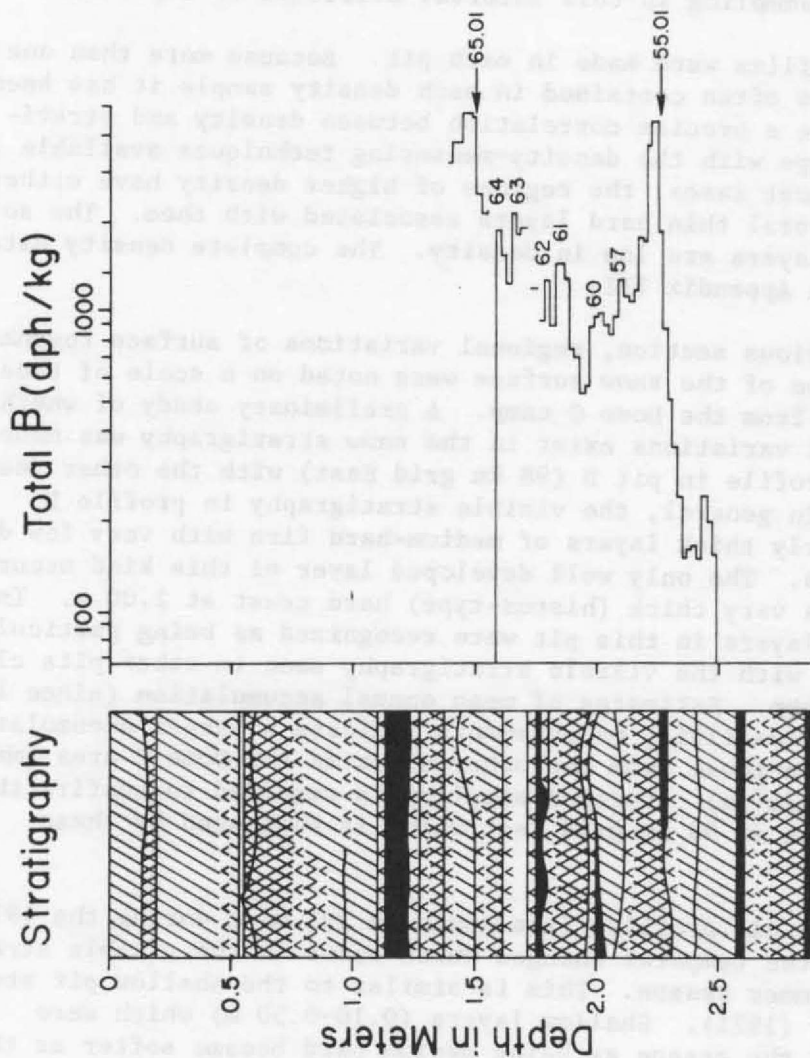


Figure 13. Profile E, January 1-3, 1979.

Another type of layer noted in the Dome C pit studies are the so-called "very soft layers" (see Figure 9 at 1.50-1.60 m and Figure 10 at 2.50-2.60 m). These are fairly thick layers, described in the field as being very soft with a friable, sandy texture, which may be similar to the "snow quicksand" layers described by Shumskii (1964, p. 259). These layers are particularly common between 1.50-3.00 m and often made snow sampling in this interval difficult or impossible.

Density profiles were made in each pit. Because more than one type of layer was often contained in each density sample it has been difficult to make a precise correlation between density and stratigraphic layer type with the density-measuring techniques available in the field. In most cases, the regions of higher density have either one thick or several thin hard layers associated with them. The soft, coarse-grained layers are low in density. The complete density data are presented in Appendix III.

In the previous section, regional variations of surface roughness and the condition of the snow surface were noted on a scale of tens of kilometers away from the Dome C camp. A preliminary study of whether similar regional variations exist in the snow stratigraphy was made by comparing the profile in pit D (98 km grid East) with the other deep pit profiles. In general, the visible stratigraphy in profile D consists of fairly thick layers of medium-hard firn with very few depth-hoar-like layers. The only well developed layer of this kind occurs directly below a very thick (hiatus-type) hard crust at 2.00 m. In the field, the layers in this pit were recognized as being particularly thick, compared with the visible stratigraphy seen in other pits closer to the Dome C camp. Estimates of mean annual accumulation (since 1965) from gross  $\beta$  radioactivity measurements indicate a larger accumulation ( $52 \text{ kg/m}^2/\text{a}$ ) than those from the other sites in the Dome C area (mean value of  $37.5 \text{ kg/m}^2/\text{a}$ ). Further sampling is required to confirm the high accumulation at 98 km grid East which is suggested by these measurements.

The shallow pit profiles (see Appendix IV) made during the 1978-79 season show the temporal changes which occur in the visible stratigraphy over a summer season. This is similar to the shallow pit study done by Koerner (1971). Shallow layers (0.10-0.50 m) which were mapped early in the season as being medium hard became softer as the summer progressed. However, the soft new snow which was present close to the surface (0.00-0.10 m) at the beginning of the season developed a thin hard crust. More detailed investigations are required to confirm these observations.

Further studies on the visible stratigraphy at Dome C were made in a series of 2- and 3-meter pits in 1979-80 by John Bolzan and Ron Coffman. Samples were again collected for microparticle, gross  $\beta$  radioactivity and  $\delta^{18}\text{O}$  studies. These laboratory results are not yet



available, but the following comments may be made on the visible stratigraphy.

Similar units of visible stratigraphy are recognized as in 1978-79 and a very good positive correlation between density and hardness was observed. Also, a relation was observed between surface conditions and the visible layering in the pits. In the grid East direction, the surface was very soft and smooth and the pit at 30 km grid East showed the most regular stratigraphy of any pit examined, with the fewest layers of hard firn. In contrast, well developed sastrugi and hard surface crusts were observed in the grid West direction and the pit at 49 km grid West had many hard undulating surfaces, indicative of buried sastrugi.

A pit which was profiled early in the 1979-80 season (December 5, 1979) near the Dome C camp was re-profiled at the end of the season (December 30, 1979), by excavating back into the original pit wall to look at temporal changes during the summer. Based on these observations, there was an overall hardening of the soft near surface (0.00-0.10 m) firn, with a corresponding increase in density. Some of the deeper layers which were medium hard early in the season had softened by the end of the season. In some layers (1.25 m, 1.50 m, 1.85 m), hoar like crystals which were recognized on December 5 were no longer present on December 30 and only thin crusts were found in their place. In other cases, new hoar-like crystals were found where there had been none at the first observation (0.35-0.45 m, 1.80 m). These observations are consistent with temporal variations seen in the 1978-79 shallow pits. In further studies an attempt should be made to quantify these changes.

Definition of Annual Units. The similarities of the Dome C snow pit observations with those described by Koerner (1971) suggests that visible stratigraphy might be used to identify annual units of accumulation. Uncertainties in the accuracy of variations in concentrations of microparticles or gross  $\beta$  activity to define annual layers led us to use those parameters primarily to investigate whether any correlation exists between high concentrations of microparticles (or  $\beta$  radioactivity) and visible layer type, and only secondarily for dating.

According to the criteria described earlier (p. 12-15), the January 1955 and January 1965 levels in each pit were identified. Based on the visible stratigraphy, several types of annual units were defined. Soft or medium-hard, thick layers (believed to represent the accumulation during the interval from autumn to spring) with a thin crust (late summer formed) above (with or without depth hoar [formed in autumn] below the crust) is found to be the most common annual unit. Thick hard layers (usually with depth hoar below) were used to define annual units. When the depth hoar was especially thick, these layers were defined as having formed during a two year interval. This interpretation was based on Gow's (1965) observations of hiatus-

type depth hoar and associated thick crusts which formed at the surface during intervals of non-accumulation. A complete stratigraphic interpretation for each pit, using these criteria, can be found in Appendix V.

Peaks in the microparticle profiles were identified independently of the visible stratigraphy, according to the criteria outlined earlier (p. 11-15). Dating of the peaks however, was made in conjunction with the maps of visible stratigraphy. Using the visible stratigraphy as a guide, the number of missing peaks in a given interval (January 1955-January 1965, for example) can be estimated. Thus in Figures 9-13, an indication such as 59/60 on a microparticle peak means that either the 1959 or 1960 peak is missing or that they have been combined into one peak. In this way, the number of missing years and thus the probability (5 percent) of losing a layer of microparticles can be estimated.

Using the visible stratigraphy again as a framework, peaks in the gross  $\beta$  radioactivity profiles were dated. This is done in such a way that the peaks coincide as closely as possible with the age determination from the visible stratigraphy. In most cases, one  $\beta$ -radioactivity peak was found in each visible stratigraphy layer. The non-correspondence between  $\beta$  and microparticle peaks is believed to be a function of many things, including the non-horizontality of deposited layers, the natural variability in the arrival time of the impurities and perhaps their mobility during burial. The interpretation of the  $\beta$ -radioactivity and microparticle profiles and their correlation are discussed further in the following sections.

Gross  $\beta$  Radioactivity. In this section, the gross  $\beta$  radioactivity profiles from the 3-m pits of the 1978-79 Dome C season are described. The usefulness of this method for the determination of accumulation rate is discussed and specific examples from the pit profiles are given. Finally, the possibility of using gross  $\beta$  radioactivity for detecting annual stratification is discussed. The gross  $\beta$  radioactivity profiles are used to define two time horizons in each snow pit section (January 1955, January 1965) which are used in the determination of mean annual accumulation for various time intervals (1955-79, 1965-79, 1955-65). This information is presented in Table 4.

Recent studies (Pourchet and others, 1983; Petit and others, 1982) on accumulation rate at Dome C have indicated the possibility of a 30 percent increase in accumulation in the period since 1965 when compared with the interval 1955-65. Results presented here support the apparent increase observed by these authors; however the exact cause of this increase is not known. Some possibilities are discussed below.

Measurement

s from 3-

It is possible that there was a true increase in the amount of precipitation during this interval. Pourchet and others, (1983), based on stable isotope and direct temperature measurements, indicate that in the last two decades there has been a slight increase ( $0.2^{\circ}\text{C}$  per decade) in the average temperature. Calculation by these authors however, suggest that a temperature increase of  $4^{\circ}\text{C}$  would be required to increase the quantity of water available for precipitation by 30 percent. Thus, this alone is not a viable explanation.

Another suggestion discussed in more detail in the following chapter, is that processes of metamorphism have contributed to a mass transfer of water vapor from the lower to upper layers. Since the layers between 1955 and 1965 have had ten additional years for this diagenesis to occur (as compared to the layers in the interval 1965-79) it seems reasonable to suppose that during this ten-year interval a certain amount of material could have been transferred out of the lower layers of firn. The possible mechanisms which could produce such a mass transfer are discussed in the next chapter.

At some sites in Antarctica gross  $\beta$  radioactivity (Lambert and others, 1977) can be used to detect annual stratification because of a seasonal peak in atmospheric radioactivity, (Lockhart and others, 1966). In our five 3-meter profiles (Figures 9-13), there is some indication of an annual peak in  $\beta$  activity. Suggested ages for these peaks are marked in parentheses on the figures. These peaks are not defined well enough to allow one to count annual layers using the  $\beta$  profiles alone when studied in conjunction with the profiles of visible stratigraphy, but one can pick out annual peaks of activity with a fair amount of accuracy. In addition, layers which appear homogeneous with regard to the visible stratigraphy and are thought to contain more than one year's accumulation because of their thickness and inhomogeneity often show two distinct  $\beta$  peaks, suggesting the existence of two annual layers (see for example in Figure 9 from 0.28-0.50 m and 0.88-1.00 m).

The peaks of  $\beta$  activity are found most often just below and rarely just above the thin hard crusts in the thick, soft-medium hard, coarse grained layers. The hard crusts, on the other hand, are usually low in activity. This is believed to be a function of the arrival time of the radioactivity and how one interprets the visible stratigraphic layers. The soft layers are interpreted as accumulation between autumn and spring and the thin hard crusts are interpreted as late summer features. A  $\beta$  concentration peak just below a thin hard crust then, is consistent with the spring to early summer arrival times predicted from atmospheric studies (Lockhart and others, 1966).

As described in the previous section, in most cases the depth hoar-like layers are generally not continuous enough laterally to be used as stratigraphic markers. However, in a few cases (see Figure 9 at 2.10 m, Figure 10 at 1.5 m and 2.4 m and Figure 12 at 2.0 m) the 1955 and 1965  $\beta$  horizons are found to correlate with well developed



crusts and depth hoar-like layers. These stratigraphic layers seem to be quite extensive in the Dome C area as a similar correlation has been noted by Pourchet (1979) for the layers occurring at the 1955 level at Dome C.

It seems possible to distinguish annual peaks in  $\beta$  activity if one has a detailed profile of the visible stratigraphy for comparison. The best defined profiles occur in the areas which have the highest snow accumulation rates (profiles B and D). This is because more samples were obtained per annual layer. In other regions of Antarctica where the accumulation rate is higher, particularly well-developed annual cycles of activity are often observed (Lambert and others, 1977; Jouzel and others, 1979). Better resolution in the  $\beta$ -radioactivity profiles should be possible at a place such as Dome C if samples are taken every centimeter rather than every two centimeters. This would give more samples per year and should provide better peak resolution. However, if one is interested simply in the determination of the mean accumulation rate, a sampling every 0.02 m is sufficient.

Microparticles. Using the criteria established at p. 11-15, microparticle peaks are identified in the four profiles at Dome C. These profiles are presented in Figures 9-12 and in Appendix II. Information from the visible stratigraphy and gross  $\beta$  radioactivity profiles help with the recognition of layers where particle peaks are absent or where two annual layers are apparently combined so that an estimate of the proportion of cases where an annual accumulation layers that are "lost" is possible. The microparticle profiles are used not only for the determination of annual layer thickness (see Appendix V) but also for assessing the relationship between microparticle peaks, visible stratigraphy (including density and hardness), and the gross  $\beta$  radioactivity profiles.

The mean background levels of microparticles  $\geq 0.63 \mu\text{m}$  (which is equivalent to the cleanest 30 percent of all samples in each snow pit section) are given in Table 5. In addition, the mean background level of particles in the size range 0.63-0.80  $\mu\text{m}$  and the upper and lower limits for the range of background as defined earlier are given for the four profiles of this study. These values agree well with mean background levels of microparticles measured by Petit (pers. comm.) (Figure 14) and indicate that sample contamination is not important. A direct comparison between units used in this study (number of particles  $\geq 0.63 \mu\text{m}/500 \mu\text{l}$ ) and those of Petit (number of particles  $\geq 0.80 \mu\text{m}/1 \text{ g}$ ) is possible because the particle size distribution is logarithmic. In most samples there are approximately twice as many particles  $\geq 0.63 \mu\text{m}$  as there are particles  $\geq 0.80 \mu\text{m}$ , so that the numbers can be directly compared to particle concentrations on the basis of 500  $\mu\text{l}$  versus 1 g. Thus the numbers quoted here can be directly compared with those of Petit. Mean background levels of this study are also similar to those of Thompson (pers. comm.) from



<u>Site Range</u>	<u>Pit sections</u> (cleanest 30%)/500 $\mu\ell$				<u>Thompson (shallow cores)</u> (cleanest 10%)/500 $\mu\ell$	<u>Petit</u> (shallow pits)/1 g
	A	B	C	D		
$\geq 0.63 \mu\text{m}$ [ /500 $\mu\ell$ ]	7687	5870	5490	5135	6000	
$\geq 0.80 \mu\text{m}$ [ / 1 g ]						6000 $\pm$ 2500
0.63-0.80 $\mu\text{m}$	2967	2319	2182	2189		
30% of (0.63-0.80 $\mu\text{m}$ )	890	696	655	657		
Threshold (upper limit for background + 30%)	3857	3015	2836	2846		
Lower limit for background - 30%	2077	1623	1527	1532		

Table 5. Microparticle data showing values of the cleanest 30% of all samples in each pit and the lower and upper limit of the background range as defined in the text. Comparable values of the mean background of microparticles from a shallow core (Thompson, pers. comm.) and from shallow pits (Petit, pers. comm.) from Dome C are also given.

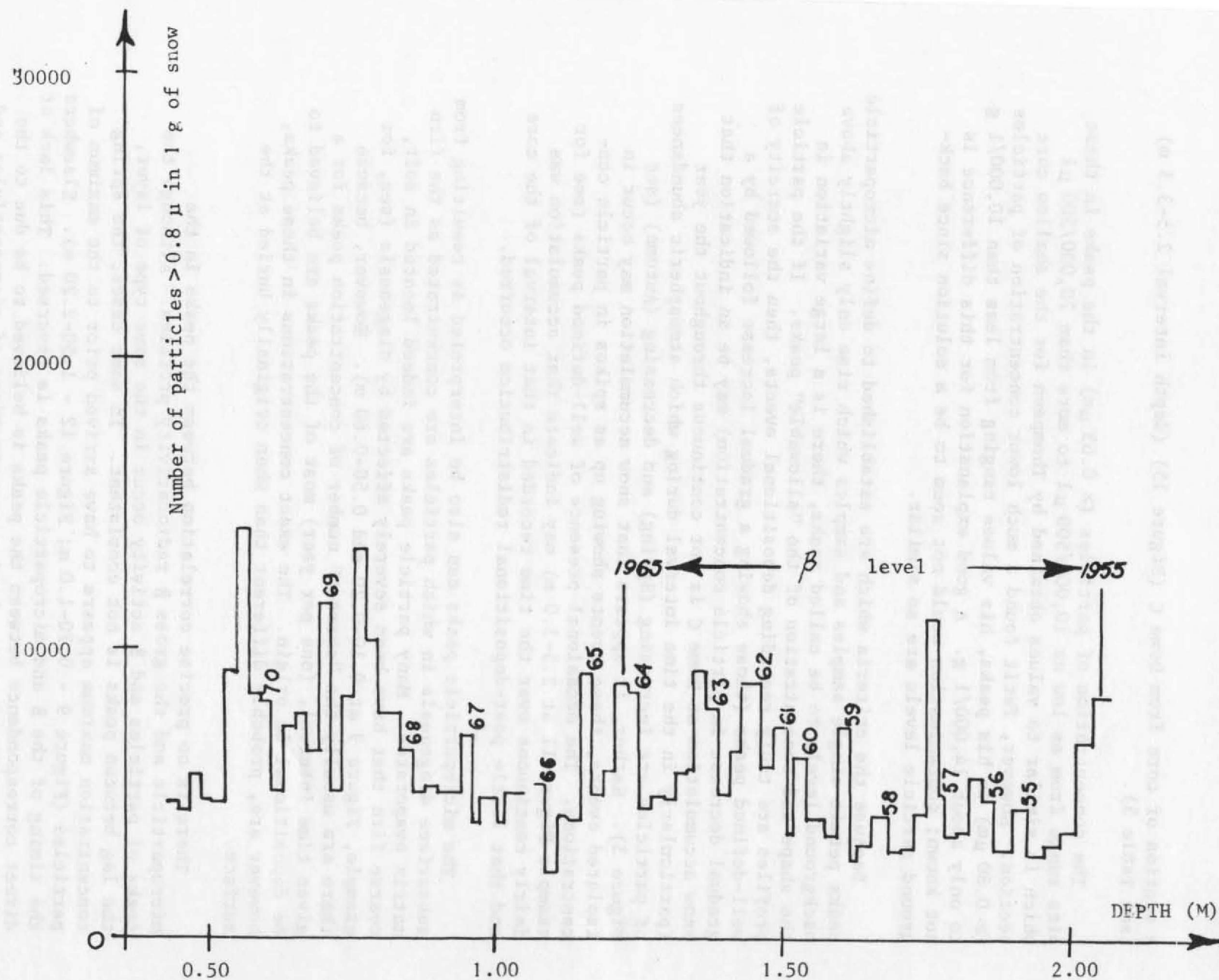


Figure 14. Microparticle profile from shallow pit at Dome C, 1975.  
(J.R. Petit) (From Thompson and others, 1981).

a section of core from Dome C (Figure 15) (depth interval 2.5-3.3 m) (see Table 5).

The concentration of particles ( $\geq 0.63 \mu\text{m}$ ) in the peaks in these pits range from as low as 10,000/500  $\mu\text{l}$  to more than 70,000/500  $\mu\text{l}$  which is similar to values obtained by Thompson for the shallow core section. However, Petit found a much lower concentration of particles ( $\geq 0.80 \mu\text{m}$ ) in his peaks, his values ranging from less than 10,000/l g to only about 14,000/l g. A good explanation for this difference is not known; contamination would not seem to be a solution since background particle levels are so similar.

Because the criteria which are established to define microparticle peaks permit single samples and samples which rise only slightly above background levels to be called peaks, there is a large variation in the shape and concentration of the "allowable" peaks. If the particle profiles are truly recording depositional events, then the scarcity of well-defined peaks (those showing a gradual increase followed by a gradual decrease in particle concentration) may be an indication that snow accumulation at Dome C is not continuous throughout the year (particularly in the time interval during which atmospheric abundances of particles are increasing (Spring) and decreasing (Autumn) (see Figure 3). Rather, it appears that snow accumulation may occur in isolated events, these events showing up as spikes in particle concentrations. The occasional presence of well-defined peaks (see for example Figure 11 at 2.5-3.0 m) may indicate that accumulation was fairly continuous over the time recorded in that interval of the core and that little post-depositional redistribution occurred.

The microparticle peaks can also be interpreted as resulting from subsurface diagenesis in which particles are concentrated as the firn matrix evaporates. Many particle peaks are indeed located in soft, coarse firn that have been severely affected by diagenesis (see, for example, Figure 9 at 0.10-0.20 and 0.50-0.60 m). However, because there are usually the "correct" number of concentration peaks for a given time interval, (one per year) most of the peaks are believed to be depositional in origin. The exact concentrations in these peaks, however are, probably different than when originally buried at the surface.

There is no precise correlation between the peaks in the microparticle and the gross  $\beta$  radiocativity profiles. Although the peaks of particles and  $\beta$  activity occur in the same type of layer, the lag between peaks is not consistent. In some cases, the spring concentration maximum appears to have arrived prior to the maximum of particles (Figure 9 - 0.70-1.0 m; Figure 12 - 1.50-2.20 m). Elsewhere the timing of the  $\beta$  and microparticle peaks is reversed. This lack of direct correspondence between the peaks is believed to be due to the complex variation in atmospheric concentrations of microparticles and

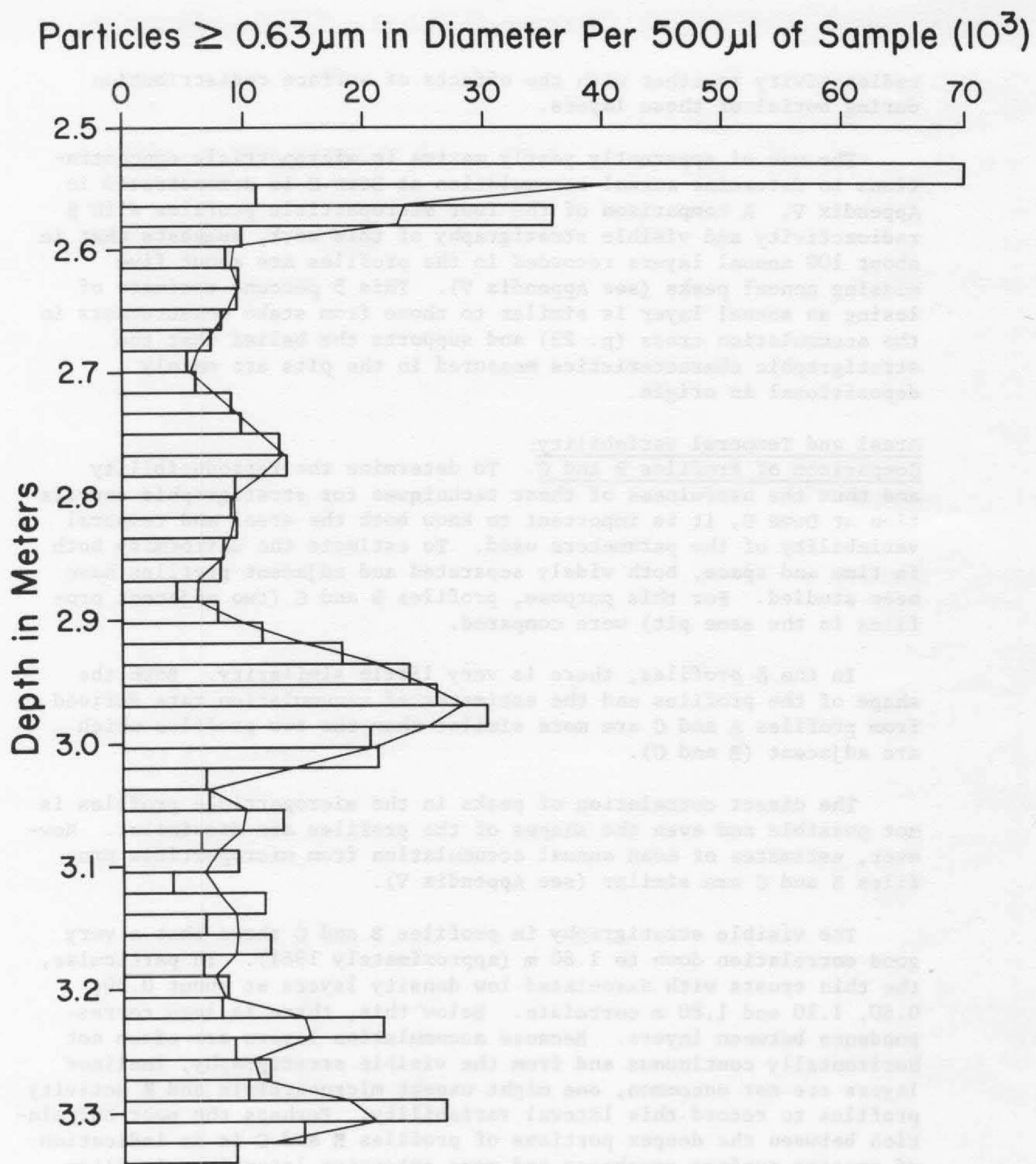


Figure 15. Microparticle profile from shallow core section, Dome C.  
(Thompson, pers. comm.)



radioactivity together with the effects of surface redistribution during burial of these layers.

The use of apparently yearly maxima in microparticle concentrations to determine annual accumulation at Dome C is demonstrated in Appendix V. A comparison of the four microparticle profiles with  $\beta$  radioactivity and visible stratigraphy of this work, suggests that in about 100 annual layers recorded in the profiles are about five missing annual peaks (see Appendix V). This 5 percent estimate of losing an annual layer is similar to those from stake measurements in the accumulation cross (p. 22) and supports the belief that the stratigraphic characteristics measured in the pits are mainly depositional in origin.

Areal and Temporal Variability:

Comparison of Profiles B and C. To determine the reproducibility and thus the usefulness of these techniques for stratigraphic correlation at Dome C, it is important to know both the areal and temporal variability of the parameters used. To estimate the uniformity both in time and space, both widely separated and adjacent profiles have been studied. For this purpose, profiles B and C (two adjacent profiles in the same pit) were compared.

In the  $\beta$  profiles, there is very little similarity. Both the shape of the profiles and the estimates of accumulation rate derived from profiles A and C are more similar than the two profiles which are adjacent (B and C).

The direct correlation of peaks in the microparticle profiles is not possible and even the shapes of the profiles are dissimilar. However, estimates of mean annual accumulation from microparticle profiles B and C are similar (see Appendix V).

The visible stratigraphy in profiles B and C shows that a very good correlation down to 1.80 m (approximately 1961). In particular, the thin crusts with associated low density layers at about 0.30, 0.60, 1.10 and 1.80 m correlate. Below this, there is less correspondence between layers. Because accumulation layers are often not horizontally continuous and from the visible stratigraphy, inclined layers are not uncommon, one might expect microparticle and  $\beta$  activity profiles to record this lateral variability. Perhaps the poor correlation between the deeper portions of profiles B and C is an indication of greater surface roughness and more extensive lateral variability prior to about 1961. This is illustrated schematically in Figure 16.

The surface roughness needed to explain such a variability is comparable with the surface roughness in the bamboo forest, namely surface undulations with wavelengths between 10 and 20 meters and amplitudes between 0.10 and 0.20 m. Figures 8b and 8e show that



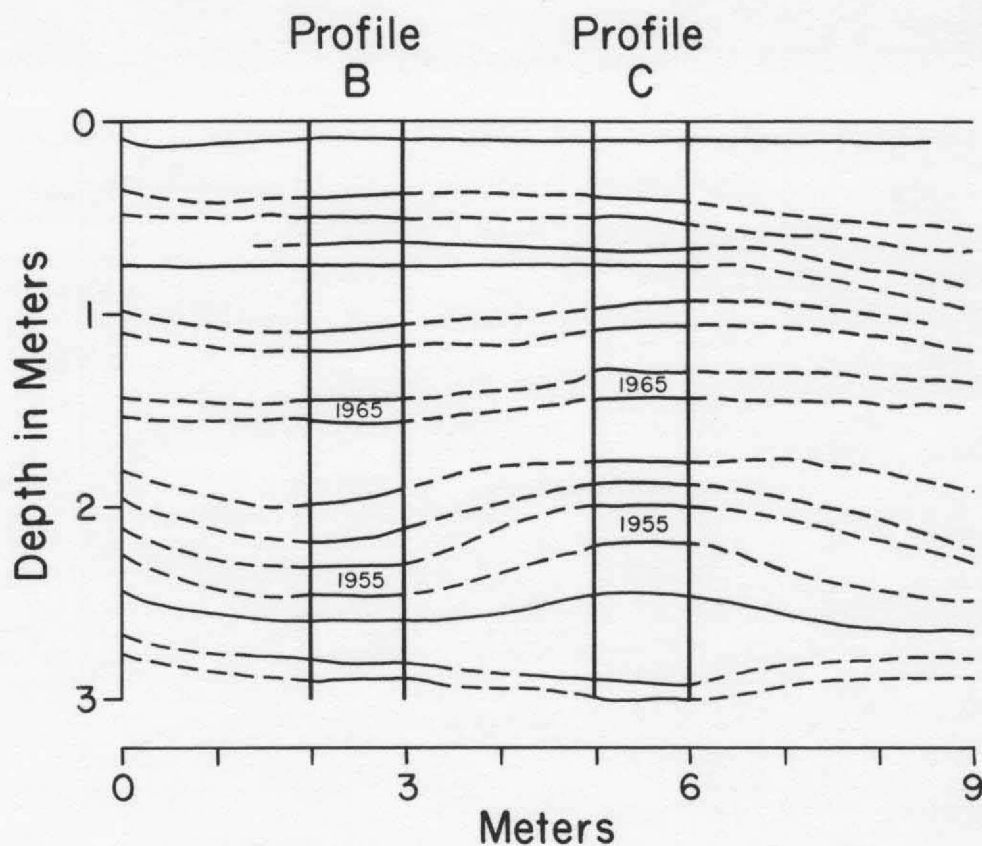


Figure 16. Schematic representation of the stratigraphy in Profiles B and C showing the preservation of undulating surfaces.

annual layers can vary in thickness by as much as 0.20 m in less than 6 m horizontally. The lesser roughness which is preserved in the upper part of profiles B and C has the same magnitude as the majority of the surface at Dome C and is believed to be more representative of normal conditions there.

Detailed comparison of the physical properties of coeval stratigraphic layers (as determined from the visible stratigraphy), in snow pits several kilometers apart reveal in some cases annual units with very similar properties. The depth hoar layer associated with the 1965 level (as described on p. 39) is even traceable to profile D (100 km distant).

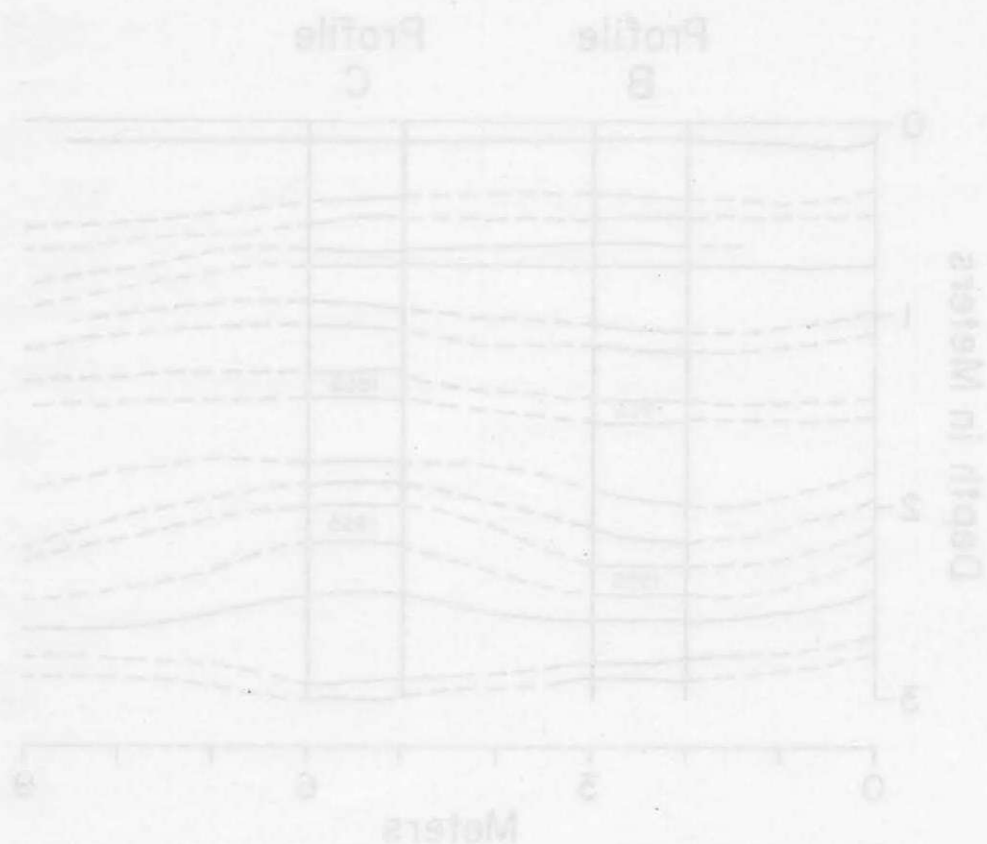


Figure 1a. Schematic representation of the stratigraphy in Profiles B and C showing the preservation of radiating structures.

radiating structures are very in thickness by as much as 0.50 m in less than a horizontal distance. The lower thickness which is preserved in the upper part of profiles B and C has the same magnitude as the radiating structures at the surface of Profile B and is believed to be due to the preservation of radiating structures.

Detailed comparison of the physical properties of several stratigraphic layers has determined from the visible stratigraphy, in some cases several kilometers apart, in some cases several miles with very similar properties. The depth here is associated with the 1965 level (as described on p. 30) is now traceable to profile B (100 m distance).

## DEPOSITIONAL AND DIAGENETIC PROCESSES

### Depositional Processes

In this section, the processes of deposition and diagenesis which are important in the formation and preservation of the stratigraphy at Dome C are examined. The patterns recorded in the snow pits at Dome C are primarily depositional. An understanding of post-depositional modifications, which affect more subtle features such as layer hardness, density, grain size and total mass of material preserved in a pit section is however important to stratigraphic interpretations.

The first question addressed is whether it is always possible to distinguish annual layers. The contrasts between summer and winter meteorologic conditions (including variations in storm frequency, strength of the temperature inversion, and solar radiation) in Antarctica are sufficiently distinct to develop seasonal stratification in the snow cover (Giovinetto, 1960; Gow, 1965). The recognition of alternating layers of approximately the "correct" number and thickness is a depth corresponding to a known age, suggests that these varying conditions are recorded in the snow at Dome C.

Annual layers are generally preserved during burial at Dome C, but complications arise due to erosion and redistribution of part or all of an accumulated layer prior to burial. After burial, diagenetic processes, such as grain growth and vapor transfer under strong near-surface temperature gradients and densification under load, affect the physical properties of the firn and the total amount of material preserved in the surface layers. Thus the observed stratification also may partly reflect conditions prevailing after burial.

Accumulation and ablation of new precipitation and redeposition of drift snow occur at irregular intervals throughout the year and produce discontinuous layers which are modified prior to burial by processes occurring at the surface. One year of accumulation stake measurements at Dome C indicate that the bulk of this accumulation occurred sometime between the end of the 1978/79 summer and the beginning of the 1979/80 summer. The belief that the bulk of the annual accumulation occurs during the autumn and winter is supported by work of Gow (1965), Barkov (1975) and Radok and Lile (1977).

Redistribution of snow at the surface and the development of topographic relief (small dunes and sastrugi) are important to the form and preservation of each accumulation layer. The processes which produce the record seen in a pit can be classified according to whether an annual layer is preserved in one site, whether it is completely or partially lost by erosion or whether it was never deposited because

for some reason the site was not conducive to the accumulation of snow. Figure 17 is a schematic representation of the possible continuum (in time and space) which might exist between surface topography and accumulation layers.

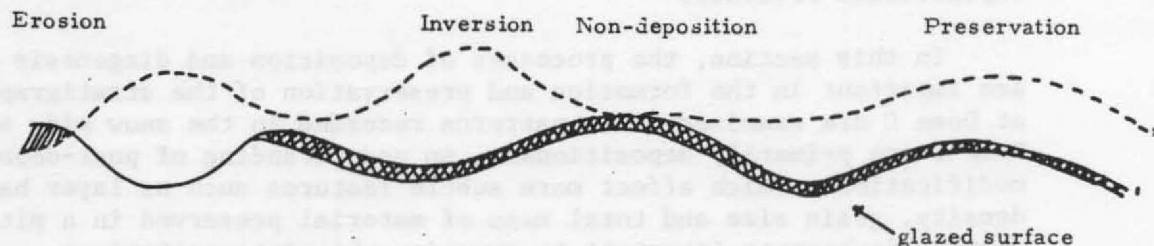


Figure 17. Schematic representation of the possible position a glazed surface with respect to other depositional units. Dashed line represents the next year's surface.

The presence or absence of a thin surface crust may be crucial to the ultimate preservation or loss of an accumulated layer. The relatively calm, clear conditions and the strong near-surface temperature gradients which exist at Dome C throughout the summer provide the conditions necessary for the formation of these crusts. Koerner (1971) and Taylor (1971) discussed the formation of such crusts at Plateau Station. Suggested mechanisms include heat and vapor transfer by evaporation and recondensation, windpacking and absorption of solar radiation, producing intergranular and intra-granular melting.

Gow (1965) discussed the formation of glazed surfaces at the South Pole. Based on accumulation stake measurements, such crusts, he believed, were surfaces of non-accumulation which form by prolonged exposure to wind and solar radiation. The apparent formation of such crusts over most of the surface at Plateau Station and Dome C during the summer can be contrasted with the situation which prevails at the South Pole, where the majority of the surface (except for 30-40 percent which is glazed (Gow, 1965) becomes softer due to extensive mass-loss during the summer. Orheim (1968) has suggested that perhaps this is an indication of a larger positive radiation balance during the summer at the South Pole than at Plateau Station.

At Dome C, sublimation crystals are observed frequently on surfaces of pronounced positive relief features, (dunes, sastrugi). If the surface at the South Pole has more extensive positive relief features, both laterally and in terms of height, than at Plateau Station or Dome C, then the processes described by Gow (1965) and Orheim (1968) should be more effective there. Such a surface would favor radiational heating and mass-loss through sublimation, due to higher angles of incidence of the sun on the surface even though Plateau Station and Dome C are at lower latitudes.



As discussed earlier, the gross surface topography (on a scale of tens of meters) is preserved throughout the summer and, to a large extent, from year to year (Figure 11 a,d). Small variations ( $\pm 0.05$  m) are observed to occur during the summer season with a slight reduction of surface elevation on the crests and small increases in the hollows. These changes are interpreted to be a manifestation of the initial stages of the process of sublimation-deflation described by Gow (1965).

In Figures 7 e and 7 f, not all the profiles indicate a preservation of the large-scale surface relief. Topographic inversion occurs where a low area one year becomes a high in the next. The exact mechanism by which this type of profile develops is not clear and further studies should investigate the development of these patterns. Perhaps this is just a random process.

If the formation of a thin surface crust in the late summer at Dome C is the key to the preservation of seasonal marker levels, then each annual layer should be interpreted as the accumulation between two summer crusts. Once this accumulation is sealed under a crust, little further surface redistribution can take place and subsequent changes in the depositional stratigraphy must be accounted for by some form of diagenesis.

#### Diagenetic Processes

In previous sections it was shown that part of the record preserved in the snow layers in pits at Dome C results from depositional processes. However certain features, such as the thin depth hoar-like layers and the thicker, very soft, low density layers, may be due to vapor loss after burial, due to air exchanges or vapor migration under temperature gradients and forced convection. These processes can lead to the formation of euhedral crystals of depth hoar and changes in the relative hardness, grain size, density and impurity concentration due to the redistribution of mass within the snow layers.

It was suggested previously that part of the 30 percent increase in the accumulation rate recorded in the depth interval 0-1.5 m as compared to the interval 1.5-2.5 m may be related to upward mass flux during negative temperature gradient metamorphism, rather than to processes of surface accumulation and preservation. The deeper (older) layers in the interval 1.5-2.5 m where strong temperature gradients are still important have been losing vapor for more years. Thus, even if accumulation were constant at the time represented by this depth interval, there would be less mass preserved in deep, old layers than was originally accumulated at the surface.

In this section, the processes which may contribute to these changes (including diffusion, conduction and convection) are discussed,



with special emphasis on the contribution of each process to the changes which occur in the stratigraphy. In addition, for formation of depth hoar and very soft, low density layers is discussed and the potential for such layers to form at Dome C is assessed. Finally, some important implications of these processes to stratigraphic interpretations are suggested.

In discussing the processes which contribute to the transformation of snow to ice, Yen (1969) described four types of snow metamorphism. Two of these, destructive and constructive metamorphism are believed to be important in this transformation and are discussed below. The other two, pressure and melt metamorphism involve both greater depths and higher temperatures than were involved in this study.

Destructive metamorphism (also known as equitemperature metamorphism) occurs in layers of snow which have a relatively constant temperature throughout. In the absence of a temperature gradient, mass flux does not occur and the transformations which take place at low temperatures are caused by vapor diffusion along pressure gradients established by differences in grain shape and curvature of crystal faces (Giddings and La Chappelle, 1962). This type of metamorphism generally results in fine-medium (0.5-1.0 mm) rounded grains of weakly bonded snow which have lost nearly all of their original snow crystal habit (Yen, 1969). This process is most effective in the first few days after deposition of new snow and is accelerated when the snow is exposed to solar radiation (Gow and Ramseier, 1963), but continues throughout the firn due to curvature contrasts particularly between crystal sides and necks.

Constructive (temperature gradient) metamorphism occurs when vapor pressure gradients are established as a result of strong temperature gradients in the snow. The snow which results from this type of metamorphism usually has enlarged grains (2-8 mm), reduced density, low strength, high air permeability, and low viscosity and brittleness as compared with the original snow (de Quervain, 1973). It is this type of metamorphism which contributes to the formation of depth hoar (Giddings and La Chappelle, 1962; Gow, 1965; Akitaya, 1974) and other soft, loosely bonded layers which have been described by several workers (Benson, 1962; Shumskii, 1969) and that were observed at Dome C.

\*At p. 28, it was shown that layers resembling depth hoar are found in most of the Dome C pits. These layers are not regularly spaced and in some cases they are not laterally continuous. Because of this, these depth hoar-like layers can not be used as a sole criterion for the determination of annual layer boundaries as was done by Gow (1965) for the South Pole. However, the occurrence

of these layers probably demonstrates the importance of temperature gradient induced metamorphism and mass flux in the near surface layers at Dome C.

The conditions required for the formation of depth hoar in polar regions are not well understood. Most of the previous work has been descriptive (Gow, 1965; Taylor, 1971) and the few theoretical (Giddings and LaChapelle, 1962) and laboratory (Akitaya, 1974) studies that have been made have considered conditions (absolute temperature, temperature gradients, density) which are not applicable to cold polar regions.

Akitaya (1974) made a detailed laboratory and field investigation on different types of depth hoar and the conditions required for their development. Solid type depth hoar which was thought to be the most similar to depth hoar forming in polar regions, was described by Akitaya as being composed of small solid crystals with sharp edges, corners and flat crystal surfaces. The importance of air space for the growth of depth hoar was also addressed in this study. Akitaya concluded that solid type depth hoar was most likely to form in fine grained, high density snow with a small air space under the influence of a relatively small negative upward temperature gradient. The importance of time in the development of depth hoar in polar regions was also mentioned by him. Where snow layers are preserved near the surface for several years, as in parts of Antarctica, depth hoar may grow and enlarge in a progressive manner.

Another aspect of Akitaya's studies on depth hoar was an investigation on how hardness and density of the snow change with the development of depth hoar. In experiments lasting from 1 to 10 days, with various temperature gradients, Akitaya found that there was little change in density with metamorphism, but that hardness of the snow did change according to the magnitude of the temperature gradient and the original snow density. For example, snow with an original density less than  $260 \text{ kg/m}^3$  was found to decrease in hardness during metamorphism, regardless of the temperature gradient and the original snow density. When the original density was greater than  $260 \text{ kg/m}^3$  hardness was found to change only slightly or increase according to the magnitude of the temperature gradient. Only in certain cases, above a density of  $300 \text{ kg/m}^3$  did the hardness decrease. A special situation described by Akitaya as perhaps occurring in polar regions is that in which a rapid increase in hardness occurs in the near surface layer of snow cover (original density -  $350 \text{ kg/m}^3$ ) as a result of a rapid drop in temperature (producing a large near-surface negative temperature gradient  $> 0.5^\circ \text{ C/cm}$ ), intense surface radiation and perhaps a strong cold wind. This mechanism, which may be related to the age hardening process described by Gow and Ramsier (1963), is thought to be important in the formation of the thin hard crusts such as at Dome C.

In order to predict whether the conditions (especially near-surface temperature gradients) required for the formation of depth hoar can occur at Dome C, a comparative study was made with the conditions at South Pole and Plateau Station using temperature data of Giovinetto (1960) (see Appendix VI) and Weller and Schwertfeger (1977), respectively. Calculations of temperature gradients, based on one year of temperature data from the South Pole, indicate that the maximum negative (upward) temperature gradients ( $-0.03$  to  $-0.6$  C/cm) occur in the upper 0.25 m of the snow cover during March and April. Temperature data from Plateau Station shows that the steepest negative gradients occur in April and May, about one month later than at the South Pole. The steepest positive gradients occur in December at both locations.

Since the absolute temperatures in polar regions are generally well below  $0^{\circ}\text{C}$ , the formation of depth hoar may be a much slower process than in other snow covered regions, requiring, perhaps several years. The importance of time to the formation of depth hoar may explain the first occurrence of well developed depth hoar at 0.30 m (which at Dome C would require between two and four years).

The understanding of temperature gradient induced metamorphism in snow, and the formation of depth hoar, involves an understanding of the processes which contribute to heat and mass flux. These processes include conduction, diffusion, and free and forced convection.

The importance of thermal conductivity of the ice network to the heat transfer in a snow layer was studied by de Quervain (1973). He determined experimentally that a major portion (75 percent) of the effective heat transfer in the snow could be attributed to conduction through the ice skeleton. Thermal conductivity is important to heat transfer and the elimination of the temperature gradient in a snow layer. Mass flux, resulting from the temperature gradients established in the snow, on the other hand, must occur through some type of molecular diffusion.

In a study on the metamorphism of snow, Bader and others (1954) concluded that the contribution to mass flux by diffusion during temperature gradient metamorphism was too small (several  $\text{mg}/\text{cm}^2/\text{day}$ ) for the temperature range from  $0^{\circ}$  to  $-10^{\circ}\text{C}$  to account for the formation of depth hoar and the mass flux which was known to occur from field and laboratory studies. It was concluded therefore that convection must also be important to the process of mass transfer.

Experimental work of Yosida (1950) showed that natural convection probably does not contribute significantly to vapor transfer through snow. This was determined by comparing the diffusion coefficients of water vapor through snow when first a negative temperature gradient and then a positive gradient was applied.



Recent studies on the importance of natural convection to mass flux in a snow layer and the conditions which must be fulfilled to initiate this natural convection, are due to Akitaya (1974) and Palm and Tveitereid (1979). The important parameters include the magnitude of the negative temperature gradient, snow layer thickness and the air permeability of the snow. These authors conclude that natural convection is likely to occur only in fairly coarse grained, old snow layers of high air permeability with a certain critical layer thickness, and a fairly high temperature gradient. The relative and absolute magnitude of these parameters have been determined theoretically by considering Rayleigh's theory of motion in a viscous fluid (Akitaya, 1974), Darcy's law to determine the motion of a mixture of air and water vapor in a snow layer (Palm and Weber, 1971) and experimentally in the laboratory (Akitaya, 1974).

The contribution of natural convection to the mass flux (loss and gain) in a snow layer has also been discussed by these authors. Palm and Tveitereid (1979) determined that when natural convection occurs in a snow layer (with a negative-upward temperature gradient) there is an overall mass loss in the lower parts of the layer and a corresponding gain in the upper part.

Forced convection resulting from pressure fluctuations established during periods of gusty winds has also been suggested as a mechanism to enhance mass transfer in snow (Yen, 1969; de Quervain, 1973). Yen (1969) studied, both experimentally and theoretically, the effects of air flow on vapor diffusivity and effective thermal conductivity of snow. He concluded that both the effective heat conduction and vapor transport are increased due to air ventilation in snow. Preliminary calculations (Appendix VII) estimating the amount of mass transfer which might occur as a result of forced convection, support the ideas of Yen. More sophisticated calculations and field experiments should investigate the contributing of forced convection to mass flux in snow.

A final important aspect of the process of temperature gradient metamorphism and the associated mass flux is that with time the process should become more efficient. The progressive increase of air permeability and the overall increase in ventilation with time will improve the conditions necessary for convection. Furthermore, because the changes in snow density (increases in some layers and decreases in others) associated with these processes will change the effective thermal conductivity of the snow, the associated temperature gradients will also change. In particular, extremely low density layers formed as a result of mass loss may show considerably steepened temperature gradients as a result of their poor thermal conductivity.

Based on these processes occurring during temperature gradient metamorphism and the necessary conditions for the formation of depth hoar, I think that the so-called depth hoar-like layers at Dome C are in fact solid-type depth hoar formed over a period of years near the

surface (upper 0.25 m) during April and May when the temperature gradients in this depth interval are the strongest. The very soft, low density layers, on the other hand, are probably layers of snow which with time have lost a considerable portion of their mass through sublimation, while still in the depth interval where temperature gradients are important.

Time is an important factor for the progressive formation of these layers. In the formation of these various diagenetic layers, molecular diffusion, enhanced by natural and forced convection are important processes. These processes when occurring progressively over a period of several years may become significant. The importance of time and the progressive changes which could occur in a snow layer are important phenomena to investigate. The revisitation of one site over a period of years should provide interesting information on the temporal changes in snow stratigraphic resulting from diagenesis.



## CONCLUSIONS

Recent studies of past climatic changes, as revealed in long ice cores, has stressed the need for understanding the development of the record preserved in these cores. This study investigated to what extent the record preserved at depth is more a function of depositional processes or of processes acting during or soon after burial. Also, problems of areal and temporal variability were studied with a view to understanding how representative (both in time and space) a particular core is for a certain region. Finally, validity of certain stratigraphic methods for dating was assessed.

Results of this investigation of surface accumulation and snow pit stratigraphy at Dome C, East Antarctica are given below.

- (1) The mean accumulation rate for 1979 as determined from 100 closely spaced (3 m apart) poles, (the "bamboo forest") was calculated to be about  $62 \text{ kg/m}^2/\text{a}$  ( $\sigma = 28$ ). In a more extensive network of poles (1 km apart) ("accumulation cross") the balance was determined to be about  $35 \text{ kg/m}^2/\text{a}$  ( $\sigma = 24$ ). The estimate from the accumulation cross is similar to determinations (using gross  $\beta$  radioactivity) from five 3-meter snow pits, in which mean annual accumulation since 1955 was  $34 \text{ kg/m}^2/\text{a}$ . Surface roughness profiles in the bamboo forest indicate that small hollows were developed on the surface at the end of the 1978-79 season, during a period of high winds. Snow accumulated preferentially in these hollows so that more sites showed abnormally high accumulations, thereby increasing the mean value. The close spacing of the stakes in the "bamboo forest" may have also contributed to preferential deposition in this site.
- (2) The probability of losing an annual accumulation layer at Dome C ranges from 0 percent (bamboo forest) to 6 percent (accumulation cross). These areally averaged determinations from surface measurements compare well with temporally averaged estimates from the snow pits in which it is estimated that between 5 percent (1 out of 20) and 6 percent (1 out of 17) of the annual layers are lost by non accumulation or erosion.
- (3) The development of an "annual accumulation layer" and the degree of surface roughness in the Dome C area were examined in the bamboo forest. Surface features of 10 to 20 m wavelength, with amplitudes of 0.10 to 0.20 m, were recognized. These features are often preserved from year to year. In some years, however, processes of accumulation may invert

or completely change these surface accumulation patterns. Changes in these surface profiles are smallest during December and January. Small changes (lowering of high spots and filling in of lows), on the order of centimeters, were observed during December and January. These are believed to be a manifestation of the process of sublimation-deflation discussed by Gow (1965).

The preservation of surface features recorded by the bamboo forest profiles is further shown in the correlation of two adjacent snow pit profiles (profiles B and C). The difficulty encountered in attempting to correlate these two profiles can be explained if one concludes that annual accumulation layers of varying dimension and lateral extent are preserved with depth. The buried layer roughness needed to explain such variability is comparable with estimates of surface roughness from the bamboo forest and estimates based on the standard deviation of accumulation rate measurements obtained from gross  $\beta$  radioactivity.

- (4) Annual units of accumulation involving thick soft layers topped by a thin hard crust (with or without depth hoar-like layers below) are recognizable and preserved with depth in a pit. The thin hard crusts are formed during the late summer by processes of near-surface diagenesis, involving effects of wind and radiation. Shallow-pit studies of the development of the near-surface snow layer confirm that these processes are occurring.
- (5) In conjunction with detailed information on the visible stratigraphy, gross  $\beta$  radioactivity is useful for the identification of annual layers. Microparticle profiles were also used to identify annual unit layers. The peaks in particle concentrations were identified independently of other methods, but a detailed visible stratigraphic map is necessary for a correct dating of these peaks.

The recognition of annual layers in the pits and the conclusions that the depositional stratigraphy is preserved with depth is further supported by work of Alley (1980) on a 50 m firn core from Dome C. In that study, visible stratigraphic units involving thin, hard, fine-grained layers and thicker, soft, coarse-grained layers (similar to those defined here) were recognized the complete length of the core.

Evidence that the annual cycles in microparticle concentration seen at the surface are preserved with depth is supported by studies of 61 sections from the French 905 m Dome C core (Thompson and others, 1981). These authors recognized "distinct" cyclical variations in microparticle concentration preserved at depth in this core. Furthermore, the mean annual accumulation derived from this interpretation, ( $32 \text{ kg/m}^2/\text{a}$ ) is comparable with current estimates at the surface.

The next step in the interpretation of the stratigraphic record preserved in snow pits and ice cores is to test the criteria which have been developed in this study. The results of the gross  $\beta$  radioactivity, and microparticle samplings which will be available, from the 1979-80 Dome C snow pit studies will be very helpful in such a test. If the 1979-80 pits can be accurately interpreted using these criteria, then these techniques can be extended to deeper firn and ice core studies.

Future field programs should investigate, in more detail, the temporal development of an annual accumulation layer over a period of years. Both surface stake measurements and detailed snow pit studies will be helpful for the understanding of the progressive changes which take place in the near surface layers. Snow pit sampling for  $\beta$  radioactivity and microparticles every centimeter is recommended to see if better peak resolution is obtainable. Studies of the temporal changes in hardness, density, and grain size of snow crystals in both hard and soft layers is suggested to help in understanding the record which is preserved with depth.

Finally, theoretical calculations combined with experimental field studies should be initiated to study the importance of mass transfer into and out of the near surface layers at Dome C. Theoretical considerations and preliminary calculations seem to suggest that mass transfer may be significantly enhanced by forced convection.

The next step in the investigation of the atmospheric record presented in snow pits and ice cores is to select the stations which have been developed in this study. The results of the snow pit activity, the atmospheric sampling which will be available from the 1955-56 snow pit stations will be very helpful in such a study. If the 1955-56 data can be accurately interpreted using these criteria, then these techniques can be extended to deeper pits and the core studies.

Before field programs should investigate, in more detail, the general development of an annual accumulation layer over a period of years. Both surface snow measurements and detailed snow pit studies will be helpful for the understanding of the progressive changes which take place in the snow surface layer. Snow pit sampling for a representative and representative every year layer is recommended to see if better peak resolution is obtainable. Studies of the temporal changes in hardness, density, and grain size of snow crystals in both hard and soft layers is suggested to help in understanding the record which is preserved with depth.

Finally, chemical calculations combined with experimental field studies should be initiated to study the importance of snow transfer into and out of the snow surface layer in deep E. Antarctica. Preliminary calculations seem to suggest that snow transfer may be significantly enhanced by forced convection.

## REFERENCES

- Akitaya, E. 1974. Studies on Depth Hoar. Contributions from the Institute of Low Temperature Science, Series A, no. 26, 67p.
- Alley, R.B. 1980. Densification and Recrystallization of Firn at Dome C, East Antarctica. The Ohio State University, Institute of Polar Studies, Rpt. 77, 62p.
- Bader, H., Haefeli, R., Bucher, E., Neher, J., Eckel, O. and Thams, C. 1954. Snow and its Metamorphism, SIPRE Translation 14, U.S. Army Snow, Ice and Permafrost Research Establishment, Wilmette, Illinois, 313p.
- Barkov, N.I. 1975. Snow Accumulation characteristics in the Vostok Station area, 1970 through 1973. Antarctic Journal of the U.S., vol. X, no. 2, 55-56.
- Benson, C.S. 1962. Stratigraphic Studies in the Snow and Firn of the Greenland Ice Sheet, SIPRE, no. 70, U.S. Army Snow, Ice and Permafrost Research Establishment, Wilmette, Illinois, 93p.
- Benson, C.S. 1970. Stratigraphic Studies in the Snow at Byrd Station, Antarctica, Compared with Similar Studies in Greenland. Antarctic Snow and Ice Studies II, A.P. Crary, ed., Antarctic Research Series vol. 16, 333-353, American Geophysical Union, Washington, D.C.
- Bentley, C., Jezek, K.C., Blankenship, D.D., Lovell, J.S. and Albert, D.G. 1979. Geophysical Investigation of the Dome C area. Antarctic Journal of the U.S., vol. XIV, no. 5, 98-100.
- Bull, C. 1971. Snow Accumulation in Antarctica; 367-421, Research in the Antarctic, L.O. Quain, ed., American Association for the Advancement of Science, Washington, D.C.
- Cameron, R.L. 1964. Glaciological Studies at Wilkes Station, Budd Coast, Antarctica. Antarctica Snow and Ice Studies, M. Mellor ed., Antarctic Res. Series vol. 2, 317-332, American Geophysical Union, Washington, D.C.
- Crozaz, G.E. 1969. Fission Products in Antarctic Snow, An Additional Reference Level in January 1965, Earth and Planetary Science Letters, vol. 6, 6-8.
- Dalrymple, P.C. 1966. A Physical Climatology of the Antarctic Plateau. Studies in Antarctic Meteorology, M.J. Rubin ed., Antarctica Res. Series vol. 9, 195-231. American Geophysical Union, Washington, D.C.



- Dansgaard, W., Johnsen, S.J., Clausen, H.B., Gundestrup, N. 1973. Stable Isotope Glaciology, Meddeleser Om Grønland, Bd. 197 Nr. 2, København, C.A. Reitzels Forlag, 53p.
- Delmas, R. and Pourchet, M. 1977. Utilisation de filtres échangeurs d'ions pour l'étude de l'activité  $\beta$  globale d'un carottage glaciologique, IAHS Publ. 118, 159-163.
- Delmas, R. and Boutron, C. 1978. Sulfate in Antarctic Snow: Spatio-Temporal Distribution, Atmospheric Environment, vol. 12, no. 1-3, 723-28.
- de Quervain, M.R. 1963. On the Metamorphism of Snow, W.D. Kingery ed., Ice and Snow: Properties, Processes and Applications, The M.I.T. Press, 377-390.
- de Quervain, M.R. 1973. Snow Structure, Heat and Mass flux through Snow in The Role of Snow and Ice in Hydrology; Proceedings of the Baniff Symposia, Sept. 1972, IAHS Pub. 107, vol. 1.
- Global Atmospheric Research Programme (GARP). 1975. The Physical Basis of Climate and Climate Modelling, Garp Publication Series, no. 16, 256p.
- Giddings, J.C. and LaChappelle, E. 1962. The formation of depth hoar, J. Geophys. Res., vol. 67, no. 6, 2377-2383.
- Giovinetto, M.B. 1960. IGY Antarctica Glaciological Data; Fieldwork 1958 and 1959 - South Pole Station. The Ohio State University, Institute of Polar Studies Rpt., 825-2, part IV, 104p.
- Gow, A.J. and Ramseier, R.O. 1963. Age Hardening of Snow at the South Pole. J. of Glaciol., vol. 4, no. 35, 521-536.
- Gow, A.J. 1965. Snow Studies in Antarctica. CRREL Res. Rpt. 177.
- Hamilton, W.L. and Langway, C.C., J4. 1967. A Correlation of micro-particle concentrations with oxygen isotope ratios in 700 year old Greenland Ice. Earth and Planetary Science Letters, vol. 3, 363, 366.
- Hammer, C.U., Clausen, H.B., Dansgaard, W., Gundestrup, N., Johnsen, S.J. and Rech, N. 1978. Dating of Greenland ice cores by Flow Models, Isotopes, Volcanic debris and Continental dust. J. of Glaciol., vol. 20, no. 82, 3-26.
- Hogan, A.W. and Barnard, S. 1978. Seasonal and Frontal Variation in Antarctica Aerosol Concentrations. J. of Applied Meteorol., vol. 17, 1458-65.

- Jouzel, J., Merlivat, L., Pourchet, M. and Lorius, C. 1979. A continuous record of artificial tritium fallout at the South Pole. *Earth and Planetary Science Letters*, vol. 45, 188-200.
- Junge, C.E. 1963. *Air Chemistry and Radioactivity*. Academic Press, N.Y., 382pp.
- Koerner, R.M. 1971. A Stratigraphic Method of determining the snow accumulation rate at Plateau Station, Antarctica and application to South Pole-Queen Maud Land Traverse 2, 1965-1966, *Antarctic Snow and Ice Studies II*, A.P. Crary ed., Antarctic Res. Series, vol. 16, 225-238. American Geophysical Union, Washington, D.C.
- Lambert, G., Lorius, C. and Ardouin, B. 1965. Datation d'une carotte de neve de la bordure de l'Antarctique par la mesure de la radioactivite naturelle et artificielle. *Earth and Planetary Science Letters*, vol. 3, 429-433.
- Lambert, G., Ardouin, B., Sanak, J., Lorius, C. and Pourchet, M. 1977. Accumulation of Snow and Radioactive Debris in Antarctica: a possible refined radiochronology beyond reference levels. *IAHS Pub.* 118, 146-157.
- Liljequist, G.H. 1956. Energy exchange of an Antarctic snow field. *Norwegian-British-Swedish-Antarctic Expedition, 1949-52. Scientific Results*, vol. 11, part I, 183p.
- Lockhart, L.B., Patterson, R.L. and Saunders, A.W. 1966. Airborne Radioactivity in Antarctica. *J. Geophys. Res.*, vol. 71, no. 8, 1985-90.
- Lorius, C. and Merlivat, L. 1977. Distribution of mean surface stable isotope values in East Antarctica: observed changes with depth in the coastal area, *IAHS Publ.* 118, 127-137.
- Lorius, C. and Donnou, D. 1978. Campagne en Antarctique, Nov. 1977-Fev. 1978, *Courrier du CNRS*, no. 30, 6-17.
- Lorius, C., Merlivat, L., Jouzel, J. and Pourchet, M. 1979. A 30,000 year isotope-climatic record from Antarctic ice. *Nature*, vol. 280, no. 5724, 644-48.
- Martell, E.A. 1959. Atmospheric Aspects of Sr-90 fallout. *Science*, vol. 129, no. 3357, 1197-1206.
- Mosley-Thompson, E.M. 1980. 911 years of Microparticle deposition at the South Pole: A Climatic Interpretation. The Ohio State University, Institute of Polar Studies, Rpt. 72, 134pp.

National Academy of Sciences: Committee on Polar Research, Antarctic Glaciology, Guidelines for U.S. Program Planning 1973-1983, 174, 66p.

Orheim, O. 1968. Surface Snow Metamorphism on the Antarctic Plateau, Norsk Polarinstitut, Arbor, 84-91.

Palm, E. and Weber, J.E. 1971. Derivation of the equations for thermal convection in a porous material, Preprint Serv. 4, Inst. of Math, Univ. of Oslo, Oslo.

Palm, E. and Tveitereid, M. 1979. On Heat and Mass Flux Through Snow. J. Geophys. Res., vol. 84, no. c-2, 745-749.

Petit, J.R., Jouzel, J., Pourchet, M. and Merlivat, L. 1982 A Detailed Study of Snow Accumulation and Stable Isotope Content in the Dome C, Antarctica. J. Geophys. Res., vol. 87, no. c-6, 4301-4308.

Picciotto, E. and Wilgain, S.E. 1963. Fission Products in Antarctic snow: a reference level for measuring snow accumulation. J. Geophys. Res., vol. 68, no. 21, 5965-72.

Picciotto, E., Crozaz, G. and DeBreuck, W. 1971. Accumulation on the South Pole-Queen Maud Land Traverse, 1964-1968, Antarctic Snow and Ice Studies II, A.P. Crary, ed., Antarctic Res. Series, vol. 16, 257-315, American Geophysical Union, Washington, D.C.

Pinglot, F. 1978. Dipositif Automatique de Mesure de la Radioactivite Beta a bas niveau d'echantillons de Neige, C.N.R.S. Publ. no. 257, 103p.

Pinglot, F. and Pourchet, M. 1979. Low-level beta counting with an automatic sample changer. Nuclear Instruments and Methods, no. 166, 483-490.

Pourchet, M. 1979. Etude del'accumulation a Dome C, Document interne, C.N.R.S., 14p.

Pourchet, M. and Pinglot, F. 1979. Determination of the Stratospheric residence time from the total beta activity of Antarctic and Greenland snows. Geophys. Res. Letters, vol. 6, 365-67.

Pourchet, M., Pinglot, F. and Lorius, C. 1983 Some Meteorological Applications of Radioactive Fallout Measurements in Antarctic Snows. J. Geophys. Res., vol. 88, no. c-10, p. 6013-6020.

Radok, U. and Lile, R.C. 1977. A Year of Snow Accumulation at Plateau Station, Meteorological Studies at Plateau Station, Antarctica, J.A. Susinger ed., Antarctic Research Series, vol. 25, 17-26. American Geophysical Union, Washington, D.C.

- Raynaud, D., Lorius, C., Budd., W.F., Young, N.W. 1979. Ice Flow Along an I.A.G.P. Flow Line and Interpretation of Data From an Ice Core in Terre Adelie, Antarctica. *J. of Glaciology*, vol. 24, no. 80, 103-115.
- Robin, G. de Q. 1975. Radio echo sounding of the Antarctic ice sheet, *Antarctic Journal of the U.S.*, vol. X, no. 4, 157-59.
- Schytt, V. 1958. *Glaciology II. Norwegian-British-Swedish Antarctic Expedition 1949-52, Scientific Results*, 4, Norsk Polarinstituit, Oslo.
- Scott Polar Research Institute. 1974. Ice sheet surface and sub-ice relief, 90°E-180°, Antarctica Radio Echo Sounding Map Series A, no. 3, Cambridge Scott Polar Research Institute.
- Seligman, G. 1936. *Snow Structure and Ski Fields*, International Glaciological Society, 3 rd. ed., 555p.
- Shumskii, P.A. 1964. *Principles of Structural Glaciology*, Dover Publications, nc., New York, 497p.
- Taylor, C.B. 1968. A Comparison of Tritium and Strontium-90 Fallout in the Southern Hemisphere, *Tellus*, 20, 569-76.
- Taylor, L.D. 1965. Glaciological studies on the South Pole traverse. The Ohio State University, Institute of Polar Studies, Rpt. 17, 25p.
- Taylor, L.D. 1971. Glaciological Studies on the South Pole Traverse, 1962-63, *Antarctic Snow and Ice Studies II*, A.P. Crary, ed., Antarctic Res. Series, vol. 16, 209-224. American Geophysical Union, Washington, D.C.
- Thompson, L.G. 1977. *Microparticles, Ice Sheets and Climate*, The Ohio State University, Institute of Polar Studies, Rpt. 64, 148p.
- Thompson, L.G., Mosley-Thompson, E. and Petit, J.R. 1981. Glaciological interpretation of microparticle concentrations from the French 905 m Dome C, Antarctica Core, Sea Level, Ice, and Climatic Change, *Proceedings of Canberra Symposium, IAHS Pub. 131*, p. 227-234.
- Weller, G. and Schwertfeger, P. 1977. Thermal Properties and Heat Transfer Processes of Low-Temperature Snow, *Meteorological Studies at Plateau Station, Antarctica*, J.A. Businger ed., Antarctic Research Series, vol. 25, 27-34. American Geophysical Union, Washington, D.C.



Whillans, I.M. 1975. Effect of Inversion Winds on Topographic Detail and Mass Balance on Inland Ice Sheets. J. of Glaciol., vol. 14, no. 70, 85-90.

Whillans, I.M. 1978. Surface mass balance variability near "Byrd Station", Antarctica, and its importance to ice core stratigraphy. J. of Glaciol., vol. 20, no. 83, 301-310.

Whillans, I.M. 1979. Glaciological Investigations in the Dome C area. Antarctic Journal of the U.S., vol. XIV, no. 3, 6.

Wilgain, S., Picciotto, E. and DeBreuck, W. 1965. Strontium 90 fallout in Antarctica. J. Geophys. Res., vol. 70, 6023-32.

Yen, Yin-Chao. 1969. Recent studies on snow properties. Advances in Hydrosience, vol. 5, 173-214.

Yosida, Z. 1950. Heat transfer by water vapor in a snow cover. Teion Kagaku A5, 93-100.



Appendix I. Accumulation Rate Data from Bamboo Forest and Accumulation Cross, December 5, 1978–November 30, 1979.

Bamboo Forest Accumulation in meters of snow.

<u>Pole</u>	<u>Accum</u>	<u>Pole</u>	<u>Accum</u>	<u>Pole</u>	<u>Accum</u>	<u>Pole</u>	<u>Accum</u>	<u>Pole</u>	<u>Accum</u>
A <sub>0</sub>	0.115	B <sub>0</sub>	0.150	C <sub>0</sub>	0.100	D <sub>0</sub>	0.280	E <sub>0</sub>	0.380
A <sub>1</sub>	0.125	B <sub>1</sub>	0.100	C <sub>1</sub>	0.065	D <sub>1</sub>	0.210	E <sub>1</sub>	0.390
A <sub>2</sub>	0.060	B <sub>2</sub>	0.055	C <sub>2</sub>	0.120	D <sub>2</sub>	0.190	E <sub>2</sub>	0.345
A <sub>3</sub>	0.150	B <sub>3</sub>	0.110	C <sub>3</sub>	0.160	D <sub>3</sub>	0.130	E <sub>3</sub>	0.295
A <sub>4</sub>	0.160	B <sub>4</sub>	0.235	C <sub>4</sub>	0.230	D <sub>4</sub>	0.180	E <sub>4</sub>	0.170
A <sub>5</sub>	0.155	B <sub>5</sub>	0.240	C <sub>5</sub>	0.260	D <sub>5</sub>	0.185	E <sub>5</sub>	0.180
A <sub>6</sub>	0.175	B <sub>6</sub>	0.195	C <sub>6</sub>	0.260	D <sub>6</sub>	0.310	E <sub>6</sub>	0.160
A <sub>7</sub>	0.160	B <sub>7</sub>	0.195	C <sub>7</sub>	0.340	D <sub>7</sub>	0.315	E <sub>7</sub>	0.150
A <sub>8</sub>	0.055	B <sub>8</sub>	0.135	C <sub>8</sub>	0.235	D <sub>8</sub>	0.240	E <sub>8</sub>	0.240
A <sub>9</sub>	0.190	B <sub>9</sub>	0.160	C <sub>9</sub>	0.295	D <sub>9</sub>	0.250	E <sub>9</sub>	0.160
F <sub>0</sub>	0.125	G <sub>0</sub>	0.155	H <sub>0</sub>	0.150	I <sub>0</sub>	0.180	J <sub>0</sub>	0.200
F <sub>1</sub>	0.290	G <sub>1</sub>	0.145	H <sub>1</sub>	0.080	I <sub>1</sub>	0.200	J <sub>1</sub>	0.225
F <sub>2</sub>	0.400	G <sub>2</sub>	0.050	H <sub>2</sub>	0.115	I <sub>2</sub>	0.200	J <sub>2</sub>	0.200
F <sub>3</sub>	0.280	G <sub>3</sub>	0.130	H <sub>3</sub>	0.145	I <sub>3</sub>	0.155	J <sub>3</sub>	0.215
F <sub>4</sub>	0.305	G <sub>4</sub>	0.135	H <sub>4</sub>	0.195	I <sub>4</sub>	0.195	J <sub>4</sub>	0.180
F <sub>5</sub>	0.110	G <sub>5</sub>	0.100	H <sub>5</sub>	0.225	I <sub>5</sub>	0.300	J <sub>5</sub>	0.110
F <sub>6</sub>	0.105	G <sub>6</sub>	0.210	H <sub>6</sub>	0.220	I <sub>6</sub>	0.140	J <sub>6</sub>	0.170
F <sub>7</sub>	0.120	G <sub>7</sub>	0.100	H <sub>7</sub>	0.185	I <sub>7</sub>	0.160	J <sub>7</sub>	0.120
F <sub>8</sub>	0.160	G <sub>8</sub>	0.140	H <sub>8</sub>	0.125	I <sub>8</sub>	0.085	J <sub>8</sub>	0.180
F <sub>9</sub>	0.220	G <sub>9</sub>	0.185	H <sub>9</sub>	0.090	I <sub>9</sub>	0.150	J <sub>9</sub>	0.105

$$\bar{X} = 0.183$$

$$\sigma = 0.075$$

A <sub>0</sub>	-0.030	B <sub>0</sub>	0.020	C <sub>0</sub>	-0.010	D <sub>0</sub>	0.100	E <sub>0</sub>	0.000
A <sub>1</sub>	0.000	B <sub>1</sub>	0.000	C <sub>1</sub>	0.040	D <sub>1</sub>	0.040	E <sub>1</sub>	0.060
A <sub>2</sub>	0.020	B <sub>2</sub>	-0.020	C <sub>2</sub>	-0.020	D <sub>2</sub>	0.060	E <sub>2</sub>	-0.020
A <sub>3</sub>	0.010	B <sub>3</sub>	-0.020	C <sub>3</sub>	0.000	D <sub>3</sub>	0.010	E <sub>3</sub>	0.070
A <sub>4</sub>	0.060	B <sub>4</sub>	0.070	C <sub>4</sub>	0.040	D <sub>4</sub>	-0.020	E <sub>4</sub>	0.000
A <sub>5</sub>	0.010	B <sub>5</sub>	0.040	C <sub>5</sub>	-0.030	D <sub>5</sub>	-0.010	E <sub>5</sub>	0.050
A <sub>6</sub>	-0.020	B <sub>6</sub>	-0.030	C <sub>6</sub>	-0.030	D <sub>6</sub>	-0.140	E <sub>6</sub>	-0.020
A <sub>7</sub>	-0.010	B <sub>7</sub>	-0.010	C <sub>7</sub>	-0.020	D <sub>7</sub>	-0.090	E <sub>7</sub>	-0.010
A <sub>8</sub>	-0.030	B <sub>8</sub>	-0.010	C <sub>8</sub>	-0.010	D <sub>8</sub>	-0.020	E <sub>8</sub>	0.000
A <sub>9</sub>	0.080	B <sub>9</sub>	-0.020	C <sub>9</sub>	-0.020	D <sub>9</sub>	-0.010	E <sub>9</sub>	-0.030
F <sub>0</sub>	-0.020	G <sub>0</sub>	-0.030	H <sub>0</sub>	-0.010	I <sub>0</sub>	-0.010	J <sub>0</sub>	-0.010
F <sub>1</sub>	-0.020	G <sub>1</sub>	-0.040	H <sub>1</sub>	-0.050	I <sub>1</sub>	-0.010	J <sub>1</sub>	-0.020
F <sub>2</sub>	0.000	G <sub>2</sub>	-0.060	H <sub>2</sub>	-0.030	I <sub>2</sub>	-0.020	J <sub>2</sub>	0.000
F <sub>3</sub>	0.150	G <sub>3</sub>	0.010	H <sub>3</sub>	-0.030	I <sub>3</sub>	-0.020	J <sub>3</sub>	0.000
F <sub>4</sub>	-	G <sub>4</sub>	-0.050	H <sub>4</sub>	-0.030	I <sub>4</sub>	-0.010	J <sub>4</sub>	-0.030
F <sub>5</sub>	-0.030	G <sub>5</sub>	-0.020	H <sub>5</sub>	-0.010	I <sub>5</sub>	-0.030	J <sub>5</sub>	-0.040
F <sub>6</sub>	0.200	G <sub>6</sub>	-0.020	H <sub>6</sub>	-0.020	I <sub>6</sub>	-0.030	J <sub>6</sub>	-0.040
F <sub>7</sub>	0.050	G <sub>7</sub>	-0.020	H <sub>7</sub>	-0.040	I <sub>7</sub>	0.010	J <sub>7</sub>	0.000
F <sub>8</sub>	-0.400	G <sub>8</sub>	-0.010	H <sub>8</sub>	-0.020	I <sub>8</sub>	-0.020	J <sub>8</sub>	-0.020
F <sub>9</sub>	0.220	G <sub>9</sub>	0.060	H <sub>9</sub>	-0.020	I <sub>9</sub>	0.000	J <sub>9</sub>	-0.010
									$\bar{X} = -0.005$
									$\sigma = 0.063$

A <sub>0</sub>	0.00	B <sub>0</sub>	0.000	C <sub>0</sub>	-0.010	D <sub>0</sub>	-0.015	E <sub>0</sub>	-0.035
A <sub>1</sub>	0.025	B <sub>1</sub>	0.050	C <sub>1</sub>	0.040	D <sub>1</sub>	-0.010	E <sub>1</sub>	-0.040
A <sub>2</sub>	0.025	B <sub>2</sub>	0.015	C <sub>2</sub>	0.000	D <sub>2</sub>	0.000	E <sub>2</sub>	-0.045
A <sub>3</sub>	-0.010	B <sub>3</sub>	0.025	C <sub>3</sub>	0.000	D <sub>3</sub>	0.000	E <sub>3</sub>	-0.015
A <sub>4</sub>	0.00	B <sub>4</sub>	-0.015	C <sub>4</sub>	0.000	D <sub>4</sub>	-0.010	E <sub>4</sub>	-0.010
A <sub>5</sub>	0.00	B <sub>5</sub>	-0.015	C <sub>5</sub>	-0.035	D <sub>5</sub>	0.045	E <sub>5</sub>	0.020
A <sub>6</sub>	0.00	B <sub>6</sub>	-0.015	C <sub>6</sub>	0.000	D <sub>6</sub>	0.000	E <sub>6</sub>	0.000
A <sub>7</sub>	-0.010	B <sub>7</sub>	-0.010	C <sub>7</sub>	-0.035	D <sub>7</sub>	-0.030	E <sub>7</sub>	-0.010
A <sub>8</sub>	0.030	B <sub>8</sub>	0.030	C <sub>8</sub>	-0.015	D <sub>8</sub>	0.015	E <sub>8</sub>	0.000
A <sub>9</sub>	0.00	B <sub>9</sub>	0.000	C <sub>9</sub>	-0.125	D <sub>9</sub>	-0.020	E <sub>9</sub>	0.010
F <sub>0</sub>	0.015	G <sub>0</sub>	0.020	H <sub>0</sub>	0.020	I <sub>0</sub>	0.000	J <sub>0</sub>	0.000
F <sub>1</sub>	0.045	G <sub>1</sub>	-0.010	H <sub>1</sub>	0.000	I <sub>1</sub>	0.000	J <sub>1</sub>	0.000
F <sub>2</sub>	-0.045	G <sub>2</sub>	0.045	H <sub>2</sub>	0.000	I <sub>2</sub>	-0.010	J <sub>2</sub>	0.000
F <sub>3</sub>	0.020	G <sub>3</sub>	0.045	H <sub>3</sub>	-0.010	I <sub>3</sub>	0.000	J <sub>3</sub>	-0.010
F <sub>4</sub>	-0.025	G <sub>4</sub>	0.040	H <sub>4</sub>	0.010	I <sub>4</sub>	0.015	J <sub>4</sub>	-0.010
F <sub>5</sub>	0.00	G <sub>5</sub>	0.060	H <sub>5</sub>	0.000	I <sub>5</sub>	-0.230	J <sub>5</sub>	0.055
F <sub>6</sub>	0.030	G <sub>6</sub>	0.000	H <sub>6</sub>	0.000	I <sub>6</sub>	0.045	J <sub>6</sub>	0.000
F <sub>7</sub>	0.030	G <sub>7</sub>	0.045	H <sub>7</sub>	0.000	I <sub>7</sub>	0.010	J <sub>7</sub>	0.015
F <sub>8</sub>	0.030	G <sub>8</sub>	0.000	H <sub>8</sub>	0.000	I <sub>8</sub>	0.035	J <sub>8</sub>	-0.010
F <sub>9</sub>	0.00	G <sub>9</sub>	0.000	H <sub>9</sub>	0.000	I <sub>9</sub>	0.000	J <sub>9</sub>	0.035
									$\bar{X} = +0.001$
									$\sigma = 0.035$

Accumulation Cross in meters of snow

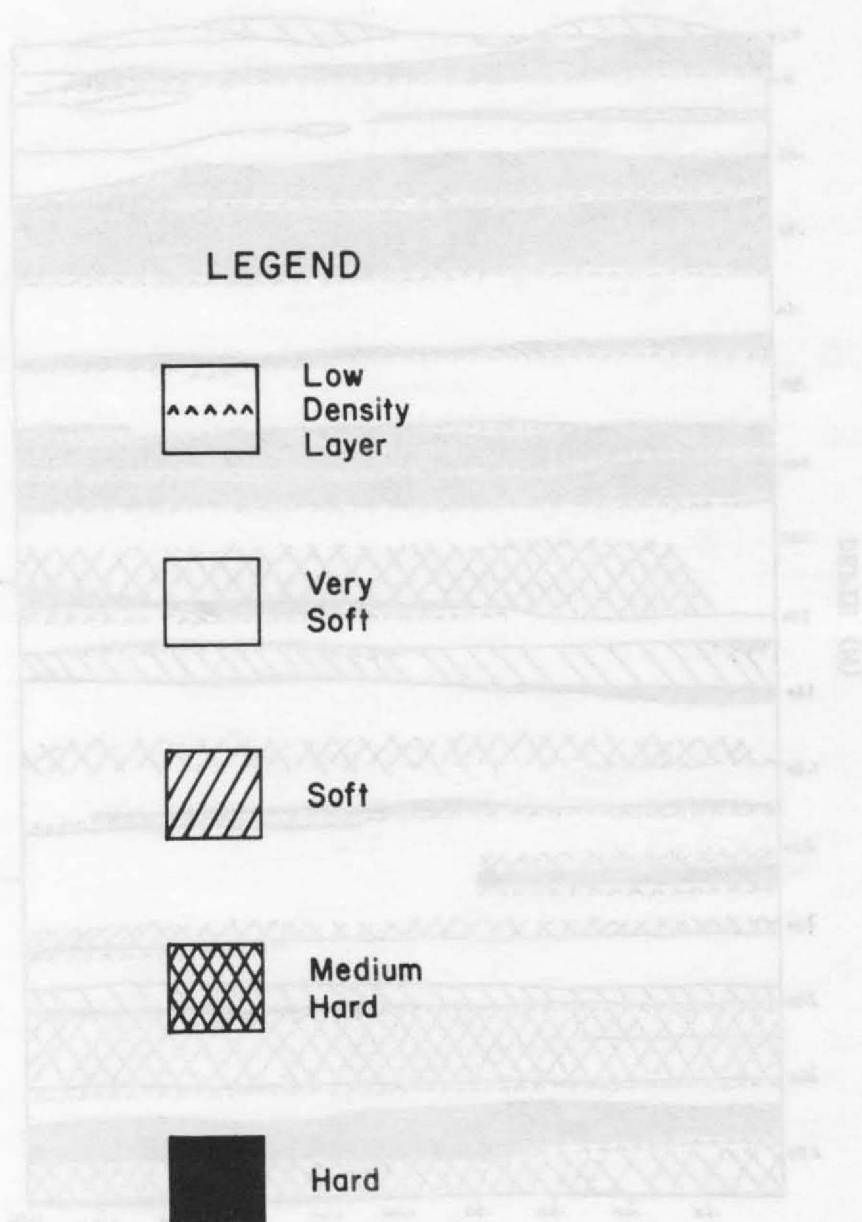
N- 6	0.15	S- 6	0.016	W- 6	0.065	E- 6	0.040
N- 7	0.11	S- 7	0.116	W- 7	0.220	E- 7	0.100
N- 8	0.07	S- 8	0.034	W- 8	0.225	E- 8	0.085
N- 9	0.075	S- 9	0.078	W- 9	0.050	E- 9	0.065
N-10	0.155	S-10	0.312	W-10	0.010	E-10	0.090
N-11	0.15	S-11	0.169	W-11	0.030	E-11	0.138
N-12	0.09	S-12	0.135	W-12	0.075	E-12	0.087
N-13	0.175	S-13	0.172	W-13	0.045	E-13	0.137
N-14	0.065	S-14	0.098	W-14	0.110	E-14	0.052
N-15	0.09	S-15	0.295	W-15	0.045	E-15	0.037
N-16	0.155	S-16	0.126	W-16	0.150	E-16	0.113
N-17	0.12	S-17	0.120	W-17	0.075	E-17	0.130
N-18	0.195	S-18	0.097	W-18	0.150	E-18	0.125
N-19	0.095	S-19	0.128	W-19	0.125	E-19	0.061
N-20	0.105	S-20	0.093	W-20	0.050	E-20	0.038
N-21	0.135	S-21	0.109	W-21	0.095	E-21	0.095
N-22	0.13	S-22	0.045	W-22	0.190	E-22	0.055
N-23	0.095	S-23	0.120	W-23	0.230	W-23	0.137
N-24	0.06	S-24	0.098	W-24	0.025	W-24	0.113
N-25	0.195	S-25	0.100	W-25	0.035	E-25	0.111
N-26	0.00	S-26	0.007	W-26	0.000		
N-27	0.02	S-27	0.108	W-27	0.070		
N-28	0.12	S-28	0.085	W-28	0.060		
N-29	0.00	S-29	0.070	W-29	0.090		
N-30	0.08	S-30	0.087	W-30	0.110		
<hr/>							
$\bar{X}$	= 0.105	$\bar{X}$	= 0.099	$\bar{X}$	= 0.093	$\bar{X}$	= 0.84
$\sigma$	= 0.053	$\sigma$	= 0.084	$\sigma$	= 0.067	$\sigma$	= 0.048



Accumulated Gross in excess of zero

W-6 0.12	W-6 0.016	W-6 0.009	W-6 0.000
W-7 0.11	W-7 0.116	W-7 0.110	W-7 0.100
W-8 0.01	W-8 0.036	W-8 0.119	W-8 0.081
W-9 0.012	W-9 0.018	W-9 0.020	W-9 0.002
W-10 0.112	W-10 0.111	W-10 0.110	W-10 0.099
W-11 0.11	W-11 0.109	W-11 0.090	W-11 0.116
W-12 0.09	W-12 0.112	W-12 0.012	W-12 0.081
W-13 0.112	W-13 0.111	W-13 0.069	W-13 0.111
W-14 0.001	W-14 0.098	W-14 0.110	W-14 0.081
W-15 0.09	W-15 0.102	W-15 0.069	W-15 0.011
W-16 0.112	W-16 0.110	W-16 0.110	W-16 0.111
W-17 0.11	W-17 0.110	W-17 0.012	W-17 0.110
W-18 0.101	W-18 0.091	W-18 0.110	W-18 0.111
W-19 0.092	W-19 0.118	W-19 0.111	W-19 0.081
W-20 0.101	W-20 0.091	W-20 0.010	W-20 0.098
W-21 0.112	W-21 0.109	W-21 0.069	W-21 0.069
W-22 0.11	W-22 0.069	W-22 0.109	W-22 0.091
W-23 0.092	W-23 0.110	W-23 0.110	W-23 0.111
W-24 0.09	W-24 0.098	W-24 0.011	W-24 0.111
W-25 0.102	W-25 0.110	W-25 0.011	W-25 0.111
W-26 0.10	W-26 0.001	W-26 0.000	W-26 0.000
W-27 0.01	W-27 0.108	W-27 0.010	W-27 0.000
W-28 0.11	W-28 0.081	W-28 0.000	W-28 0.000
W-29 0.00	W-29 0.010	W-29 0.000	W-29 0.000
W-30 0.08	W-30 0.081	W-30 0.110	W-30 0.110
$\Sigma = 0.102$	$\Sigma = 0.099$	$\Sigma = 0.081$	$\Sigma = 0.081$
$\sigma = 0.011$	$\sigma = 0.009$	$\sigma = 0.009$	$\sigma = 0.009$

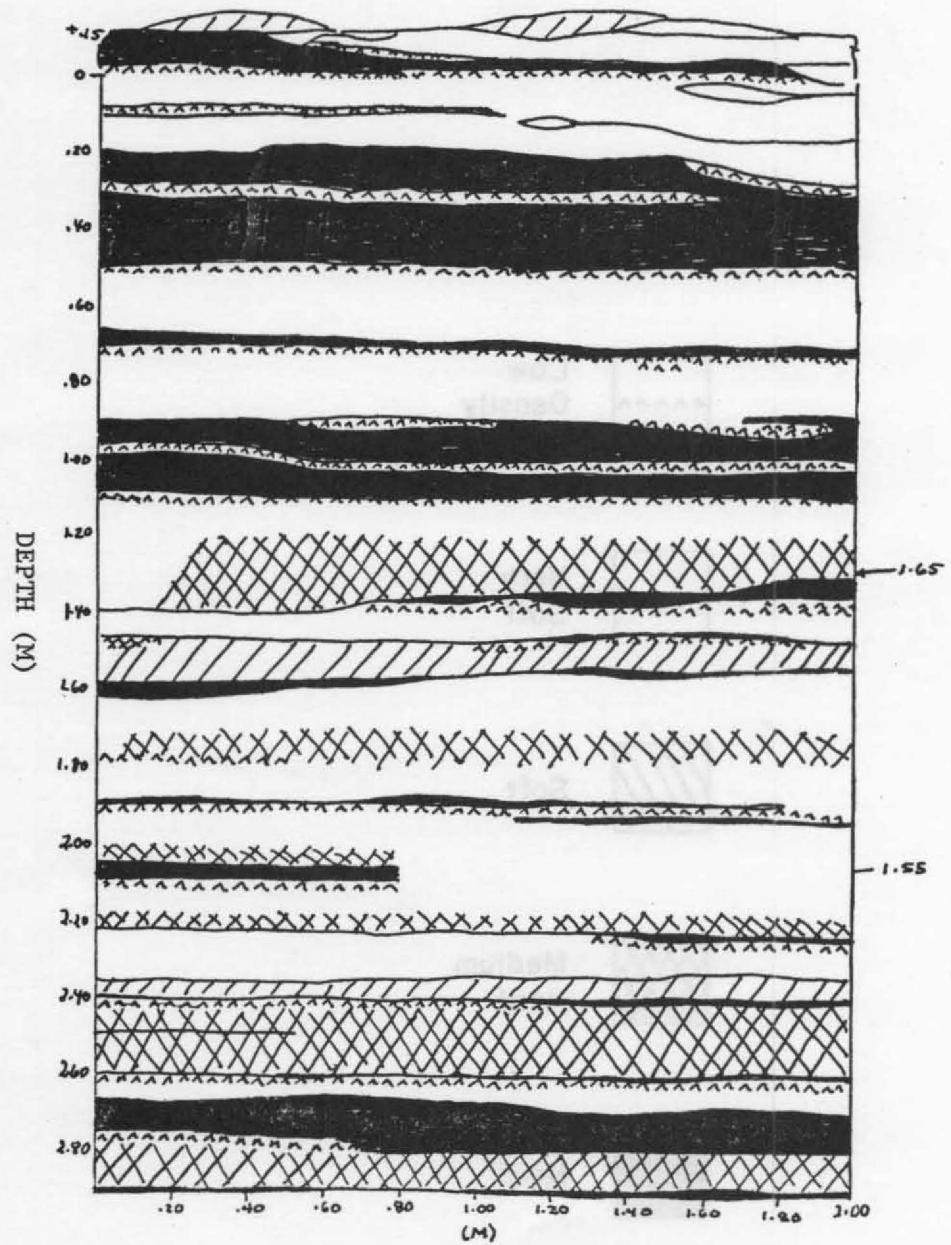
Appendix II. Complete figures of visible stratigraphy, gross  $\beta$  Radioactivity, and microparticle stratigraphy.



VISIBLE

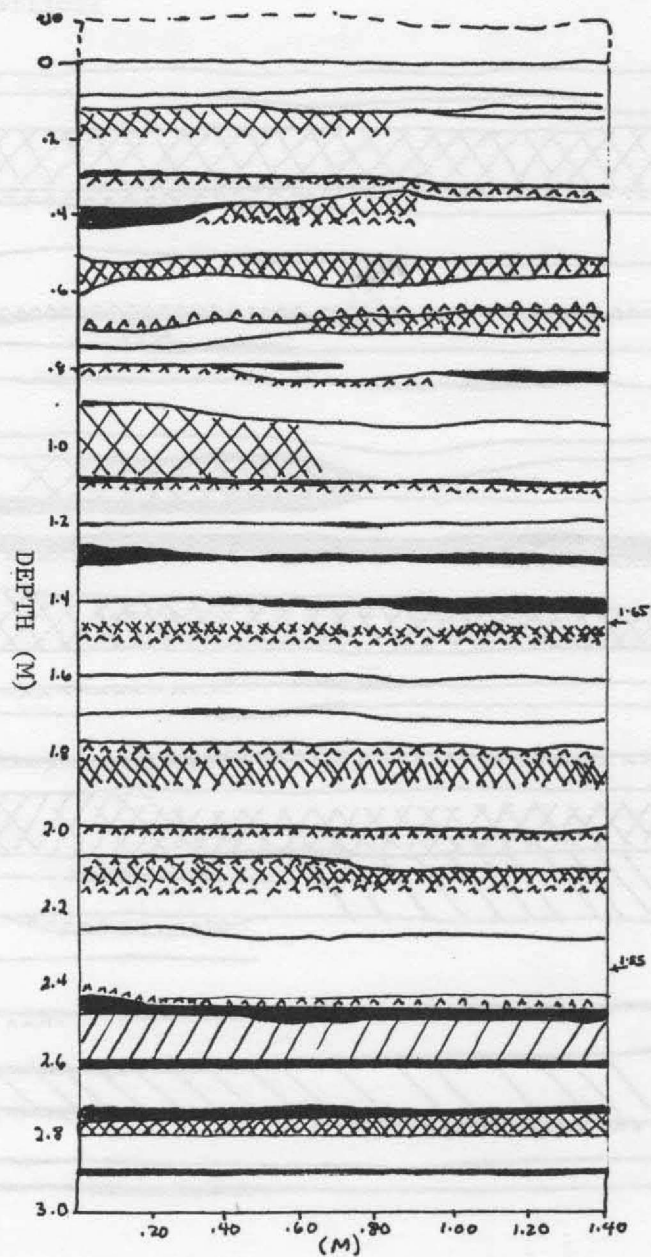
STRATIGRAPHY

Profile A



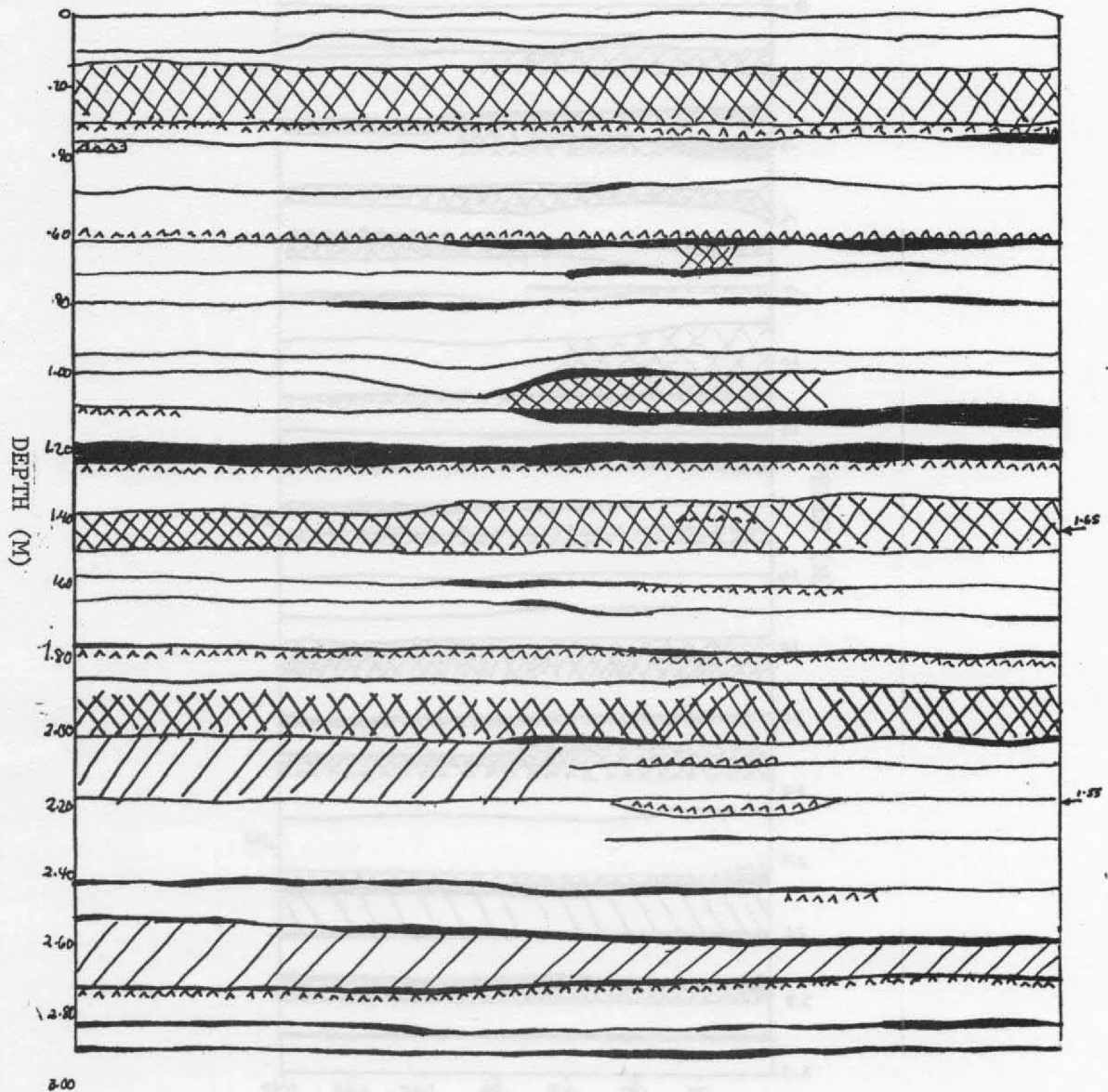
VISIBLE  
STRATIGRAPHY

Profile B



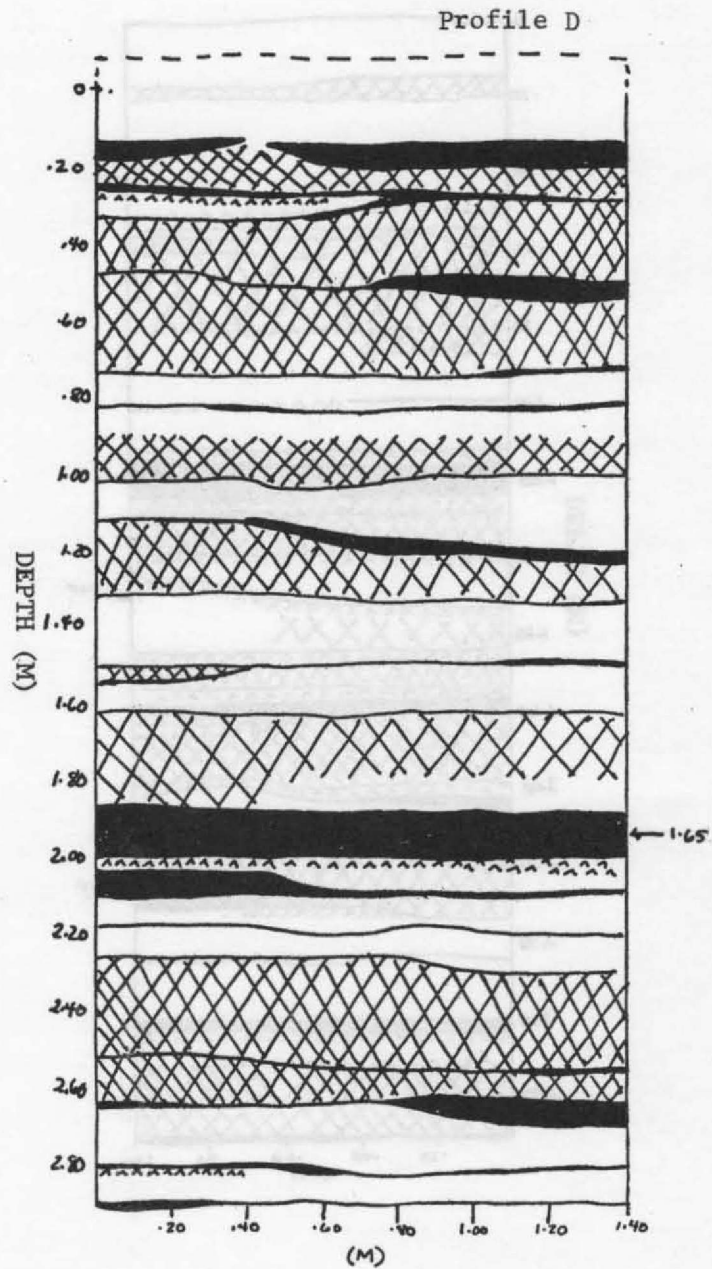
VISIBLE  
STRATIGRAPHY

Profile C





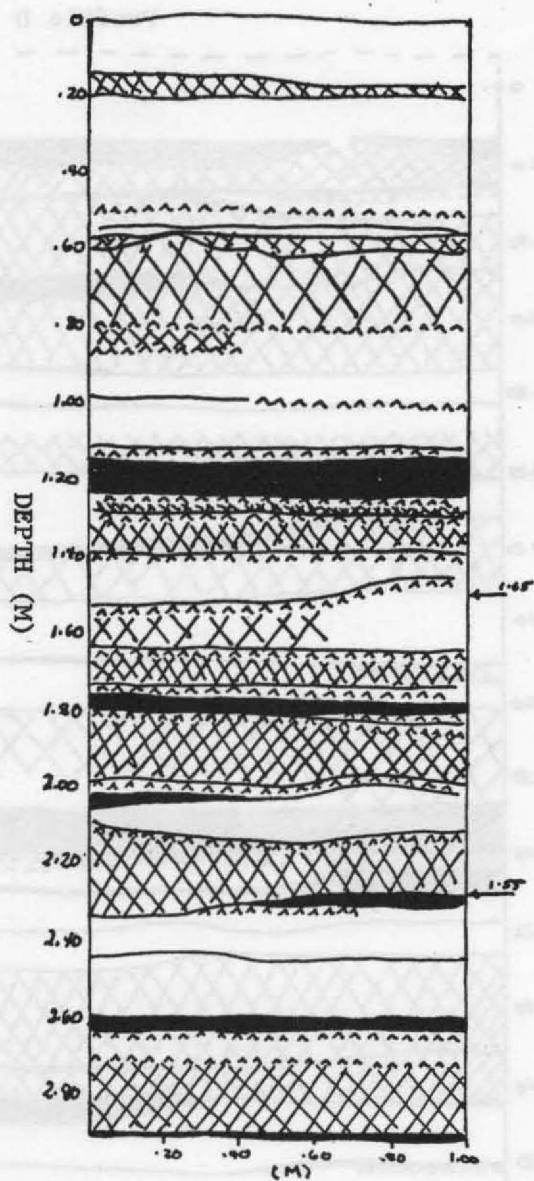
VISIBLE  
STRATIGRAPHY

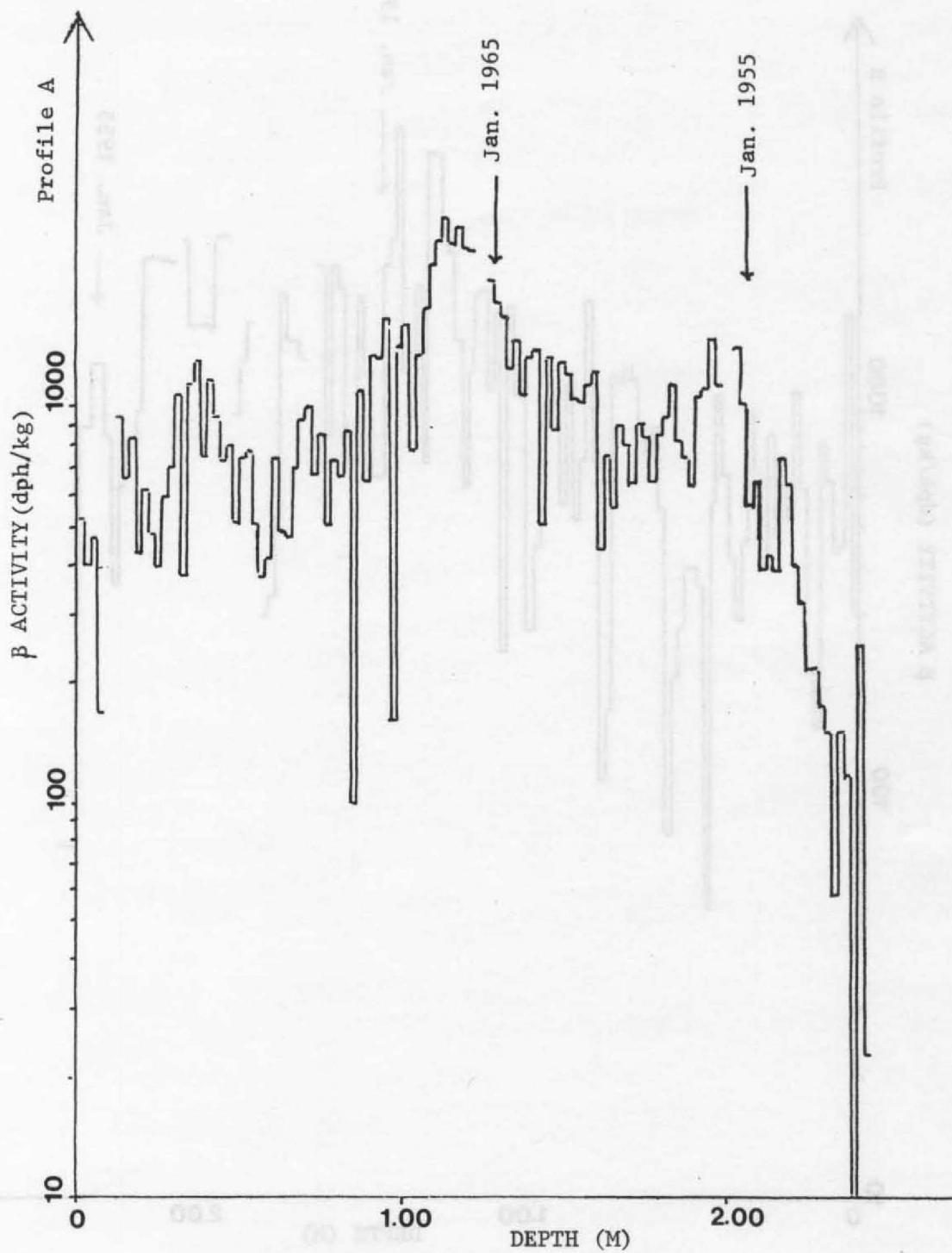


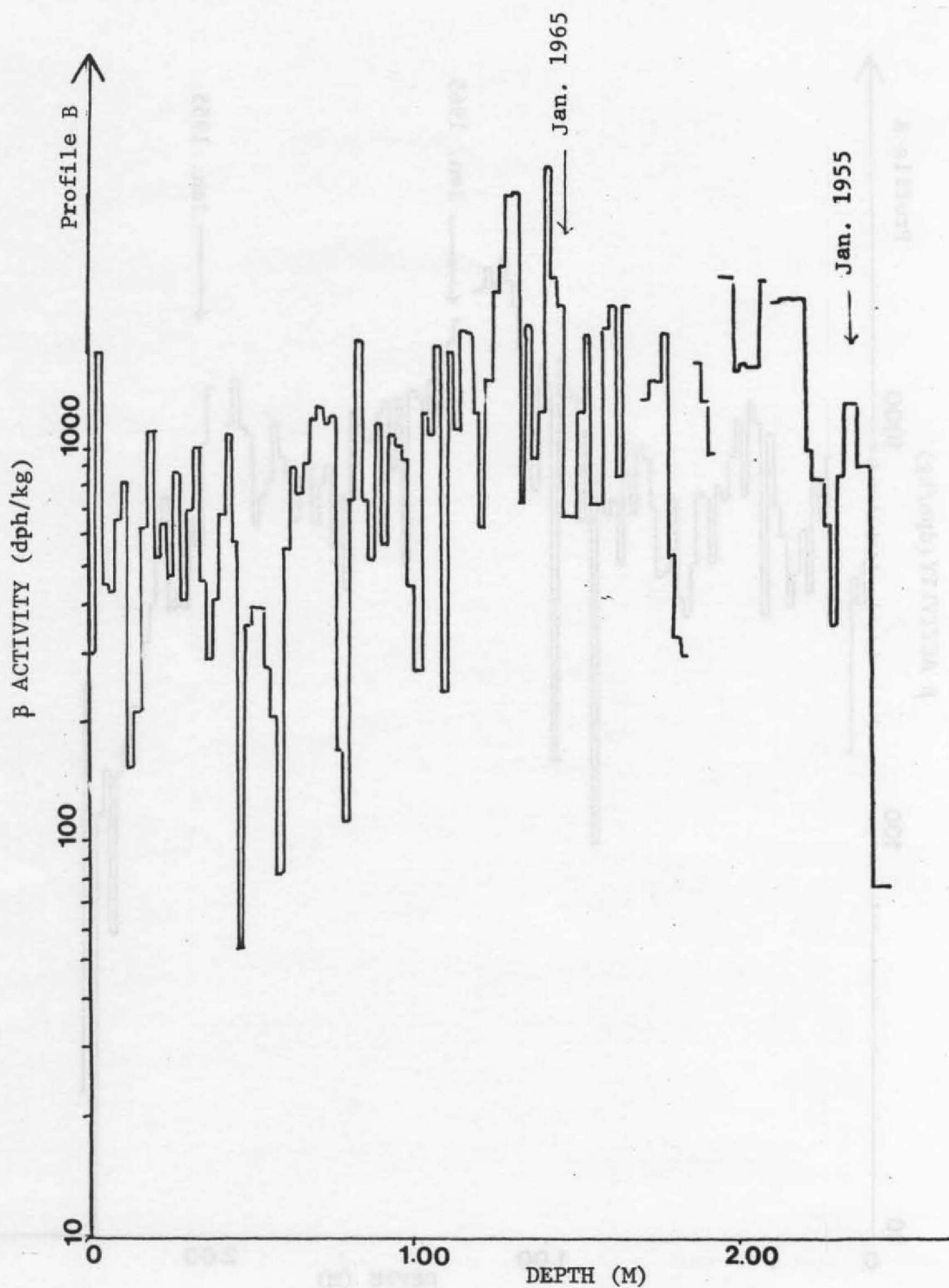
VISIBLE

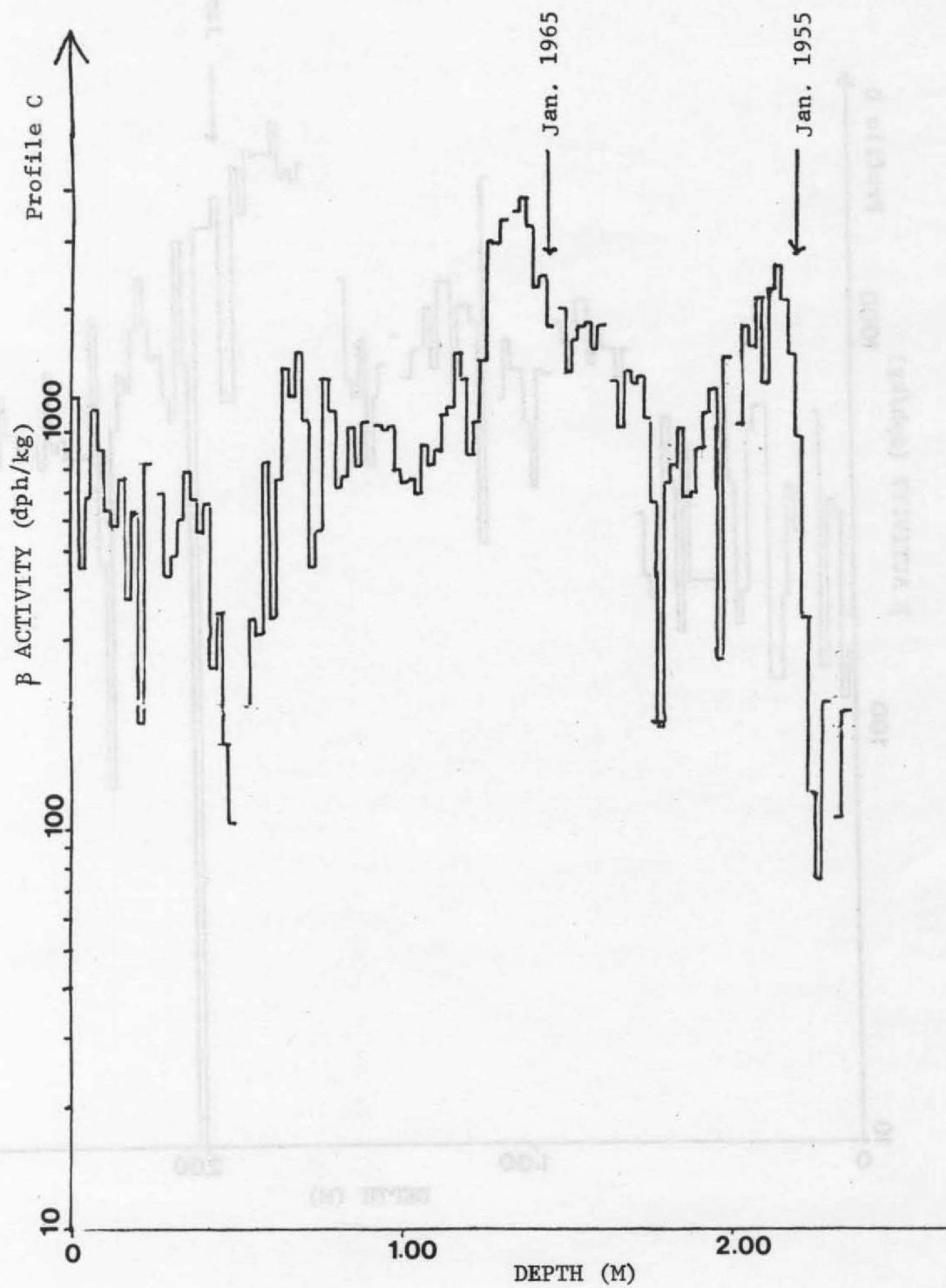
STRATIGRAPHY

Profile E

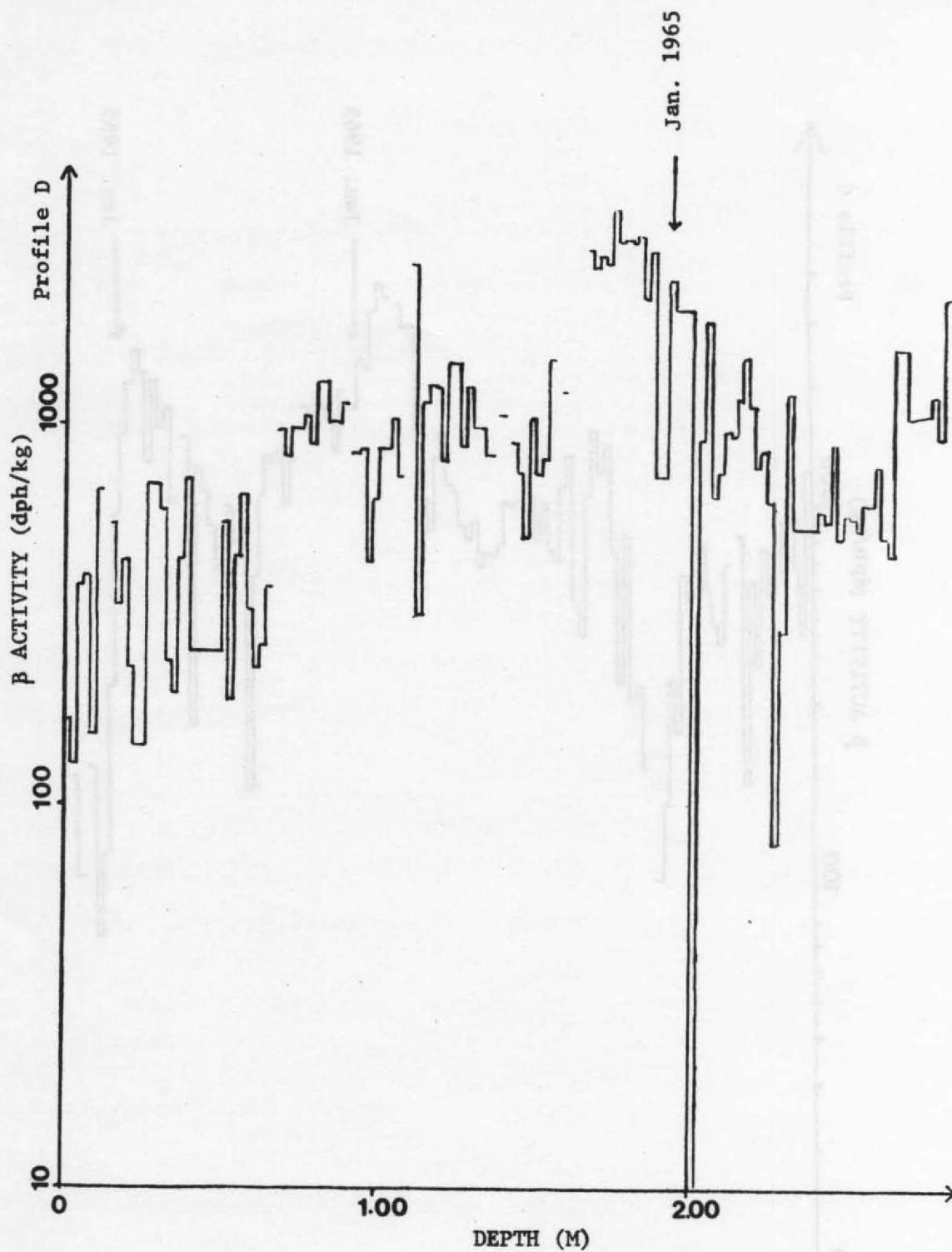


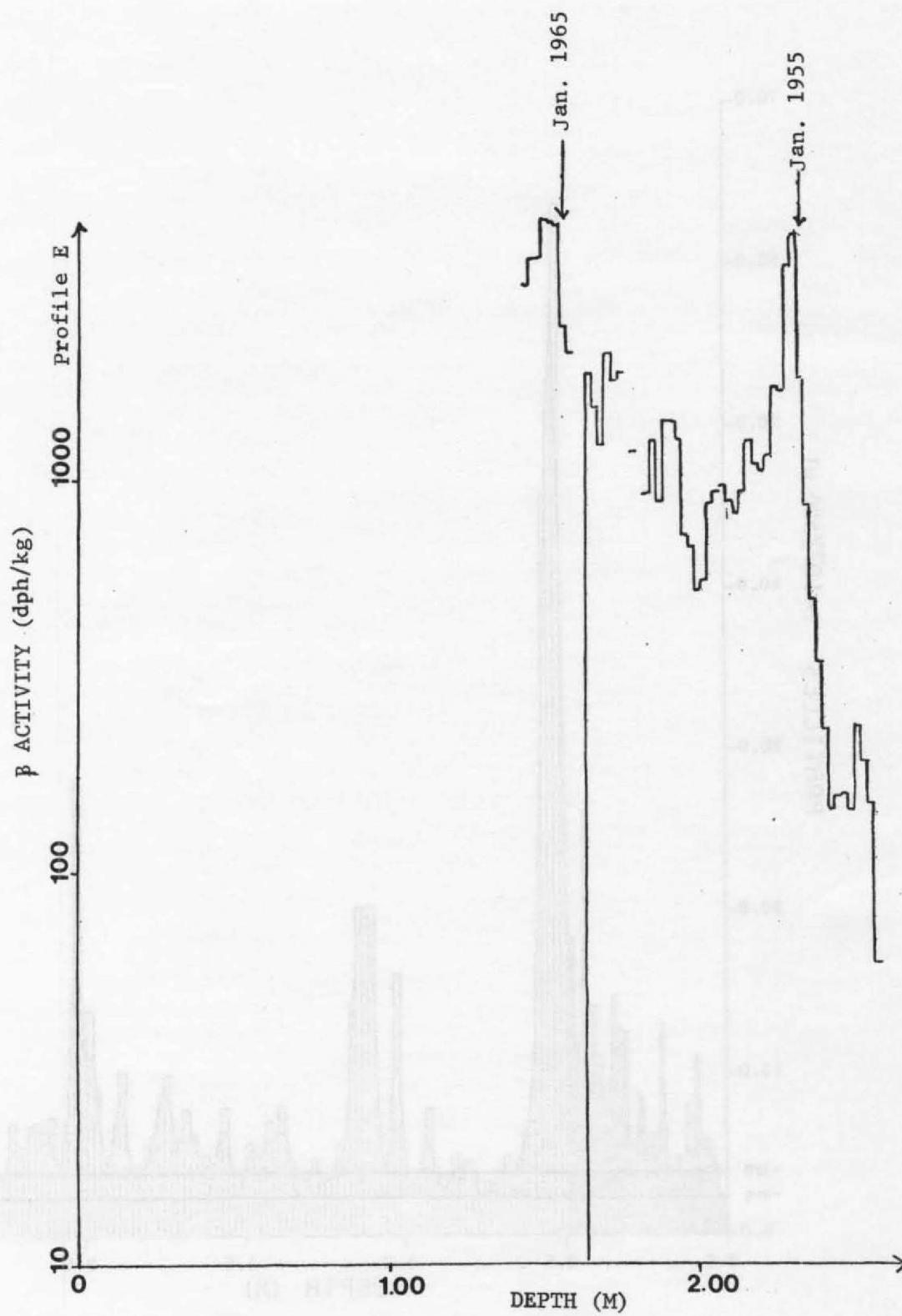


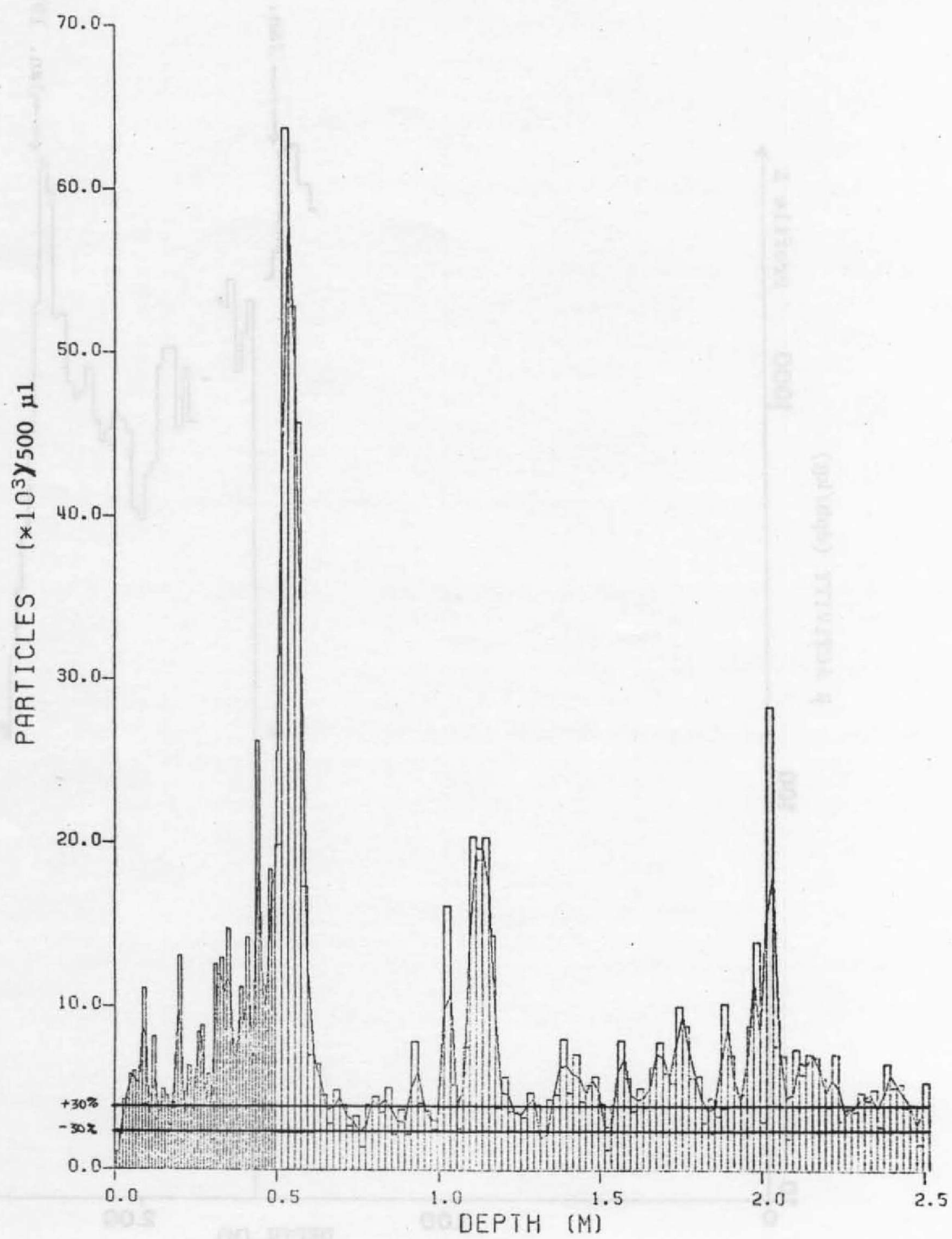


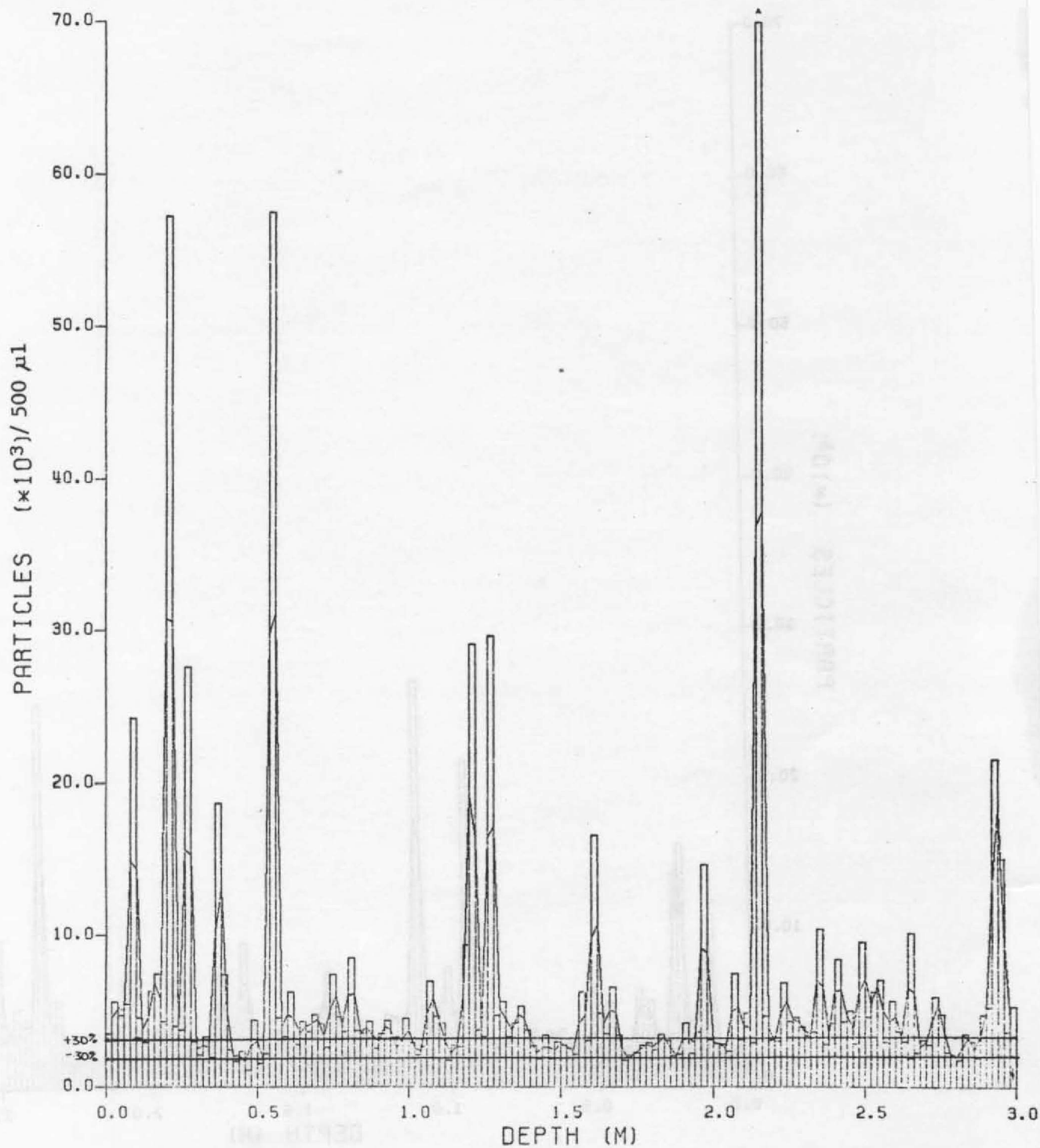


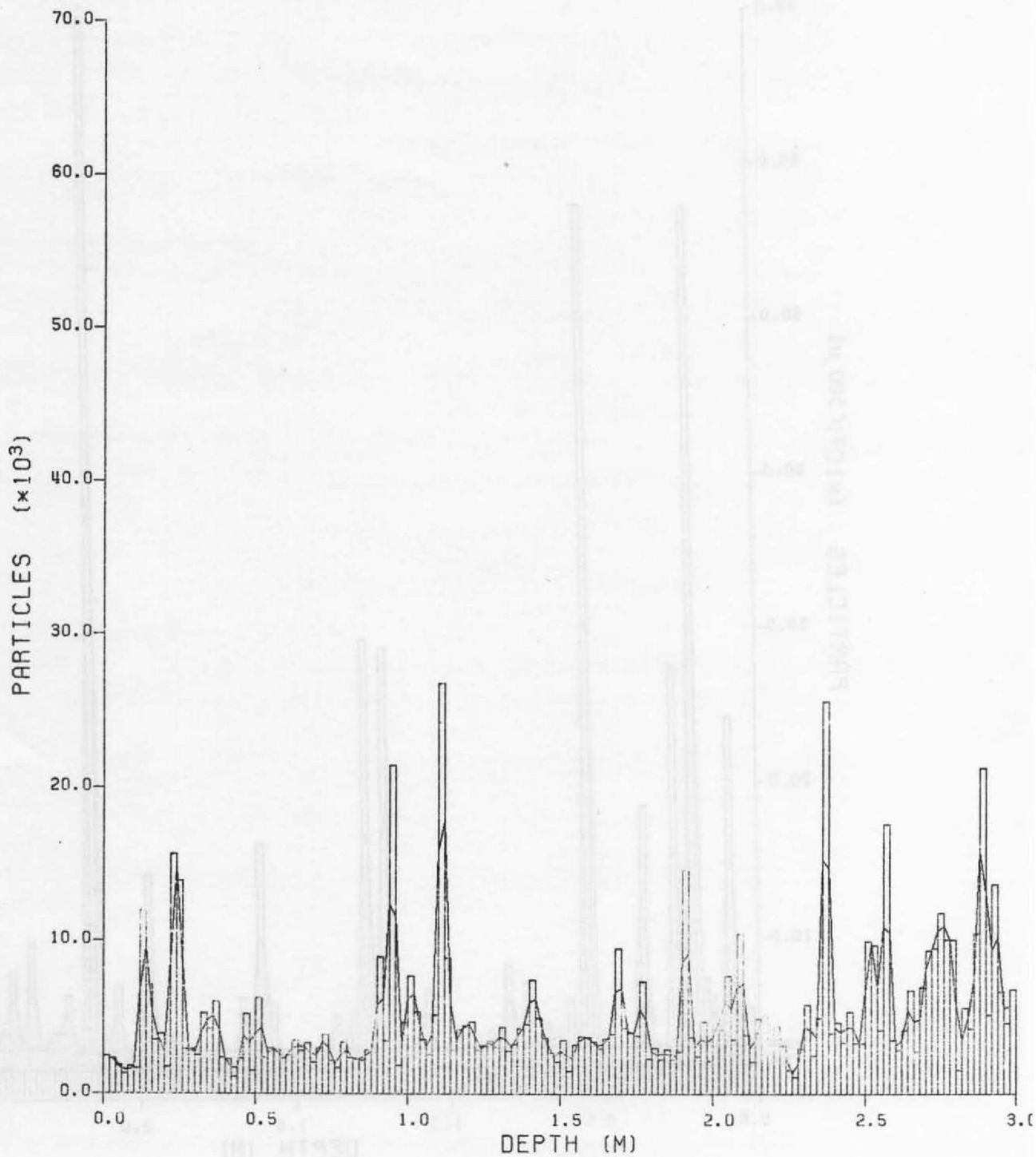




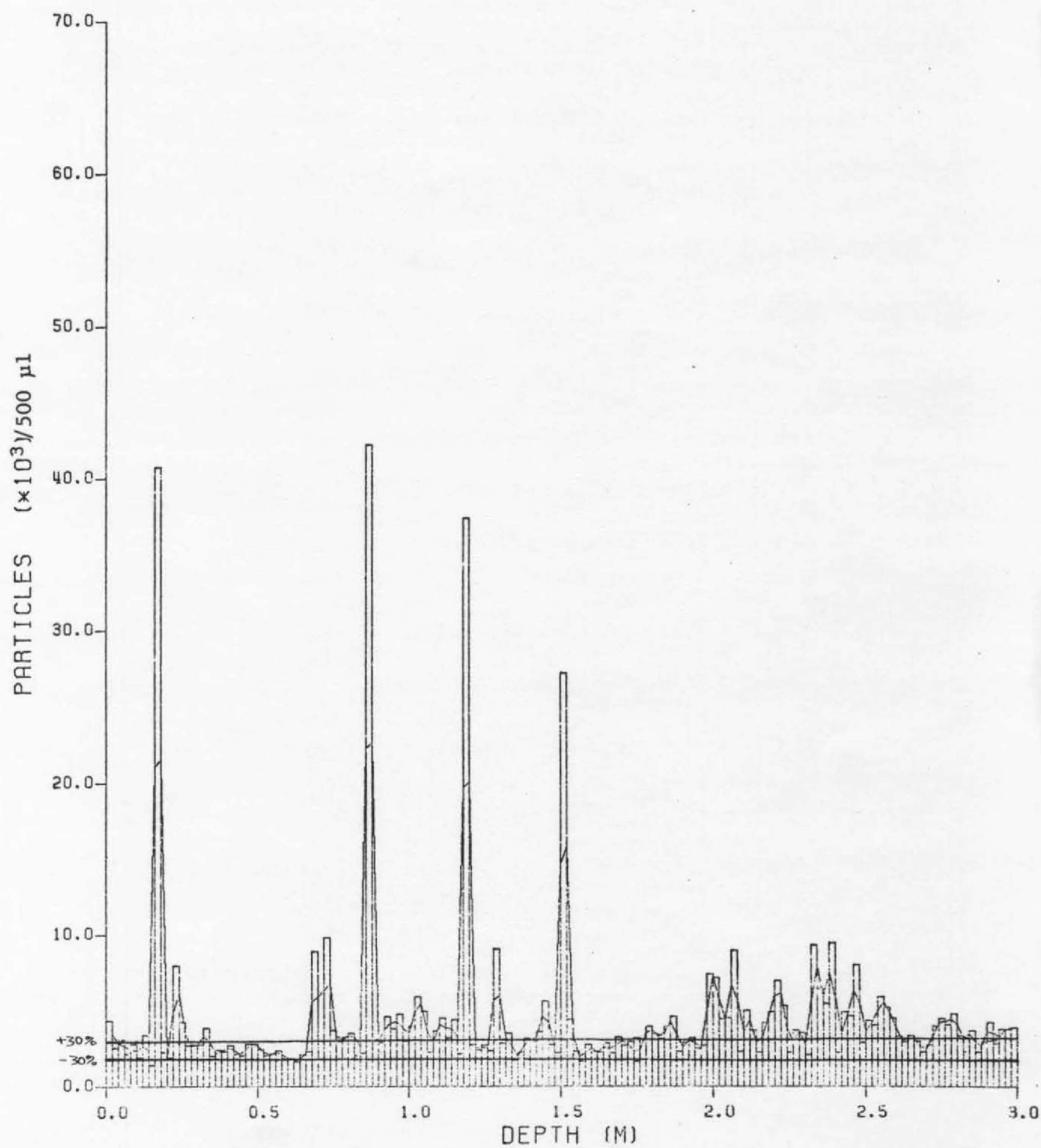




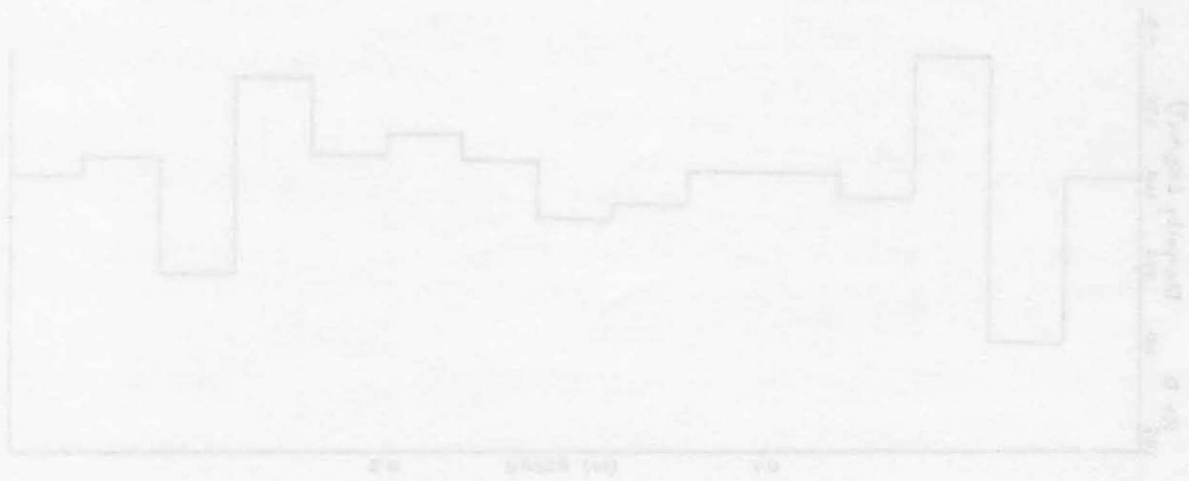




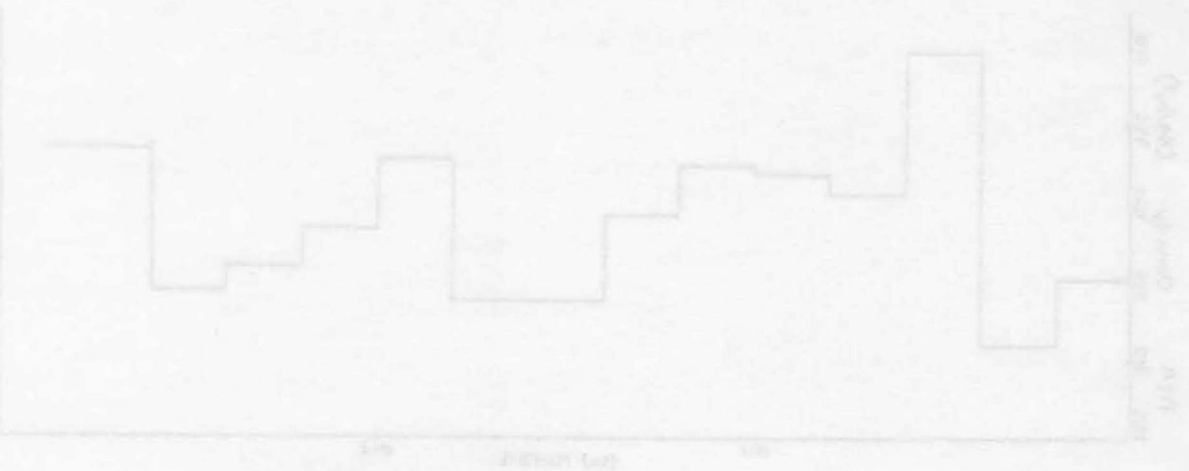
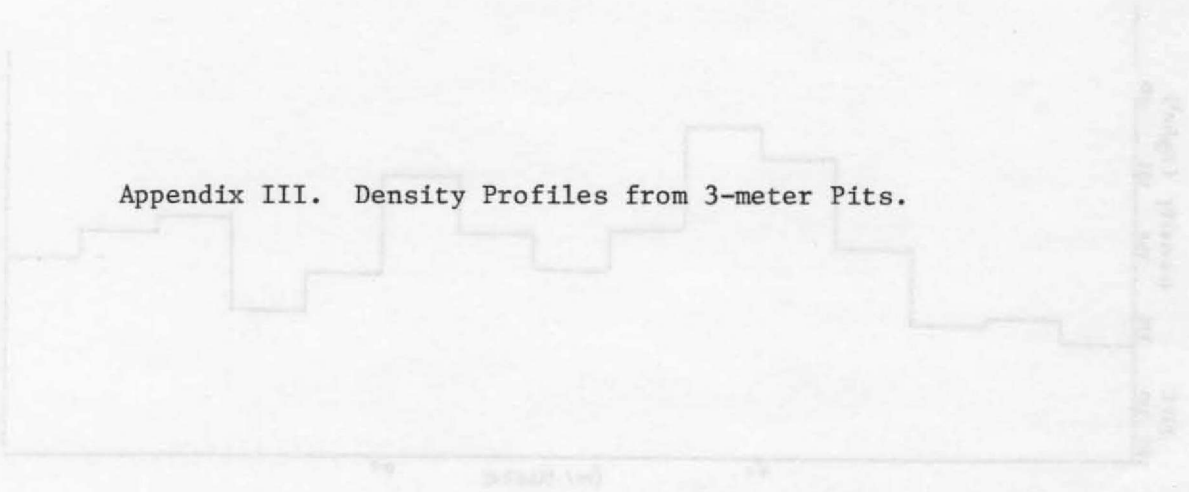


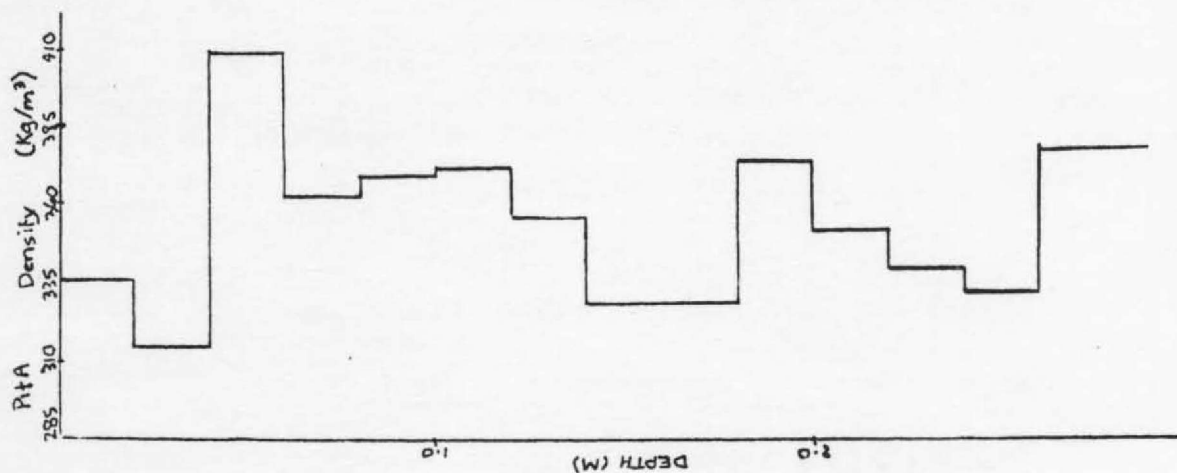
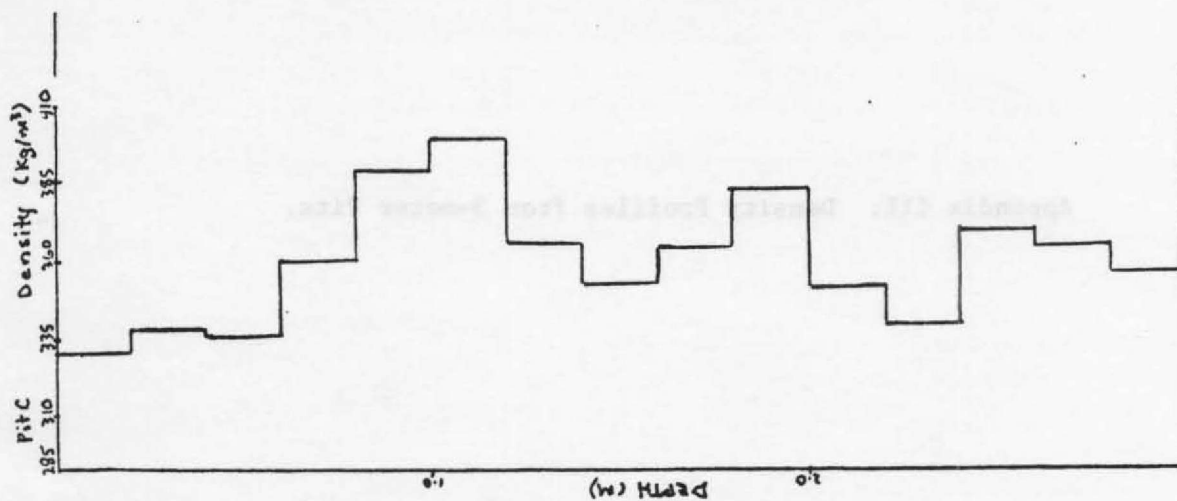
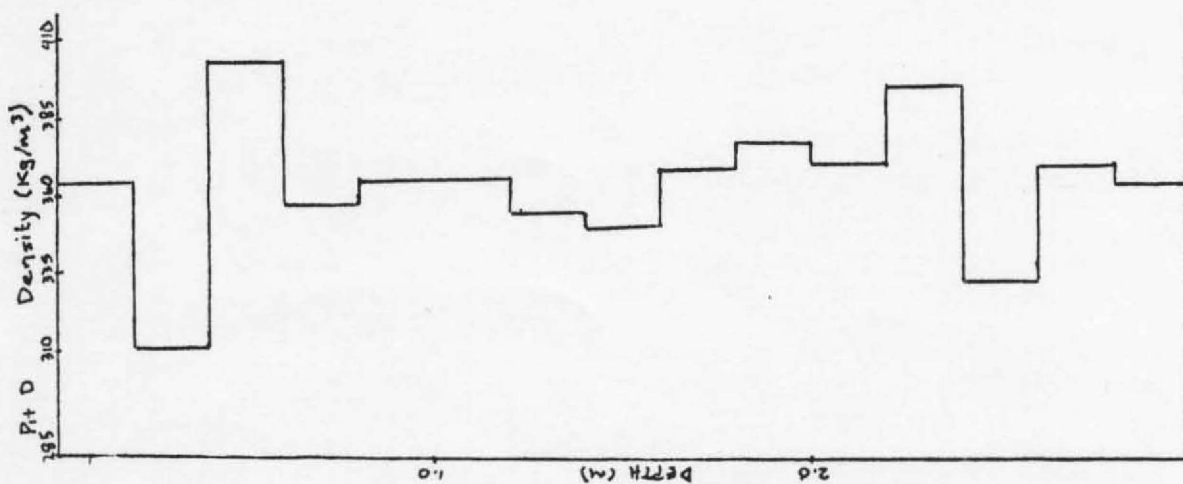


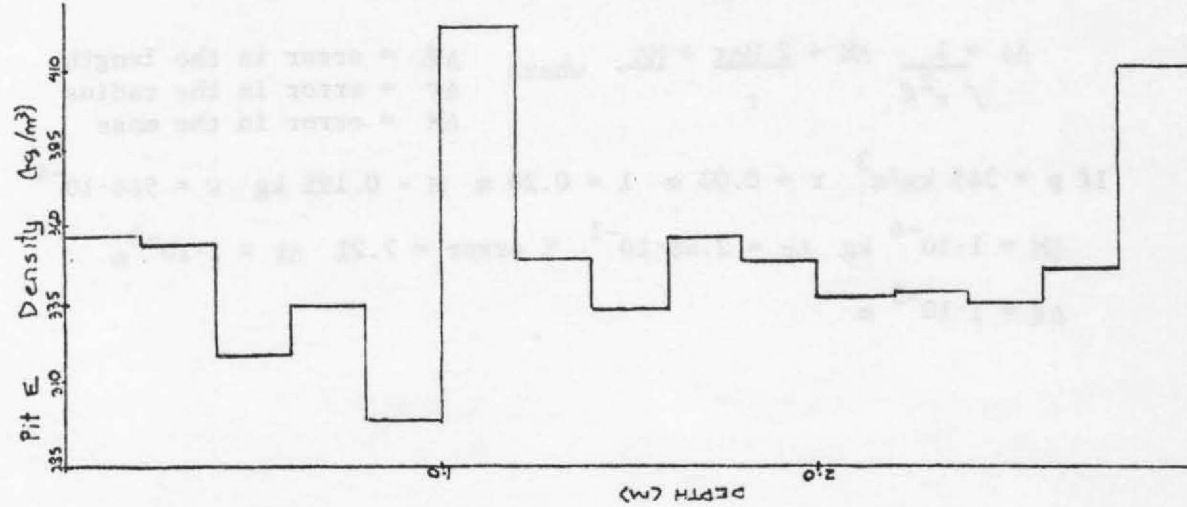
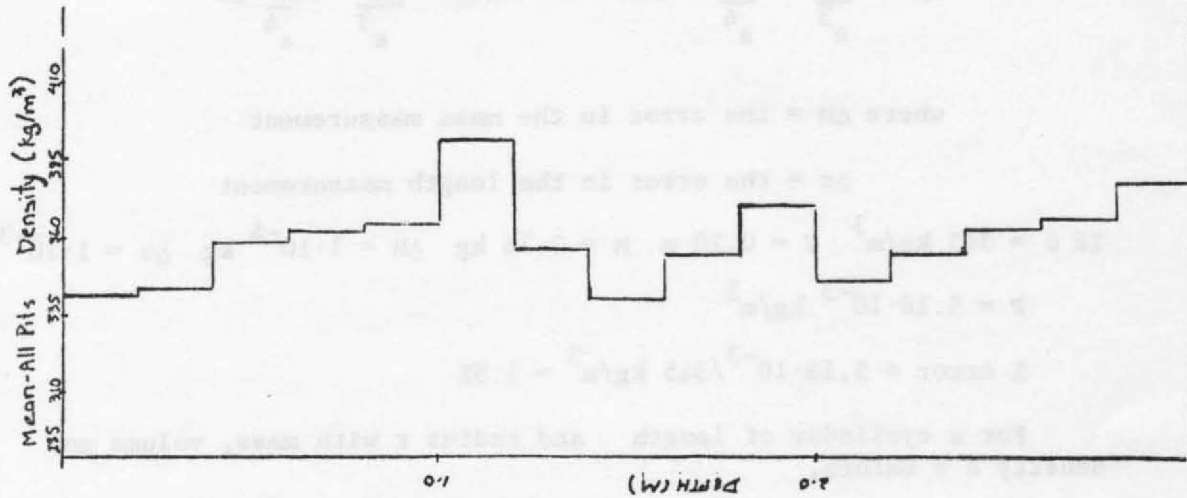
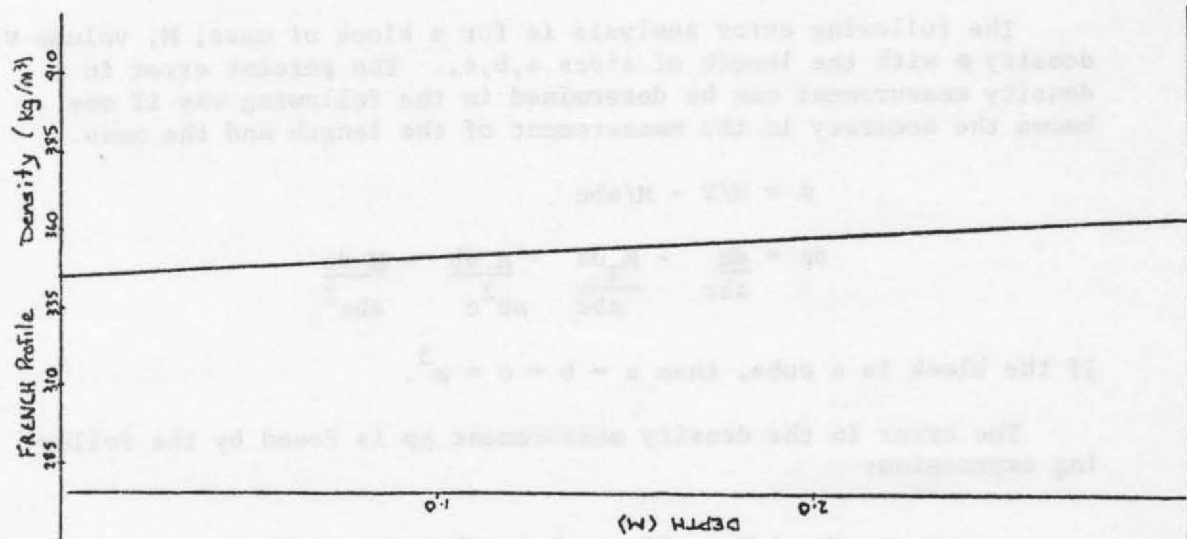




Appendix III. Density Profiles from 3-meter Pits.









### Error Analysis for Density Measurements

The following error analysis is for a block of mass,  $M$ , volume  $V$ , density  $\rho$  with the length of sides  $a, b, c$ . The percent error in a density measurement can be determined in the following way if one known the accuracy in the measurement of the length and the mass.

$$\rho = M/V = M/abc$$

$$d\rho = \frac{dM}{abc} - \frac{M_2 da}{abc} - \frac{M db}{ab^2 c} - \frac{M dc}{abc^2}$$

If the block is a cube, than  $a = b = c = a^3$ .

The error in the density measurement  $\Delta\rho$  is found by the following expression:

$$\Delta\rho = \frac{\Delta M}{a^3} + \frac{M}{a^4} (\Delta a + \Delta b + \Delta c) = \frac{\Delta M}{a^3} + \frac{M}{a^4} \Delta a$$

where  $\Delta M$  = the error in the mass measurement

$\Delta a$  = the error in the length measurement

$$\text{If } \rho = 345 \text{ kg/m}^3 \quad V = 0.20 \text{ m}^3 \quad M = 2.76 \text{ kg} \quad \Delta M = 1 \cdot 10^{-4} \text{ kg} \quad \Delta a = 1 \cdot 10^{-3} \text{ m}$$

$$P = 5.18 \cdot 10^{-3} \text{ kg/m}^3$$

$$\% \text{ error} = 5.18 \cdot 10^{-3} / 345 \text{ kg/m}^3 = 1.5\%$$

For a cylinder of length  $l$  and radius  $r$  with mass, volume and density  $\rho$  as before,

$$\Delta\rho = \frac{1}{\sqrt{r^2 l}} \Delta M + \frac{2 M \Delta r}{r} + \frac{M \Delta l}{l^2} \quad \text{where} \quad \begin{array}{l} \Delta l = \text{error in the length} \\ \Delta r = \text{error in the radius} \\ \Delta M = \text{error in the mass} \end{array}$$

$$\text{If } \rho = 345 \text{ kg/m}^3 \quad r = 0.03 \text{ m} \quad l = 0.20 \text{ m} \quad M = 0.195 \text{ kg} \quad V = 566 \cdot 10^{-4} \text{ m}^3$$

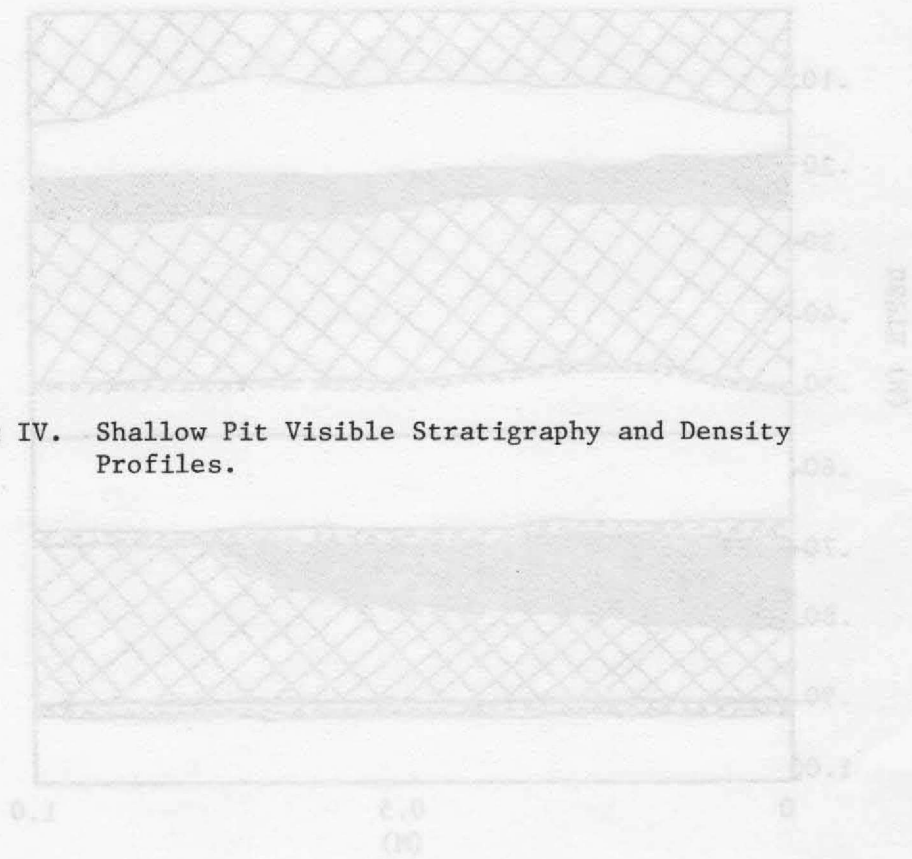
$$\Delta M = 1 \cdot 10^{-4} \text{ kg} \quad \Delta\rho = 2.48 \cdot 10^{-1} \quad \% \text{ error} = 7.2\% \quad \Delta r = 1 \cdot 10^{-3} \text{ m}$$

$$\Delta l = 1 \cdot 10^{-3} \text{ m}$$

# APPENDIX IV SHALLOW PIT VISIBLE STRATIGRAPHY

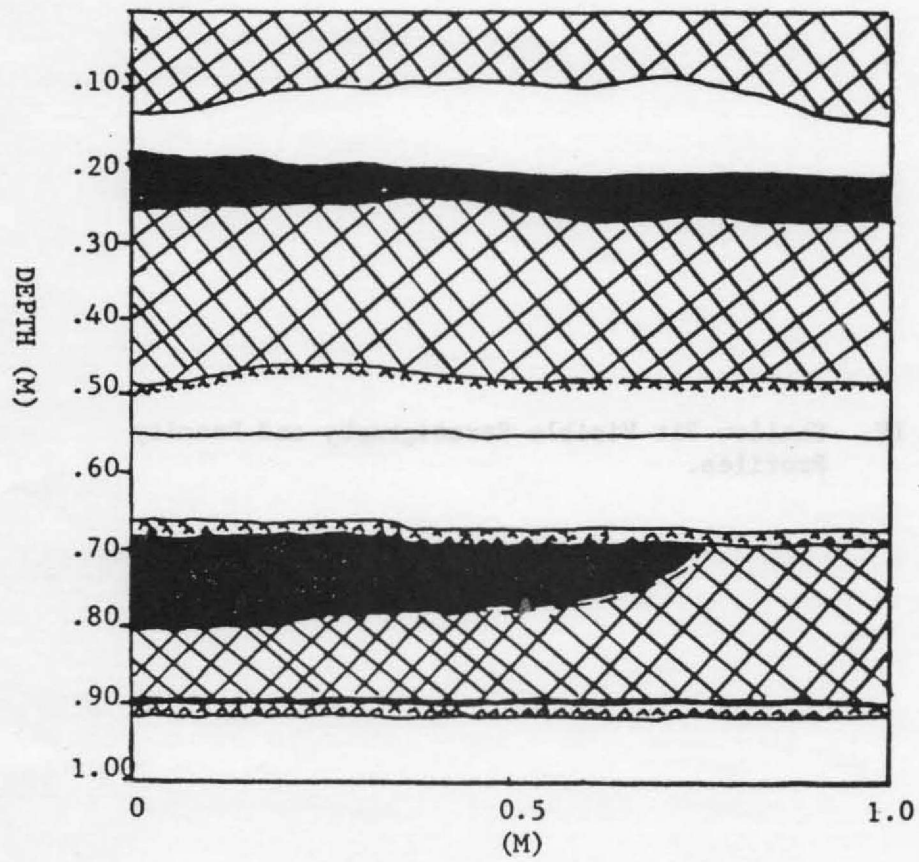
FIG. 12-10a, b, c, d, e, f, g, h, i, j, k, l, m, n, o, p, q, r, s, t, u, v, w, x, y, z, aa, ab, ac, ad, ae, af, ag, ah, ai, aj, ak, al, am, an, ao, ap, aq, ar, as, at, au, av, aw, ax, ay, az, ba, bb, bc, bd, be, bf, bg, bh, bi, bj, bk, bl, bm, bn, bo, bp, bq, br, bs, bt, bu, bv, bw, bx, by, bz, ca, cb, cc, cd, ce, cf, cg, ch, ci, cj, ck, cl, cm, cn, co, cp, cq, cr, cs, ct, cu, cv, cw, cx, cy, cz, da, db, dc, dd, de, df, dg, dh, di, dj, dk, dl, dm, dn, do, dp, dq, dr, ds, dt, du, dv, dw, dx, dy, dz, ea, eb, ec, ed, ee, ef, eg, eh, ei, ej, ek, el, em, en, eo, ep, eq, er, es, et, eu, ev, ew, ex, ey, ez, fa, fb, fc, fd, fe, ff, fg, fh, fi, fj, fk, fl, fm, fn, fo, fp, fq, fr, fs, ft, fu, fv, fw, fx, fy, fz, ga, gb, gc, gd, ge, gf, gg, gh, gi, gj, gk, gl, gm, gn, go, gp, gq, gr, gs, gt, gu, gv, gw, gx, gy, gz, ha, hb, hc, hd, he, hf, hg, hh, hi, hj, hk, hl, hm, hn, ho, hp, hq, hr, hs, ht, hu, hv, hw, hx, hy, hz, ia, ib, ic, id, ie, if, ig, ih, ii, ij, ik, il, im, in, io, ip, iq, ir, is, it, iu, iv, iw, ix, iy, iz, ja, jb, jc, jd, je, jf, jg, jh, ji, jj, jk, jl, jm, jn, jo, jp, jq, jr, js, jt, ju, jv, jw, jx, jy, jz, ka, kb, kc, kd, ke, kf, kg, kh, ki, kj, kk, kl, km, kn, ko, kp, kq, kr, ks, kt, ku, kv, kw, kx, ky, kz, la, lb, lc, ld, le, lf, lg, lh, li, lj, lk, ll, lm, ln, lo, lp, lq, lr, ls, lt, lu, lv, lw, lx, ly, lz, ma, mb, mc, md, me, mf, mg, mh, mi, mj, mk, ml, mm, mn, mo, mp, mq, mr, ms, mt, mu, mv, mw, mx, my, mz, na, nb, nc, nd, ne, nf, ng, nh, ni, nj, nk, nl, nm, nn, no, np, nq, nr, ns, nt, nu, nv, nw, nx, ny, nz, oa, ob, oc, od, oe, of, og, oh, oi, oj, ok, ol, om, on, oo, op, oq, or, os, ot, ou, ov, ow, ox, oy, oz, pa, pb, pc, pd, pe, pf, pg, ph, pi, pj, pk, pl, pm, pn, po, pp, pq, pr, ps, pt, pu, pv, pw, px, py, pz, qa, qb, qc, qd, qe, qf, qg, qh, qi, qj, qk, ql, qm, qn, qo, qp, qq, qr, qs, qt, qu, qv, qw, qx, qy, qz, ra, rb, rc, rd, re, rf, rg, rh, ri, rj, rk, rl, rm, rn, ro, rp, rq, rr, rs, rt, ru, rv, rw, rx, ry, rz, sa, sb, sc, sd, se, sf, sg, sh, si, sj, sk, sl, sm, sn, so, sp, sq, sr, ss, st, su, sv, sw, sx, sy, sz, ta, tb, tc, td, te, tf, tg, th, ti, tj, tk, tl, tm, tn, to, tp, tq, tr, ts, tt, tu, tv, tw, tx, ty, tz, ua, ub, uc, ud, ue, uf, ug, uh, ui, uj, uk, ul, um, un, uo, up, uq, ur, us, ut, uu, uv, uw, ux, uy, uz, va, vb, vc, vd, ve, vf, vg, vh, vi, vj, vk, vl, vm, vn, vo, vp, vq, vr, vs, vt, vu, vv, vw, vx, vy, vz, wa, wb, wc, wd, we, wf, wg, wh, wi, wj, wk, wl, wm, wn, wo, wp, wq, wr, ws, wt, wu, wv, ww, wx, wy, wz, xa, xb, xc, xd, xe, xf, xg, xh, xi, xj, xk, xl, xm, xn, xo, xp, xq, xr, xs, xt, xu, xv, xw, xx, xy, xz, ya, yb, yc, yd, ye, yf, yg, yh, yi, yj, yk, yl, ym, yn, yo, yp, yq, yr, ys, yt, yu, yv, yw, yx, yy, yz, za, zb, zc, zd, ze, zf, zg, zh, zi, zj, zk, zl, zm, zn, zo, zp, zq, zr, zs, zt, zu, zv, zw, zx, zy, zz

Appendix IV. Shallow Pit Visible Stratigraphy and Density Profiles.



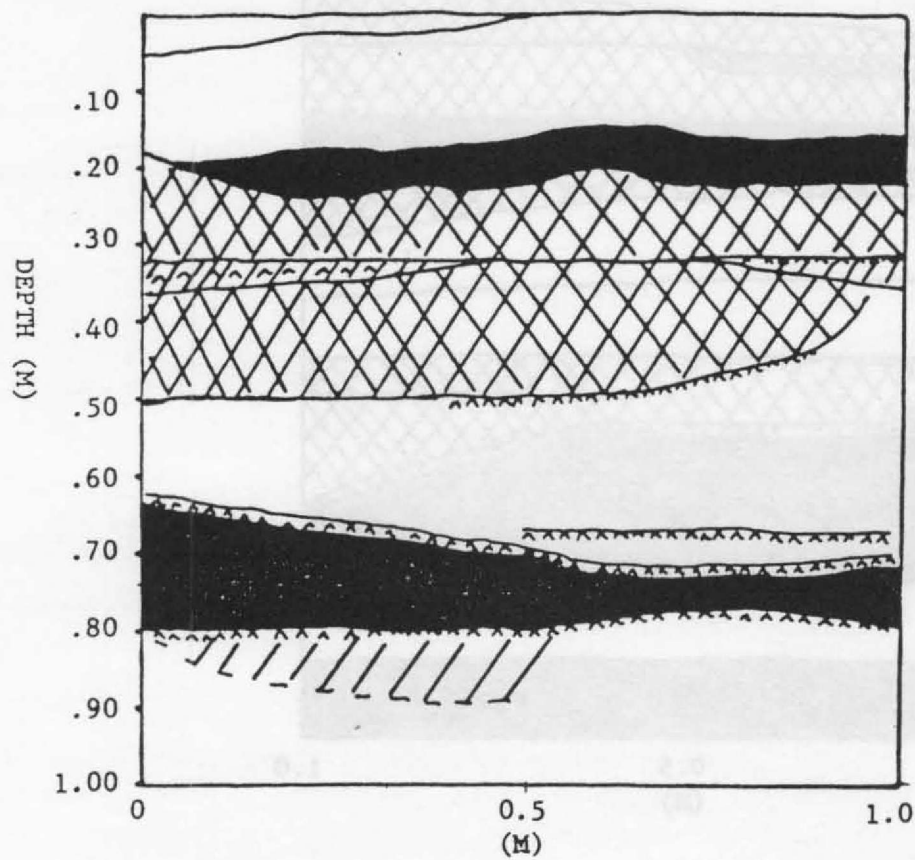
VISIBLE  
STRATIGRAPHY

Pit II- Dec. 9, 1978



VISIBLE  
STRATIGRAPHY

Pit III- Dec. 14, 1978

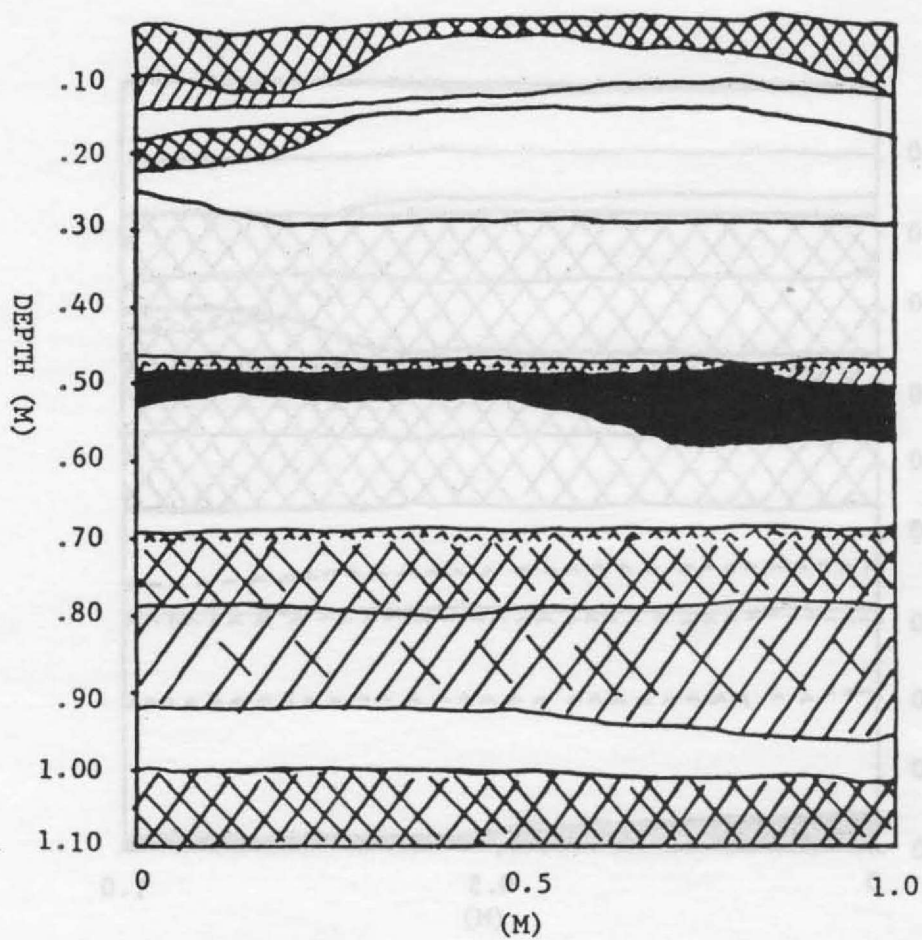






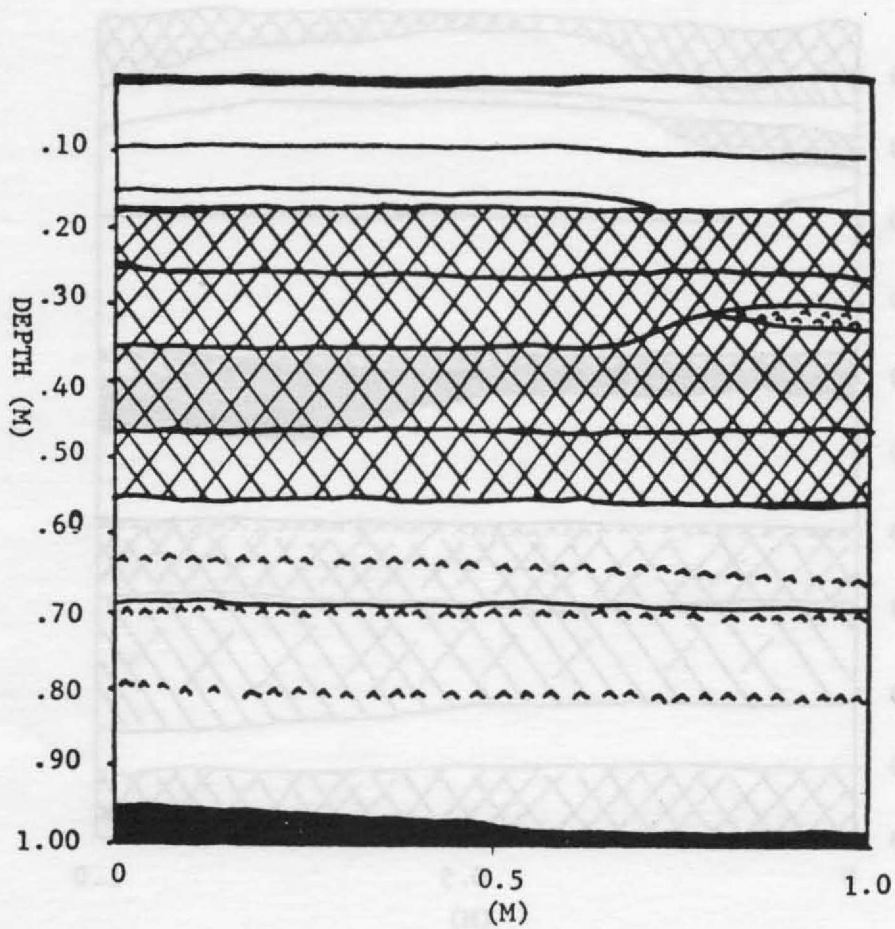
VISIBLE  
STRATIGRAPHY

Pit V- Dec. 29, 1978



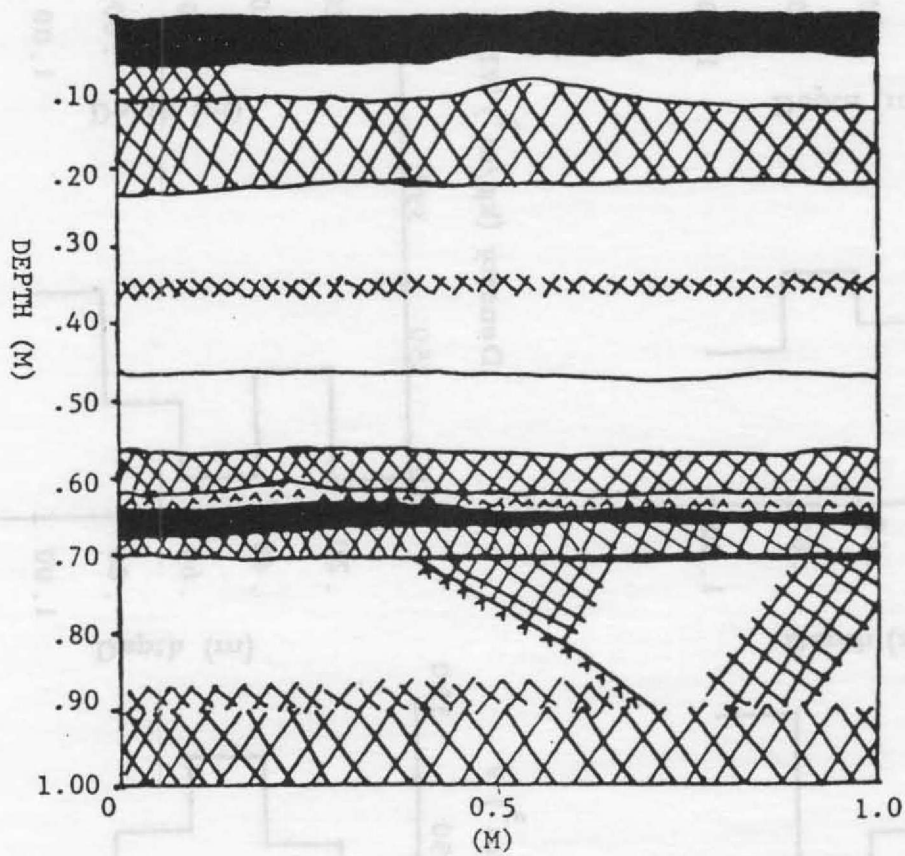
VISIBLE  
STRATIGRAPHY

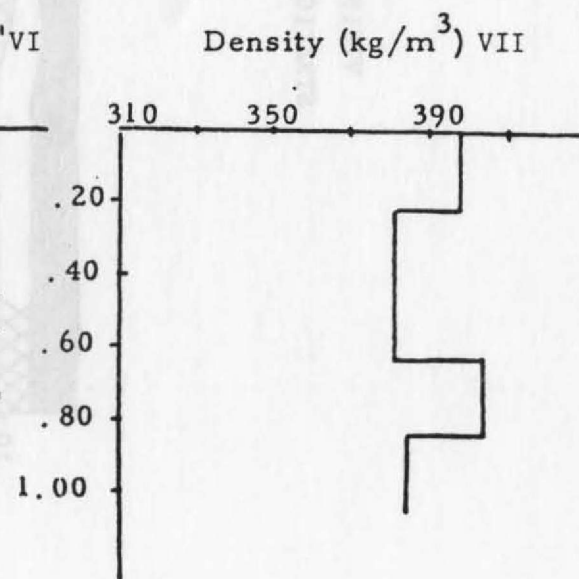
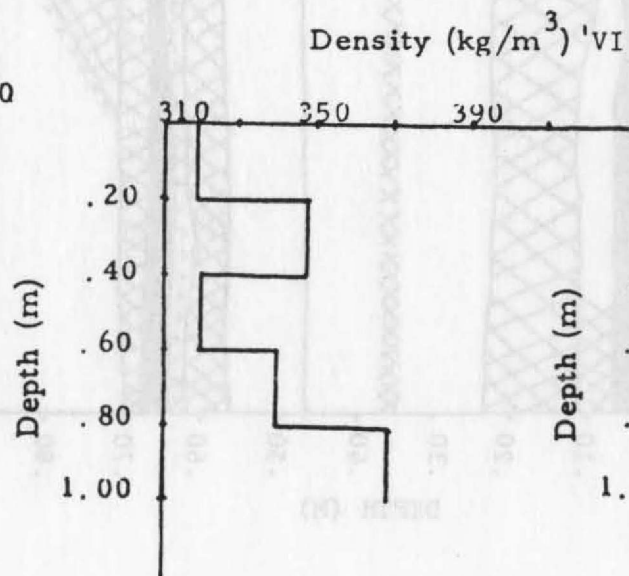
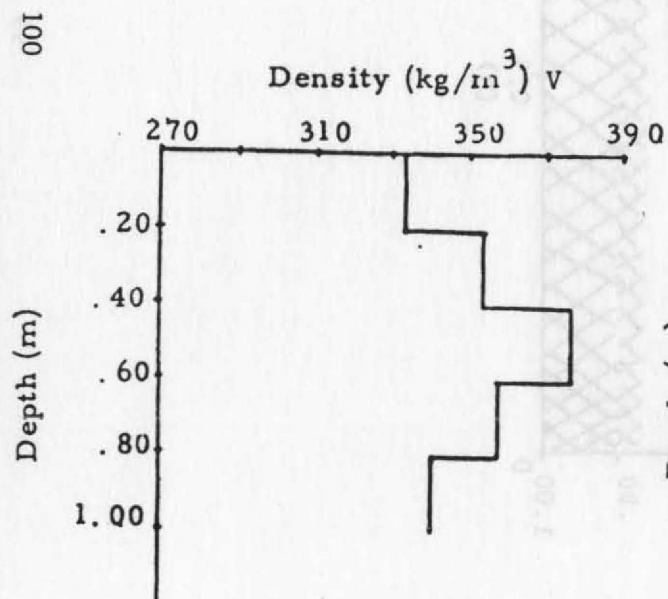
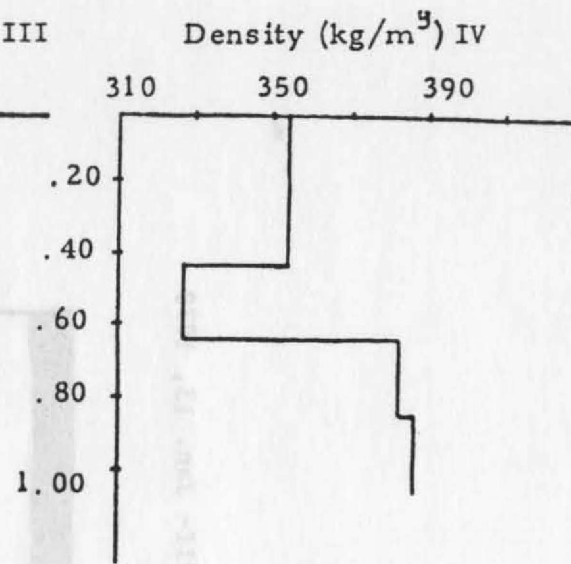
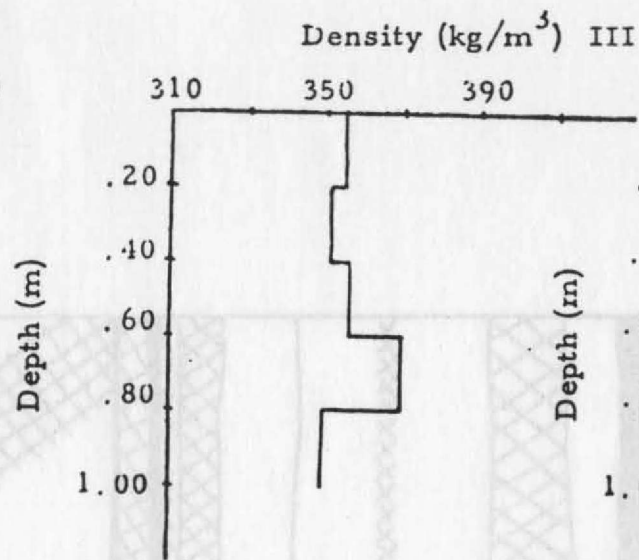
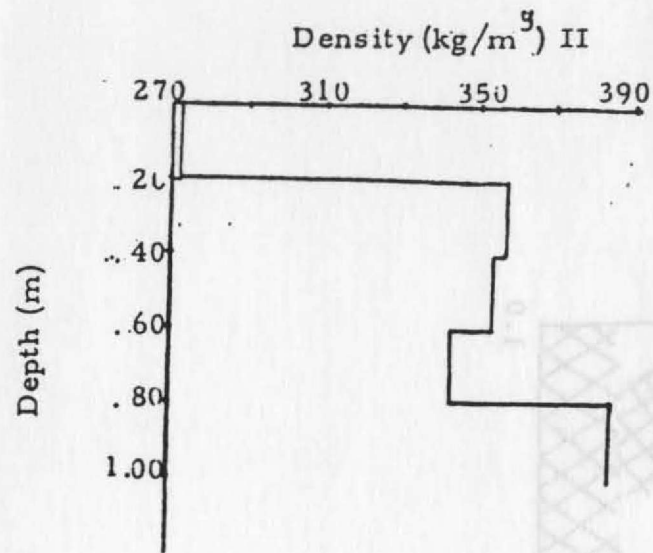
Pit VI- Jan. 6, 1979



VISIBLE  
STRATIGRAPHY

Pit VII- Jan. 13, 1979









# Stratigraphic Interpretations

## Profile A

### Visible Stratigraphy

### Microparticles

<u>Yr.</u>	<u>Interval (m)</u>	<u>Layer Thickness (m snow)</u>
78	+0.12-0.00	0.12
77	0.00-0.08	0.08
76	0.08-0.18	0.10
75]	0.18-0.28	0.10
74]		
73]	0.28-0.50	0.22
72]		
71	0.50-0.68	0.18
70	0.68-0.88	0.20
69]	0.88-1.00	0.12
68]		
67	1.00-1.10	0.10
66	1.10-1.20	0.10
65	1.20-1.38	0.18
64]	1.38-1.48	0.10
63]		
62	1.48-1.58	0.10
61]	1.58-1.70	0.12
60]		
59	1.70-1.80	0.10

<u>Yr.</u>	<u>Interval (m)</u>	<u>Layer Thickness (m snow)</u>
76	0.00-0.14	0.14
75	0.14-0.22	0.08
74	0.22-0.29	0.07
73	0.29-0.38	0.09
72	0.38-0.47	0.09
71	0.47-0.67	0.20
70	0.67-0.77	0.10
69	0.77-0.89	0.12
68	0.89-0.99	0.10
67	0.99-1.07	0.08
66	1.07-1.24	0.17
65	1.24-1.33	0.09
64]	1.33-1.45	0.12
63]		
62	1.45-1.53	0.08
61	1.53-1.61	0.08
60]	1.61-1.72	0.11
59]		

## Profile A (continued)

Stratigraphic InterpretationsVisible StratigraphyMicroparticles

<u>Yr.</u>	<u>Interval (m)</u>	<u>Layer Thickness (m snow)</u>
58	1.80-1.88	0.88
57	1.88-2.00	0.12
56	2.00-2.06	0.06
55	2.06-2.18	0.12
54	2.18-2.22	0.04
53	2.22-2.36	0.14
52	2.36-2.40	0.04
51	2.40-2.60	0.20
50	2.60-2.68	0.08
49	2.68-2.80	0.12
48	2.80-2.90	0.10

$$\bar{X} = 0.10$$

$$\sigma = 0.06$$

<u>Yr.</u>	<u>Interval (m)</u>	<u>Layer Thickness (m snow)</u>
58	1.72-1.83	0.11
57	1.83-1.93	0.10
56	1.93-2.01	0.08
55	2.01-2.09	0.08
54	2.09-2.21	0.12
53	2.21-2.27	0.06
52	2.27-2.37	0.10
51	2.37-2.49	0.12

$$\bar{X} = 0.10$$

$$\sigma = 0.04$$

## Profile B

Stratigraphic InterpretationsVisible StratigraphyMicroparticles

<u>Yr.</u>	<u>Interval (m)</u>	<u>Layer Thickness (m snow)</u>
78	+0.10-0.08	0.18
77	0.08-0.13	0.05
76	0.13-0.30	0.17
75	0.30-0.38	0.08
74	0.38-0.50	0.12
73	0.50-0.56	0.06
72	0.56-0.68	0.12
71	0.68-0.76	0.08
70	0.76-0.80	0.04
69	0.80-0.90	0.10
68	0.90-1.08	0.18
67	1.08-1.20	0.12
66	1.20-1.28	0.08
65	1.28-1.38	0.10
64	1.38-1.50	0.12
63	1.50-1.58	0.08
62	1.58-1.70	0.12
61	1.70-1.78	0.08
60	1.78-1.90	0.12
59	1.90-2.00	0.10

<u>Yr.</u>	<u>Interval (m)</u>	<u>Layer Thickness (m snow)</u>
78	0.00-0.04	0.04
77	0.04-0.13	0.09
76	0.13-0.31	0.18
75	0.31-0.47	0.16
74	0.47-0.63	0.16
73	0.63-0.79	0.16
72	0.79-0.89	0.10
71	0.89-0.96	0.06
70	0.96-1.04	0.06
69	1.04-1.14	0.10
68	1.14-1.25	0.11
67	1.25-1.33	0.08
66	1.33-1.42	0.09
65	1.42-1.52	0.10
64	1.52-1.65	0.13
63		
62	1.65-1.76	0.11
61	1.76-1.88	0.12
60	1.88-1.93	0.05
59	1.93-2.02	0.09

Profile B (continued)

Stratigraphic Interpretations

Visible Stratigraphy

Microparticles

Yr.	Interval (m)	Layer Thickness (m snow)
58	2.00-2.06	0.06
57	2.06-2.14	0.08
56	2.14-2.26	0.12
55	2.26-2.42	0.16
54	2.42-2.46	0.04
53	2.46-2.60	0.14
52	2.60-2.72	0.12
51	2.72-2.80	0.08
50	2.80-2.90	0.10

$$\bar{X} = 0.10$$

$$\sigma = 0.04$$

Yr.	Interval (m)	Layer Thickness (m snow)
58	2.02-2.09	0.07
57	2.09-2.20	0.11
56	2.20-2.31	0.11
55	2.31-2.37	0.06
54	2.37-2.47	0.10
53	2.47-2.57	0.10
52	2.57-2.70	0.13
51	2.70-2.80	0.10
50	2.80-3.00	0.20

$$\bar{X} = 0.10$$

$$\sigma = 0.04$$

			Profile C		
			<u>Stratigraphic Interpretations</u>		
<u>Visible Stratigraphy</u>			<u>Microparticles</u>		
<u>Yr.</u>	<u>Interval (m)</u>	<u>Layer Thickness (m snow)</u>	<u>Yr.</u>	<u>Interval (m)</u>	<u>Layer Thickness (m snow)</u>
78	0.00-0.10	0.10	78	0.00-0.06	0.06
77	0.10-0.14	0.04	77	0.06-0.21	0.15
76	0.14-0.28	0.14	76	0.21-0.31	0.10
75	0.28-0.36	0.08	75	0.31-0.42	0.11
74	0.36-0.50	0.14	74	0.42-0.58	0.16
73	0.50-0.60	0.10	73	0.58-0.69	0.11
72	0.60-0.72	0.12	72	0.69-0.76	0.07
71	0.72-0.80	0.08	71	0.76-0.86	0.10
70	0.80-0.95	0.15	70	0.86-0.97	0.11
69	0.95-1.00	0.05	69	0.97-1.07	0.10
68	1.00-1.10	0.10	68	1.07-1.15	0.08
67	1.10-1.19	0.09	67	1.15-1.23	0.08
66	1.19-1.25	0.06	66	1.23-1.33	0.10
65	1.25-1.40	0.15	65	1.33-1.48	0.15
64	1.40-1.50	0.10	64	1.48-1.53	0.05
63	1.50-1.58	0.08	63	1.53-1.63	0.10
62	1.58-1.62	0.04	62	1.63-1.73	0.10
61	1.62-1.78	0.16	61	1.73-1.79	0.06
60	1.78-1.82	0.04	60	1.79-1.95	0.16
59	1.82-1.86	0.04	59		



Profile C (continued)

Stratigraphic Interpretations

Visible Stratigraphy

Microparticles

<u>Yr.</u>	<u>Interval (m)</u>	<u>Layer Thickness (m snow)</u>
58	1.86-2.04	0.08
57	2.10-2.20	0.06
56	2.10-2.20	0.10
55	2.20-2.42	0.20
54	2.42-2.52	0.10
53	2.52-2.72	0.20
52	2.72-2.82	0.10
51	2.82-2.90	0.08

$$\bar{X} = 0.10$$

$$\sigma = 0.05$$

<u>Yr.</u>	<u>Interval (m)</u>	<u>Layer Thickness (m snow)</u>
58	1.95-1.99	0.04
57]	1.99-2.13	0.14
56]		
55	2.13-2.26	0.13
54	2.26-2.48	0.22
53	2.48-2.61	0.13
52	2.61-2.81	0.20
51	2.81-3.00	0.19

$$\bar{X} = 0.11$$

$$\sigma = 0.05$$

Profile D

Stratigraphic Interpretations

Visible Stratigraphy

Microparticles

<u>Yr.</u>	<u>Interval (m)</u>	<u>Layer Thickness (m snow)</u>
78	+0.06--0.12	0.18
77	0.12-0.17	0.05
76	0.17-0.25	0.08
75	0.25-0.33	0.08
74	0.33-0.48	0.01
73	0.48-0.74	0.26
72	0.74-0.82	0.08
71	0.82-0.90	0.08
70	0.90-1.02	0.12
69	1.02-1.12	0.10
68	1.12-1.32	0.20
67	1.32-1.50	0.18
66	1.50-1.62	0.12
65	1.62-1.86	0.24
64	1.86-2.00	0.14
63	2.00-2.08	0.08
62	2.08-2.18	0.10
61	2.18-2.26	0.08
60	2.26-2.52	0.26
59	2.52-2.64	0.12

<u>Yr.</u>	<u>Interval (m)</u>	<u>Layer Thickness (m snow)</u>
78	0.00-0.20	0.20
77	0.20-0.28	0.08
76	0.28-0.51	0.23
75	0.51-0.77	0.26
74	0.77-0.85	0.08
73	0.85-0.91	0.06
72	0.91-0.99	0.08
71	0.99-1.07	0.08
70	1.07-1.17	0.10
69	1.17-1.24	0.06
68	1.24-1.36	0.12
67	1.36-1.48	0.12
66	1.48-1.67	0.19
65	1.67-1.89	0.22
64	1.89-2.09	0.20
63	2.09-2.15	0.06
62	2.15-2.25	0.10
61	2.25-2.41	0.16
60	2.41-2.50	0.08
59	2.50-2.69	0.19

## Profile D (continued)

<u>Visible Stratigraphy</u>			<u>Stratigraphic Interpretations</u>			<u>Microparticles</u>		
<u>Yr.</u>	<u>Interval (m)</u>	<u>Layer Thickness (m snow)</u>		<u>Yr.</u>	<u>Interval (m)</u>	<u>Layer Thickness (m snow)</u>		
58	2.64-2.80	0.16		58	2.69-2.87	0.18		
57	2.80-2.90	0.10		57	2.87-3.00	0.13		
56	2.90-3.00	0.10		56	3.00-3.10	0.10		
55	3.00-3.10	0.10		55	3.10-3.20	0.10		
54	3.10-3.20	0.10		54	3.20-3.30	0.10		
53	3.20-3.30	0.10		53	3.30-3.40	0.10		
52	3.30-3.40	0.10		52	3.40-3.50	0.10		
51	3.40-3.50	0.10		51	3.50-3.60	0.10		
50	3.50-3.60	0.10		50	3.60-3.70	0.10		
49	3.60-3.70	0.10		49	3.70-3.80	0.10		
48	3.70-3.80	0.10		48	3.80-3.90	0.10		
47	3.80-3.90	0.10		47	3.90-4.00	0.10		
46	3.90-4.00	0.10		46	4.00-4.10	0.10		
45	4.00-4.10	0.10		45	4.10-4.20	0.10		
44	4.10-4.20	0.10		44	4.20-4.30	0.10		
43	4.20-4.30	0.10		43	4.30-4.40	0.10		
42	4.30-4.40	0.10		42	4.40-4.50	0.10		
41	4.40-4.50	0.10		41	4.50-4.60	0.10		
40	4.50-4.60	0.10		40	4.60-4.70	0.10		
39	4.60-4.70	0.10		39	4.70-4.80	0.10		
38	4.70-4.80	0.10		38	4.80-4.90	0.10		
37	4.80-4.90	0.10		37	4.90-5.00	0.10		
36	4.90-5.00	0.10		36	5.00-5.10	0.10		
35	5.00-5.10	0.10		35	5.10-5.20	0.10		
34	5.10-5.20	0.10		34	5.20-5.30	0.10		
33	5.20-5.30	0.10		33	5.30-5.40	0.10		
32	5.30-5.40	0.10		32	5.40-5.50	0.10		
31	5.40-5.50	0.10		31	5.50-5.60	0.10		
30	5.50-5.60	0.10		30	5.60-5.70	0.10		
29	5.60-5.70	0.10		29	5.70-5.80	0.10		
28	5.70-5.80	0.10		28	5.80-5.90	0.10		
27	5.80-5.90	0.10		27	5.90-6.00	0.10		
26	5.90-6.00	0.10		26	6.00-6.10	0.10		
25	6.00-6.10	0.10		25	6.10-6.20	0.10		
24	6.10-6.20	0.10		24	6.20-6.30	0.10		
23	6.20-6.30	0.10		23	6.30-6.40	0.10		
22	6.30-6.40	0.10		22	6.40-6.50	0.10		
21	6.40-6.50	0.10		21	6.50-6.60	0.10		
20	6.50-6.60	0.10		20	6.60-6.70	0.10		
19	6.60-6.70	0.10		19	6.70-6.80	0.10		
18	6.70-6.80	0.10		18	6.80-6.90	0.10		
17	6.80-6.90	0.10		17	6.90-7.00	0.10		
16	6.90-7.00	0.10		16	7.00-7.10	0.10		
15	7.00-7.10	0.10		15	7.10-7.20	0.10		
14	7.10-7.20	0.10		14	7.20-7.30	0.10		
13	7.20-7.30	0.10		13	7.30-7.40	0.10		
12	7.30-7.40	0.10		12	7.40-7.50	0.10		
11	7.40-7.50	0.10		11	7.50-7.60	0.10		
10	7.50-7.60	0.10		10	7.60-7.70	0.10		
9	7.60-7.70	0.10		9	7.70-7.80	0.10		
8	7.70-7.80	0.10		8	7.80-7.90	0.10		
7	7.80-7.90	0.10		7	7.90-8.00	0.10		
6	7.90-8.00	0.10		6	8.00-8.10	0.10		
5	8.00-8.10	0.10		5	8.10-8.20	0.10		
4	8.10-8.20	0.10		4	8.20-8.30	0.10		
3	8.20-8.30	0.10		3	8.30-8.40	0.10		
2	8.30-8.40	0.10		2	8.40-8.50	0.10		
1	8.40-8.50	0.10		1	8.50-8.60	0.10		

$$\bar{x} = 0.13$$

$$\sigma = 0.06$$

$$\bar{x} = 0.14$$

$$\sigma = 0.06$$

Profile E

Stratigraphic Interpretations

Visible Stratigraphy

Microparticles

<u>Yr.</u>	<u>Interval (m)</u>	<u>Layer Thickness (m snow)</u>
78	0.00-0.14	0.14
77	0.14-0.20	0.06
76	0.20-0.48	0.28
75	0.48-0.54	0.06
74	0.54-0.60	0.06
73	0.60-0.80	0.20
72	0.80-0.88	0.08
71	0.88-0.90	0.11
70	0.99-1.12	0.13
69	1.12-1.24	0.12
68	1.24-1.28	0.04
67	1.28-1.40	0.12
66	1.40-1.54	0.14
65	1.54-1.64	0.10

<u>Yr.</u>	<u>Interval (m)</u>	<u>Layer Thickness (m snow)</u>
64	1.64-1.73	0.09
63	1.73-1.80	0.07
62]	1.80-2.00	0.20
61]		
60	2.00-2.06	0.06
59]	2.06-2.12	0.06
58]		
57	2.12-2.32	0.20
56	2.32-2.45	0.13
55	2.45-2.60	0.15
54	2.60-2.64	0.04
53	2.64-2.70	0.06
52	2.70-2.90	0.20

$$\bar{X} = 0.11$$

$$\sigma = 0.07$$

Depth Interval (m)

Date	05-20	05-20	05-1-00	05-1-00
Jan. 19	-	-	-	+0.08
Jan. 20	-	-	-	+0.07
Jan. 21	-	-	-	+0.07
Feb. 1	+0.10	+0.07	-	+0.08
Feb. 2	-	-	-	-
Feb. 17	-0.10	-0.11	-0.08	+0.08
Feb. 18	-0.10	-0.08	-0.08	+0.07
Feb. 18	+0.10	+0.09	+0.08	+0.08
Feb. 19	+0.08	+0.08	+0.08	+0.08
Feb. 20	+0.10	+0.10	+0.08	+0.07
Feb. 21	-	-	-	+0.07

Appendix VI. Temperature Gradient Calculations from South Pole.

Feb. 18	+0.07	+0.08	+0.08
Feb. 17	0.00	+0.08	+0.08
Feb. 16	-0.11	-0.07	-0.08
Feb. 15	+0.08	+0.08	+0.08
Feb. 14	-	-	-
Feb. 13	-0.12	-0.07	-0.08
Mar. 1	-0.07	-0.08	-
Mar. 2	-0.10	-0.08	-0.10
Mar. 3	-0.07	-0.08	-0.08
Mar. 4	-0.08	-0.08	-0.08
Mar. 5	-0.08	-0.08	-0.08
Mar. 6	-0.08	-0.08	-0.08
Mar. 7	-0.08	-0.08	-0.08
Mar. 8	-0.08	-0.08	-0.08
Mar. 9	-0.08	-0.08	-0.08
Mar. 10	-0.08	-0.08	-0.08
Mar. 11	-0.08	-0.08	-0.08
Mar. 12	-0.08	-0.08	-0.08
Mar. 13	-0.08	-0.08	-0.08
Mar. 14	-0.08	-0.08	-0.08
Mar. 15	-0.08	-0.08	-0.08
Mar. 16	-0.08	-0.08	-0.08
Mar. 17	-0.08	-0.08	-0.08
Mar. 18	-0.08	-0.08	-0.08
Mar. 19	-0.08	-0.08	-0.08
Mar. 20	-0.08	-0.08	-0.08
Mar. 21	-0.08	-0.08	-0.08
Mar. 22	-0.08	-0.08	-0.08



Depth Interval ( $^{\circ}\text{C}/\text{cm}$ )

<u>Date</u>	<u>.05-.25</u>	<u>.05-.50</u>	<u>.05-1.00</u>	<u>1.00-3.00</u>
Jan. 19	-	-	-	+.068
Jan. 27	-	-	-	+.053
Jan. 31	-	-	-	+.063
Feb. 3	+.110	+.073	-	+.060
Feb. 7	-.085	-.037	-	-
Feb. 8	-	-	-	+.056
Feb. 12	-.190	-.113	-.056	+.048
Feb. 16	-.120	-.086	-.058	+.037
Feb. 18	+.390	+.197	+.080	+.034
Feb. 19	+.285	+.180	+.091	+.034
Feb. 20	+.200	+.137	+.087	+.035
Feb. 21	-.085	-.009	-.017	+.037
Feb. 22	+.025	+.024	+.030	+.037
Feb. 23	.000	+.009	+.014	+.038
Feb. 24	-.115	-.051	-.020	+.038
Feb. 25	+.060	+.020	+.031	+.038
Feb. 26	-	-	-	+.038
Feb. 27	-.175	-.073	-.028	+.036
Mar. 2	-.405	-.208	-	-
Mar. 6	-.350	-.188	-.126	+.025
Mar. 9	-.165	-.093	-.080	+.018
Mar. 12	.000	-.004	-.034	+.012
Mar. 15	-.580	-.304	-.190	+.010
Mar. 17	-.385	-.220	-.169	+.005
Mar. 18	-.100	-.080	-.107	+.005
Mar. 19	-.180	-.080	-.100	+.000
Mar. 20	-.195	-.086	-.095	+.003
Mar. 21	+.035	+.016	-.040	-.004
Mar. 22	-.160	-.071	-.069	-.004

Depth Interval ( $^{\circ}\text{C}/\text{cm}$ )

Date	<u>.05-.25</u>	<u>.05-.50</u>	<u>.05-1.00</u>	<u>1.00-3.00</u>
Mar. 23	-.660	-.293	-.184	-.004
Mar. 24	-.565	-.251	-.187	-.004
Mar. 25	-.500	-.222	-.184	-.006
Mar. 26	-.455	-.202	-.180	-.008
Mar. 31	-.480	-.213	-	-
Apr. 3	-.360	-.197	-.158	-.019
Apr. 6	-.360	-.184	-.135	-.022
Apr. 9	-.270	-.160	-.133	-.024
Apr. 12	-.225	-.131	-.116	-.116
Apr. 15	-.245	-.066	-.123	-.030
Apr. 18	-	-	-.164	-.033
Apr. 21	-.460	-.111	-.164	-.034
Apr. 24	-.285	-.069	-.117	-.035
Apr. 27	-.110	-.030	-.077	-.036
Apr. 30	-.220	-.057	-.100	-.036
May 3	+.175	+.070	-.002	-.037
May 6	-.245	-.064	-.087	-.036
May 9	+.030	.000	-.023	-.035
May 12	.000	+.028	-.037	-.034
May 15	-.045	-.020	-.018	-.032
May 18	-.075	-.071	-.051	-.028
May 21	+.210	+.082	+.025	-.028
May 24	-	-	-	-.027
May 27	-.070	-.042	-.024	-.023
May 30	-.040	-.077	-.054	-.023
June 3	+.070	+.004	-.007	-.024
June 6	+.085	+.055	+.007	-.024
June 9	-.085	-.073	-.049	-.025
June 12	+.070	+.002	-.030	-.025
June 15	-.165	-.173	-.116	-.027
June 16	-.200	-.180	-.128	-

Depth Interval ( $^{\circ}\text{C}/\text{cm}$ )

<u>Date</u>	<u>.05-.25</u>	<u>.05-.50</u>	<u>.05-1.00</u>	<u>1.00-3.00</u>
June 17	-.300	-.213	-.147	-
June 18	-.155	-.160	-.126	-.030
June 19	-.230	-.228	-.157	-
June 20	-.210	-.195	-.145	-
June 21	-.170	-.191	-.145	-.036
June 22	-.095	0.133	-.122	-
June 23	+.060	+.026	-.041	-
June 24	+.350	+.204	+.060	-.039
June 27	-.075	-.017	-.015	-.033
June 30	-.185	-.137	-.084	-.030
July 4	-	-	-	-.028
July 6	-.105	-.055	-.015	-.023
July 9	+.140	+.073	+.013	+.020
July 12	-.130	-.100	-.061	-.021
July 15	+.085	+.009	-.012	-.021
July 18	-.105	-.076	-.038	-.022
July 21	-.035	-.022	-.015	-.020
July 24	-.260	-.226	-.133	-.020
July 27	-.030	-.042	-.046	-.021
July 30	+.005	+.035	+.035	-.018
Aug. 3	-.050	-.062	-.034	-.016
Aug. 6	-.105	-.171	-.103	-.020
Aug. 9	-.220	-.222	-.152	-.024
Aug. 12	-.110	-.053	-.049	-.028
Aug. 15	-.105	-.100	-.069	-.029
Aug. 18	+.055	-.013	-.024	-.028
Aug. 21	+.010	+.007	-.005	-.030
Aug. 24	-.030	+.009	+.008	-.028
Aug. 27	-.080	-.088	-.045	-.026
Aug. 31	-.250	-.224	-.127	-.025
Sept. 3	+.095	+.042	-.002	-.025

Depth Interval ( $^{\circ}\text{C}/\text{cm}$ )

<u>Date</u>	<u>.05-.25</u>	<u>.05-.50</u>	<u>.05-1.00</u>	<u>1.00-3.00</u>
Sept. 6	-.185	-.082	-.049	-.024
Sept. 9	-.245	-.108	-.069	-.025
Sept. 12	+.215	+.095	+.035	-.024
Sept. 15	+.315	+.140	+.081	-.023
Sept. 18	-.555	-.246	-.104	-.020
Sept. 21	-.175	-.208	-.128	-.020
Sept. 24	+.435	+.362	+.165	-.023
Sept. 27	-	-	-	-.009
Sept. 30	-.055	-.046	-.005	-.011
Oct. 3	-.180	-.131	-.060	-.010
Oct. 6	-.135	-.088	-.050	-.009
Oct. 12	-	-	-	-.004
Oct. 15	-.100	-.017	+.005	-.007
Oct. 18	+.080	+.048	+.017	+.0005
Oct. 21	+.295	+.206	+.092	-.000125
Oct. 24	+.170	+.122	+.074	-.0013
Oct. 27	+.040	+.164	+.106	+.000125
Oct. 30	+.200	+.255	+.176	-.000122
Nov. 3	+.060	+.113	+.098	+.0065
Nov. 6	+.075	+.080	+.070	+.017
Nov. 9	+.080	+.108	-	-
Nov. 12	+.150	+.155	+.122	+.014
Nov. 15	-	-	-	+.014

Depth Interval (C/cm)

1.00-1.01	.97-1.00	.95-.98	.93-.95	Index
+.030	+.040	+.045	+.185	Sept. 8
+.032	+.040	+.108	+.205	Sept. 9
+.034	+.035	+.092	+.215	Sept. 12
+.033	+.081	+.140	+.315	Sept. 13
+.030	+.104	+.204	+.255	Sept. 18
+.030	+.138	+.208	+.175	Sept. 21
+.033	+.165	+.205	+.435	Sept. 24
+.009	-	-	-	Sept. 27
+.011	+.005	+.044	+.055	Sept. 30
+.010	+.060	+.131	+.180	Oct. 3
+.009	+.020	+.088	+.175	Oct. 6
+.004	-	-	-	Oct. 12
+.003	+.005	+.013	+.100	Oct. 15
+.0005	+.013	+.045	+.080	Oct. 18
+.00015	+.005	+.208	+.205	Oct. 21
+.0017	+.034	+.155	+.150	Oct. 24
+.00015	+.108	+.184	+.040	Oct. 25
+.00015	+.150	+.255	+.300	Oct. 30
+.0003	+.008	+.113	+.060	Nov. 3
+.013	+.030	+.080	+.075	Nov. 6
-	-	+.108	+.060	Nov. 9
+.014	+.155	+.155	+.150	Nov. 12
+.014	-	-	-	Nov. 15



The following calculations assume in a very rough way the latent heat of fusion of ice is transferred to the heat transfer layer of a point mass cover. The calculation considers the heat transfer associated with evaporation of ice (sublimation from ice to vapor).

Consider that all the heat which penetrates the film during the summer is lost by forced convection in the summer. The cold air entering the film is warmed by association with the film and is then associated with respect to ice and collides with the surface of the film. Convection exchanges air above the snow with air between the film grains. Subsequent loss of this air involves vapor and heat loss. Heat of the heat is in the form of latent heat of evaporation of ice, the heat capacity of dry air is negligibly small.

Consider a volume of film ( $V_f$ ) in the heat transfer layer of a point mass sheet. The density of this film is ( $\rho_f$ ) and the volume of air in the film is given by  $V = (V_f - V_{ice})$ . The concentration of aqueous vapor present in the block of film can be calculated from the perfect gas law

$$n = \frac{P_f V}{RT_f} \quad (1) \quad n = \frac{P_f V}{RT_f}$$

## Appendix VII. Calculations Considering the importance of forced convection to mass flux.

$V$  = volume of air space  
 $T$  = temperature in  $^{\circ}K$ ,  $T_f$  and  $T_a$  are temperatures with  $T_f > T_a$   
 $n$  = universal gas constant  
 $n$  = concentration of aqueous vapor

As the cold air which enters the film in the summer is warmed from  $T_a$  to  $T_f$ , the change in vapor mass is

$$\Delta n = \frac{P_f V}{R} \left[ \frac{1}{T_f} - \frac{1}{T_a} \right] \quad (2) \quad \Delta n = \frac{P_f V}{R} \left[ \frac{1}{T_f} - \frac{1}{T_a} \right]$$

The energy to form this vapor is drawn from the ice matrix. This loss of energy cools the film. The amount of cooling  $T_f$  from this air exchange can be calculated as follows:

$$Q = \frac{L_f \Delta n}{C_p} \quad (3) \quad T_f = \frac{L_f \Delta n}{C_p}$$

$L_f$  = latent heat of sublimation (which is the sum of the heat required to raise ice to the melting point plus the latent heat of sublimation at  $0^{\circ}C$ )  
 $C_p$  = heat capacity of ice  
 $T_f$  = temperature drop associated with evaporation

The following calculations assess in a very rough way the importance of forced convection to mass transfer in the near surface layers of a polar snow cover. The calculation considers the heat transfer associated with evaporation of ice (sublimation from ice to vapor).

Consider that all the heat which penetrates the firn during the summer is lost by forced convection in the autumn. The cold air entering the firn is warmed by association with the firn and it remains saturated with respect to ice and collects moisture by evaporation of the firn. Convection exchanges air above the snow with air between the firn grains. Subsequent loss of this air involves vapor and heat loss. Most of the heat is in the form of latent heat of evaporation of ice; the heat capacity of dry air is negligibly small.

Consider a volume of firn ( $V_f$ ) in the near surface layer of a polar ice sheet. The density of this firn is ( $\rho_f$ ) and the volume of air in the firn is given by  $V = (\rho_{ice} - \rho_f / \rho_{ice}) V_f$ . The concentration ( $m$ ), of aqueous vapor present in the block of firn can be calculated from the perfect gas law:

$$(1) \quad m = \frac{P V W}{R T}$$

W = molecular weight of water  
P = vapor pressure of aqueous vapor over ice at T.  
V = volume of air space  
T = temperature in  $^{\circ}\text{K}$   $T_1$  and  $T_2$  are temperatures with  $T_1 > T_2$ .  
R = Universal Gas Constant  
m = concentration of aqueous vapor

As the cold air which enters the firn in the autumn is warmed from  $T_2$  to  $T_1$ , the change in vapor mass  $\Delta m$  is:

$$(2) \quad \Delta m = \frac{VW}{R} \left[ \frac{P_1}{T_1} - \frac{P_2}{T_2} \right]$$

The energy to form this vapor is drawn from the ice matrix. This loss of energy cools the firn. The amount of cooling,  $T'$ , from this air exchange can be calculated as follows:

$$(3) \quad T' = \frac{\Delta m L_s}{M_f C_i}$$

$L_s$  = Latent heat of sublimation (which is the sum of the heat required to raise ice to the melting point plus the latent heat of sublimation at  $0^{\circ}\text{C}$ .  
 $M_f$  = Mass of firn originally present  
 $C_i$  = Heat capacity of ice  
 $T'$  = Temperature drop associated with evaporation

Assume that the cooling which occurs in the autumn can be attributed to the sublimation from ice to vapor. The number of air exchanges needed to change the temperature of the firn by  $\Delta T$  is roughly calculated as follows:

$$(4) \quad N = \frac{\Delta T}{T_1} \quad \Delta T = T_1 - T_2 \text{ (where } T_1 > T_2 \text{)}$$

$N$  = number of exchanges/year

and the total mass lost each year ( $M^*$ ) by these exchanges is:

$$(5) \quad M^* = N \Delta m \quad M^* = \text{mass of water vapor removed in each year}$$

Combining equations (3), (4), and (5):

$$(6) \quad M^* = \frac{\Delta T M_f C_i}{L_s}$$

The number of years required to remove a certain percent of the original mass of firn can now be calculated:

$$(7) \quad \frac{n = x \% M_f}{M^*} \quad \begin{array}{l} n = \text{number of years} \\ x = \text{percent of the original mass lost by evaporation} \end{array}$$

Similarly, the amount of mass removed in a certain number of years can also be calculated:

$$(8) \quad M_n = n M^* \quad M_n = \text{mass lost in } n \text{ years}$$

An example of these calculations is shown below with the following values considered to be typical for Dome C.

When  $T_1 = -20^\circ\text{C}$  (253 K),  $P_1 = 0.776 \text{ mmHg}$  or  $1.02 \cdot 10^{-3} \text{ atm}^1$

When  $T_2 = -40^\circ\text{C}$  (233 K),  $P_2 = 0.966 \text{ mmHg}$  or  $1.27 \cdot 10^{-4} \text{ atm}^1$

$$\rho_f = 350 \text{ kg/m}^3$$

$$\rho_{\text{ice}} = 917 \text{ kg/m}^3$$

$$L_s = 6.76 \cdot 10^{-5} \text{ cal/kg} \text{ (}\# \text{)}$$

$$C_i = 5.0 \cdot 10^2 \text{ cal/C-kg} \text{ (}\#\# \text{)}$$

$$R = 8.2 \cdot 10^{-5} \text{ l-atm/k-mole} \text{ (}\#\#\# \text{)}$$

$$W = 1.8 \cdot 10^{-2} \text{ kg/mole}^1$$

# Yen (1969)

## C.R.C. Handbook of Chemistry and Physics, Weast, R.D. ed., The Chemical Rubber Company, 50th ed., Cleveland, 1970.

### Murphy, D.B. and Rousseau, V., Foundations of College Chemistry, 2nd ed., The Ronald Press, New York, 1975.

3. Consider a unit volume of firn ( $1 \text{ m}^3$ ) with a density  $\rho_f$  350 kg/ $\text{m}^3$ . The concentration of aqueous vapor present in this firn is calculated from equation 1.

The change in vapor mass when cold air with a temperature  $T_2 = 40^\circ\text{C}$  is introduced into firn with a temperature  $T_1 = -20^\circ\text{C}$  is calculated from equation 2. This change in mass,  $\Delta m = 4.7 \cdot 10^{-8}$  kg/exchange.

The amount of cooling,  $T'$  from this exchange is calculated from equation 3.

$$T' = 1.8 \cdot 10^{-7} \text{ }^\circ\text{C/exchange}$$

The number of air exchanges  $N$  required to cool the firn by  $T$  is calculated from equation 4.

$$N = 1.1 \cdot 10^8 \text{ exchanges}$$

The total mass of aqueous vapor lost during these exchanges is determined from equation 5.

$$M^* = 5.2 \text{ kg}$$

The most prominent low density layers at Dome C were found between 1.5 and 3.0 meters. With an average annual accumulation of about 0.10 m of snow/year, snow at 1.5 m is about 15 years old. Using equation 8, it can be calculated that in 15 years, 78 kg of firn would be lost from a cubic meter of firn with an original density of  $350 \text{ kg/m}^3$ . This is almost one-quarter of the original mass of firn and thus, is considered to be an extreme value.

In addition to ignoring the heat transfer associated with thermal conduction, this calculation ignores the contributions from the reverse situation in which warm moist air is exchanged with cold dry air in the firn, adding mass to the firn. However since the cold dry air in the firn is relatively stable, this process may cause deposition only in the very near surface layers. With depth, the contribution from this process becomes less important.

The mass loss calculated from this model is considered to be a maximum for several reasons. Two important factors which introduce an uncertainty in these calculations are the following:

- (1) An uncertainty exists in whether the amount of air required for these exchanges can physically be passed through the firn in the time required by this model.
- (2) An uncertainty exists in how much of the summer warm wave can actually be cooled by this process. If, as de Quervain (1972) suggests, that thermal conductivity of the ice matrix contributes to 75 percent of the effective conductivity in the firn, then the maximum cooling which can be attributed to forced convection, as described in this model, is only 25 percent.

Despite the rough nature of these calculations and the uncertainties discussed above, it appears that forced convection is potentially an important process contributing to heat and mass transfer in low temperature firn. Modifications to this model should incorporate the effects of varying wind speeds and progressive changes in absolute temperature throughout the year. Changes in density of the firn resulting from mass loss (decreases) and those due to increased load (increases) must be balanced against one another. Finally, a scaling factor should be incorporated relating to the extent to which this process actually contributes to temperature changes and mass transfer. A value of 25 percent of the total annual heat exchange is suggested as a maximum limit to the contribution from this process.